DIGITALCOMMONS
@WAYNESTATE

Wayne State University

Wayne State University Dissertations

1-1-2014

Lanthanide-Based Precatalysts For Carbon-Carbon Bond-Forming Reactions In Aqueous Media

Derek James Averill
Wayne State University,

Follow this and additional works at: http://digitalcommons.wayne.edu/oa_dissertations

Part of the Chemistry Commons

Recommended Citation
Averill, Derek James, "Lanthanide-Based Precatalysts For Carbon-Carbon Bond-Forming Reactions In Aqueous Media" (2014). *Wayne State University Dissertations.* Paper 1084.

This Open Access Dissertation is brought to you for free and open access by DigitalCommons@WayneState. It has been accepted for inclusion in Wayne State University Dissertations by an authorized administrator of DigitalCommons@WayneState.

LANTHANIDE-BASED PRECATALYSTS FOR CARBON–CARBON BOND FORMING REACTIONS IN AQUEOUS MEDIA.

by

DEREK JAMES AVERILL

DISSERTATION

Submitted to the Graduate School

of Wayne State University,

Detroit, Michigan

in partial fulfillment of the requirements

for the degree of

DOCTOR OF PHILOSOPHY

2014

MAJOR: CHEMISTRY

Approved by:

_____

Advisor Date

_____

_____

_____

DEDICATION

To my parents who raised me with infinite love

ACKNOWLEDGMENTS

I am forever grateful for the patience of my graduate advisor Professor Matthew J. Allen. Matt was able to challenge, support, and encourage me throughout the entirety of my graduate career.

I would like to express great thanks to Dr. David Becker at Oakland Community College. The impact he had on me during my general chemistry course was incredible. Dr. Becker has inspired me since the day we met.

I am very lucky to have had an undergraduate advisor who worked directly with me in the lab. The skills I learned from Professor Ferman Chavez at Oakland University prepared me to start my graduate work without hesitation.

I am thankful for all of the advice of my committee members; Professor Charles H. Winter, Professor Sarah Trimpin, and Professor William D. Wulff.

I would like to acknowledge my lab mates for all their help, laughs, and food over the years. I was lucky enough to share a lab bench with Buddhima Mahanama, she made great food and I could make her laugh at a moments notice.

I appreciate all of the support from the Wayne State Chemistry department.

I thank Melissa Barton for all of the help over the years.

I thank my former lab mate (Stephanie Neal) who is now my wife (Stephanie Averill) for giving me her desk and “WSU Chemistry Department” coffee cup after she graduated.

I want to thank my parents for letting me “experiment” in the garage as I grew up. In the garage, I learned how to troubleshoot problems with skateboards, bicycles, mopeds, and cars. The garage is where I learned how to form hypotheses, test them, and come to a conclusion.

Stephanie, I bet you thought that was the only acknowledgement you would get. Thank you for your patience with my jokes! Stephanie is my best friend, adventure partner, and the love of my life.

TABLE OF CONTENTS

Dedication……ii

Acknowledgments……..…iii

List of Tables….……...….vii

List of Figures……...viii

List of Schemes..……xii

List of Abbreviations……xiii

List of Symbols…….xiv

CHAPTER ONE: Tools for Studying Aqueous Enantioselective Lanthanide–Catalyzed Mukaiyama Aldol Reactions...……..1

1.1 Introduction……....1

1.2 Part 1: Development of enantioselective water-tolerant lanthanide-based precatalysts for Mukaiyama aldol reactions.……..2

1.3 Part 2: Crystal structure determination of precatalysts……..6

1.4 Part 3: Luminescence measurements to study Eu^{3+}-based precatalysts……..……..8

1.5 Part 4: ^{1}H-NMR experiments to study Ln^{3+}-based precatalysts…..……17

1.6 Part 5: Computational studies of Mukaiyama aldol reactions…….20

1.7 Thesis context……..23

CHAPTER TWO: The Role of Water in Lanthanide-Catalyzed Carbon–Carbon Bond Formation……....24

2.1 Introduction…….24

2.2 Results and Discussion……25

2.3 Experimental Section……...32

2.4 Conclusions……..34

CHAPTER THREE: Synthesis, Spectroscopic Characterization, and Reactivity of Water-Tolerant Eu^{3+}-Based precatalysts……...……...35

3.1 Introduction……...……..35

3.2 Results and Discussion…….…...37

3.3 Luminescence measurements for the study of Eu^{3+} coordination environment……..…38

3.4 ^{1}H-NMR characterization of ligands with Eu^{3+}……...44

3.5 Testing of precatalyst reactivity and selectivity in the aqueous Mukaiyama enantioselective aldol reaction…….....46

3.6 Experimental section……49

3.7 Conclusions……..…54

CHAPTER 4: Summary and Future Direction…….55

4.1 Introduction……..55

4.2 Summary of results from chapters two and three……55

4.3 Future direction……56

Appendix A……58

Appendix B……60

Appendix C……84

Appendix D……89

References…..……97

Abstract……...102

Autobiographical Statement……104

LIST OF TABLES

Table 1.1 Aqueous enantioselective Mukaiyama aldol reaction results…….....4

Table 1.2 Selectivity data for the reaction shown in **Scheme 1.2** using different Ln^{3+} ions with ligand **1.5**……6

Table 1.3. Selectivity, reactivity, and coordination changes among different Eu^{3+}-based precatalysts using the ligands from **Figure 1.6**……..……12

Table 1.4. Water-coordination numbers for Eu^{3+} with ligands **1.5** and **1.13–1.17**……...15

Table 1.5. Relative free energies, key structural parameters, and existence probability of lower transition states, with ΔΔG less than 2 kcal/mol..……21

Table 2.1. Mean water-coordination numbers (*q*) of (a) $Eu(OTf)_3$ and (b) $Eu(NO_3)_3$ in mixtures of H_2O/THF……..……...27

Table 2.2. Mean steady state reaction rates of 7 mol % $Eu(OTf)_3$ (a) or 7 mol % $Eu(NO_3)_3$ (b) catalyzed Mukaiyama aldol reactions……..……30

Table 3.1. Water-coordination numbers for Eu^{3+} with ligands **1.5** and **1.13–1.17**……...41

Table 3.2. Aqueous Mukaiyama aldol yields and selectivities catalyzed by $Eu(OTf)_3$ with ligands **1.5** and **1.13–1.17**……..……..……46

LIST OF FIGURES

Figure 1.1. Chiral ligands used for lanthanide-catalyzed water-tolerant enantioselective Mukaiyama aldol reactions…….…..3

Figure 1.2. Graph of selectivity data for the reaction shown in **Scheme 1.2** using different Ln^{3+} ions and ligand **1.4**. Increased selectivity is observed as the ionic radii of Ln^{3+} increase from Yb^{3+} to Ce^{3+}. Adapted with permission from S. Kobayashi, T. Hamada, S. Nagayama and K. Manabe, *Org. Lett*., 2001, **3**, 165. Copyright 2001 American Chemical Society……5

Figure 1.3. X-ray crystal structure of $[Pr(NO_3)_2 \cdot \mathbf{1.4}]^+$. Hydrogen atoms have been omitted for clarity. Adapted with permission from S. Kobayashi, T. Hamada, S. Nagayama and K. Manabe, *Org. Lett*., 2001, **3**, 165. Copyright 2001 American Chemical Society……...7

Figure 1.4. X-ray crystal structure of Yb^{3+}-based precatalyst showing a chelated acetate moiety and its hydrogen bonding interactions to nearby water molecules. Reprinted with permission from R. S. Dickens, S. Aime, A. S. Batsanov, A. Beeby, M. Botta, J. I. Bruce, J. A. K. Howard, C. S. Love, D. Parker, R. D. Peacock and H. Puschmann, *J. Am. Chem. Soc*. 2002; **124**, 12697. Copyright 2002 American Chemical society…...8

Figure 1.5. Top, Water-coordination number of $Eu(OTf)_3$ (○), and $Eu(NO_3)_3$ (□) as a function of % H_2O in THF (v/v). Error is represented by standard error of the mean of between 3 and 9 measurements. Bottom, Steady-state reaction rates of 7 mol % $Eu(OTf)_3$- (○) or $Eu(NO_3)_3$-catalyzed (□) Mukaiyama aldol reactions in 0–40% H_2O in THF (v/v). Regression lines represent the dependence of rate on solvent composition and anion identity. Reprinted with permission by Averill, D. J.; Dissanayake, P.; Allen, M. J. The Role of Water in Lanthanide-Catalyzed Carbon–Carbon Bond Formation. Molecules 2012, 17, 2073–2081. http://www.mdpi.com/1420-3049/17/2/2073.....11

Figure 1.6. Hexadentate ligands used to study changes in selectivity and reactivity based on ligand identity……12

Figure 1.7. Proposed equilibrium leading to the activation and selective nucleophilic attack of benzaldehyde. Adapted with permission from Y. Mei, P. Dissanayake and M. J. Allen, *J. Am. Chem. Soc*. 2010, 132, 12871. Copyright 2010 American Chemical Society……..……..13

Figure 1.8. Proposed transition state for the asymmetric Mukaiyama aldol reaction using hexadentate ligands **1.5** and **1.8**–**1.13** and Eu^{3+} as a precatalyst. Adapted with permission from Y. Mei, P. Dissanayake and M. J. Allen, *J. Am. Chem. Soc*. 2010, 132, 12871. Copyright 2010 American Chemical Society…….....14

Figure 1.9. Hexadentate ligands studied in the presence of Eu^{3+}……15

Figure 1.10. Proposed equilibria involving multiple Eu^{3+} species. Reprinted with permission from D. J. Averill and M. J. Allen, *Inorg. Chem*. 2014, **53**, 6257. Copyright 2014 American Chemical Society……..……...15

Figure 1.11. Emission spectra of $Eu(OTf)_3$ in 9:1 $EtOH/H_2O$ with (dotted line) and without (solid line) a hexadentate ligand. Adapted with permission from D. J. Averill and M. J. Allen, *Inorg. Chem*. 2014, **53**, 6257. Copyright 2014 American Chemical Society……...……16

Figure 1.12. Emission intensity ratios of Eu^{3+} (616 nm/591 nm) versus equivalents of ligand for Eu^{3+} with **1.5** (△), **1.13** (▲), **1.14** (◆), **1.15** (◇), **1.16** (○), and **1.17** (□). Increases in magnitude of the emission intensity quotient (616 nm/591 nm) arise from increases in crystal field splitting of Eu^{3+}. Adapted with permission from D. J. Averill and M. J. Allen, *Inorg. Chem*. 2014, **53**, 6257. Copyright 2014 American Chemical Society……...……...17

Figure 1.13. (A) ^{1}H-NMR spectrum of **1.14** in 9:1 $EtOD/D_2O$. (B) ^{1}H-NMR spectrum of **1.14** in 9:1 $EtOD/D_2O$ at –40 °C with 0.25 equiv of $Eu(OTf)_3$. Arrows point to signals observed in the presence of excess ligand (the temperature of –40 °C was required to resolve the signals between 4 and 2 ppm). These new signals are attributed to a Eu^{3+}–L_n ($n > 1$) species. (C) ^{1}H-NMR spectrum of **1.14** in 9:1 $EtOD/D_2O$ with 2 equiv of $Eu(OTf)_3$. Arrows point to signals observed in the presence of excess Eu^{3+}. The new upfield signals are attributed to $Eu^{3+}{}_n$–L ($n \geq 1$) species. Adapted with permission from D. J. Averill and M. J. Allen, *Inorg. Chem*. 2014, **53**, 6257. Copyright 2014 American Chemical Society……..……19

Figure 1.14. Fragments F1, F2, F3, and F4 used by Morokuma and co-workers to study the Mukaiyama aldol reaction by the artificial force-induced reaction method. Reprinted with permission from M. Hatanaka and K. Morokuma, *J. Am. Chem. Soc*. 2013, **135**, 13972…….…..22

Figure 1.15. Reaction pathway as calculated by the artificial force-induced reaction method. Reprinted with permission from M. Hatanaka and K. Morokuma, *J. Am. Chem. Soc*. 2013, **135**, 13972.....22

Figure 2.1. The water-tolerant Mukaiyama aldol reaction between silyl enol ether **1.6**, and benzaldehyde **1.2**, studied in this work……..25

Figure 2.2. Water-coordination numbers as a function of solvent ratio for $Eu(OTf)_3$ (○) and $Eu(NO_3)_3$ (□) in mixtures of H_2O and THF. Experiments were performed with 7 mol % precatalyst. Water-coordination numbers of $Eu(OTf)_3$ (○) in 5, 10, 20, 30, and 40% H_2O in THF (v/v) are from reference 11c…….....……..27

Figure 2.3. Yields of the reaction shown in **Figure 2.1** catalyzed by $Eu(OTf)_3$ or $Eu(NO_3)_3$ after 48 h as a function of solvent composition. Conditions: solvent mixtures of 1 to 40% H_2O in THF (v/v) containing 7 mol % $Eu(OTf)_3$ (○) or $Eu(NO_3)_3$ (□).....28

Figure 2.4. HPLC traces of 7 mol % $Eu(OTf)_3$-catalyzed Mukaiyama aldol reaction in 10% H_2O/THF (v/v) after 2, 18, 34, 50, and 66 min. The increase in peak 3 with time corresponds to an increase in product concentration. The y-axis shows absorbance at 210 nm in arbitrary units.....29

Figure 2.5. Plot of the formation of product, **1.7**, as a function of time. Conditions: 7 mol % $Eu(OTf)_3$ in 10% H_2O/THF (v/v) after 1080, 2040, 3000, and 3960 s. The steady state reaction rate derived from this plot is the slope of the best fit line and is 1.39 $\mu M\ s^{-1}$. Error bars represent the standard error of the mean of three independently prepared samples……...……..30

Figure 2.6. Steady state reaction rates of 7 mol % $Eu(OTf)_3$- (○) or $Eu(NO_3)_3$- catalyzed (□) Mukaiyama aldol reactions in 0–40% H_2O/THF mixtures (v/v). Regression lines represent the rate dependence on anion identity and solvent composition. Note: 10% H_2O in THF (v/v) corresponds to the solvent composition at which $Eu(OTf)_3$ is saturated with water (**Figure 2.2**). Error bars represent the standard error of the mean of three independently prepared samples……...……..….31

Figure 3.1. C_2-symmetric ligands used to prepare Eu^{3+}-based precatalysts…….36

Figure 3.2. Representation of unchelated Eu^{3+} and a Eu^{3+}-containing complex of **1.14** with *q* values of 9 and 3, respectively (counteranions have been omitted for clarity). One complex is shown on the right of the equilibrium to demonstrate the point of the figure, but multiple species are likely in the actual solution…….……..41

Figure 3.3. Normalized emission spectra (λex = 395 nm) of $Eu(OTf)_3$ in EtOH/H_2O 1:9 with (dotted line) and without (solid line) 0.6 equiv of ligand **1.14**. The bands at 591 and 616 nm arise from the $^5D_0 \rightarrow {}^7F_1$ and hypersensitive $^5D_0 \rightarrow {}^7F_2$ transitions, respectively. Similar spectra were observed for the other ligands in this chapter..…42

Figure 3.4. Emission intensity ratios of Eu^{3+} (616 nm/591 nm) versus equiv of ligand for Eu^{3+} with **1.5** (△), **1.13** (▲), **1.4** (◆), **1.15** (◇), **1.16** (○), and **1.17** (□). Increases in magnitude of the emission intensity quotient (616 nm/591 nm) arise from increases in crystal field splitting of Eu^{3+}……...……43

Figure 3.5. **A**. ^{1}H-NMR spectrum of **1.14** in 9:1 EtOD/D_2O. **B**. ^{1}H-NMR spectrum of **1.14** in 9:1EtOD/D_2O at –40 °C with 0.25 equiv of $Eu(OTf)_3$. Arrows point to signals observed in the presence of a subsess of Eu^{3+} (the temperature of –40 °C was required to resolve the signals between 4 and 2 ppm). These new signals are attributed to a Eu^{3+}-L*n* (*n* > 1) species. **C**. ^{1}H-NMR spectrum of **1.14** in 9:1 EtOD/D_2O with 2 equiv of $Eu(OTf)_3$. Arrows point to signals observed in the presence of excess Eu^{3+}. The new upfield signals are attributed to a Eu^{3+} *n*-L (*n* ≥ 1) species……45

Figure 3.6. (left) Proposed selective nucleophilic attack at the *si* face of benzaldehyde (high selectivity and reactivity is observed). (middle) Precatalysts are non-selective when R is OH or NH_2. (right) Ligands **1.14–1.16** with Eu^{3+} are unable to block nucleophilic attack at either face of benzaldehyde likely due to the stereochemistry at the position of R^2 causing less blocking than with ligand **1.5**. Coordinated water has been omitted for clarity, additionally ligand **1.13** has been drawn in the carboxylic acid form although it likely exists in the deprotonated state while coordinated to Eu^{3+} in aqueous media……...48

Figure 3.7. Proposed equilibria involving multiple Eu^{3+} species with reactivity summarized under the species. This equilibria is based on luminescence-decay, steady-state luminescence measurements, and ^{1}H-NMR data with reactivity and selectivity from Mukaiyama aldol reaction results……49

LIST OF SCHEMES

Scheme 1.1. Example of a Ln^{3+}-catalyzed Mukaiyama aldol reaction……...3

Scheme 1.2. Ln^{3+}-catalyzed Mukaiyama aldol reaction used to monitor selectivity with precatalysts that use ligands **1.4** or **1.5**……...……..…..5

Scheme 1.3. Proposed aqueous lanthanide triflate-catalyzed Mukaiyama aldol catalytic cycle. Adapted with permission from P. Dissanayake and M. J. Allen, *J. Am. Chem. Soc.*, 2009, **131**, 6342. Copyright 2009 American Chemical Society.....10

Scheme 1.4. Mukaiyama aldol reaction used to study the influence of reaction rate by *q*.....11

Scheme 3.1 Aqueous Mukaiyama aldol reaction.....35

Scheme 3.2. Syntheses of ligands **1.14–1.17**……38

Scheme 3.3. Aqueous Mukaiyama aldol reaction performed with ligands **1.5** and **1.13–1.17**……..……...46

LIST OF ABBREVIATIONS

Abbreviation	Term
Ln	lanthanide
OTf	triflate
NO_3	nitrate
THF	tetrahydrofuran
EtOD	CD_3CD_2OD
calcd	calculated
equiv	equivalents
HRESIMS	high-resolution electrospray ionization mass spectrometry
HPLC	high-performance liquid chromatography
er	enantiomeric ratio
dr	diastereomeric ratio
TLC	thin layer chromatography
COSY	correlation spectroscopy
DEPT	distortionless enhancement by polarization transfer
HMQC	heteronuclear multiple-bond correlation spectroscopy

LIST OF SYMBOLS

Symbol	Name
q	number of inner-sphere water molecules
Δq	difference of water-coordination number before and after addition of substrate.
ø	dihedral angle
$\Delta\Delta G$	relative free energy
${\tau_{H_2O}}^{-1}$	luminescence decay rate in H_2O
${\tau_{D_2O}}^{-1}$	luminescence decay rate in D_2O

CHAPTER ONE

Tools for Studying Aqueous Enantioselective Lanthanide-Catalyzed Mukaiyama Aldol Reactions.

Portions of this chapter have been adapted or reprinted with permission from: (1) Averill, D. J.; Allen, M. J. *Catal. Sci. Technol.* 2014**,** in press DOI: 10.1039/C4CY01117A (2) S. Kobayashi, T. Hamada, S. Nagayama and K. Manabe, *Org. Lett.*, 2001, **3**, 165. Copyright 2001 American Chemical Society. (3) R. S. Dickens, S. Aime, A. S. Batsanov, A. Beeby, M. Botta, J. I. Bruce, J. A. K. Howard, C. S. Love, D. Parker, R. D. Peacock and H. Puschmann, *J. Am. Chem. Soc.* 2002; **124**, 12697. Copyright 2002 American Chemical Society. (4) P. Dissanayake and M. J. Allen, *J. Am. Chem. Soc.*, 2009, **131**, 6342. Copyright 2009 American Chemical Society. (5) Averill, D. J.; Dissanayake, P.; Allen, M. J. The Role of Water in Lanthanide-Catalyzed Carbon–Carbon Bond Formation. Molecules 2012, 17, 2073–2081. http://www.mdpi.com/1420-3049/17/2/2073. (6) Y. Mei, P. Dissanayake and M. J. Allen, *J. Am. Chem. Soc.* 2010, 132, 12871. Copyright 2010 American Chemical Society. (7) D. J. Averill and M. J. Allen, *Inorg. Chem.* 2014, **53**, 6257. Copyright 2014 American Chemical Society. (8) M. Hatanaka and K. Morokuma, *J. Am. Chem. Soc.* 2013, **135**, 13972.

1.1 Introduction

The trivalent lanthanide ions (Ln^{3+}) are of great importance due to their photophysical properties, Lewis acidity, stability in aqueous media, and reusability.[1] Because of these features, Ln^{3+}-based precatalysts are popular alternatives to moisture sensitive Lewis acids such as $AlCl_3$, $TiCl_4$, $SnCl_4$, and $SiCl_4$.[2] In select cases, Ln^{3+} ions

can be combined with chiral ligands to form enantioselective precatalysts for bond-forming reactions.[3] The improvement of chiral Ln-based precatalysts is limited by the need to understand reaction pathways and key precatalyst features such as metal-complex stability and coordination geometry. Toward this goal, spectroscopic measurements and computational studies have been used to unveil reaction pathways and precatalyst stabilies for carbon–carbon bond-forming reactions. This chapter is focused on developments since the turn of the century and is composed of five parts that will contextualize the work described in this thesis: (1) development of enantioselective water-tolerant lanthanide-based precatalysts for Mukaiyama aldol reactions; (2) crystal structure determination of precatalysts; (3) luminescence measurements to study Eu^{3+}-based precatalysts; (4) ^{1}H-NMR experiments to study Ln^{3+}-based precatalysts; and (5) computational studies of Mukaiyama aldol reactions. Comprehensive reviews that describe older work, non-lanthanide precatalysts, and reactions other than Mukaiyama aldol can be found elsewhere.[4]

1.2 Part 1: Development of enantioselective water-tolerant lanthanide-based precatalysts for Mukaiyama aldol reactions.

The Ln^{3+}-catalyzed Mukaiyama aldol reaction is of great interest to synthetic chemists because it is a water-tolerant carbon–carbon bond-forming reaction that can produce β-hydroxy carbonyls (**Scheme 1.1**), which are important functional groups found in and used to synthesize many biologically active compounds.[5] Further, the reaction can be carried out in aqueous media, and high enantiomeric ratios can be achieved with the use of chiral precatalysts.[3a-d,6] Recovery and reuse of Ln^{3+}-based precatalysts has been demonstrated with no significant loss of reactivity, making Ln^{3+}-based precatalysts a topic of study for sustainable chemistry applications.[7]

Scheme 1.1. Example of a Ln^{3+}-catalyzed Mukaiyama aldol reaction.

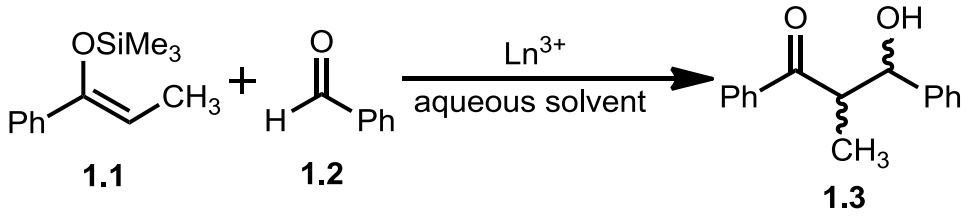

To date, several ligands have been synthesized to prepare enantioselective, water-tolerant, Ln^{3+}-based precatalysts for Mukaiyama aldol reactions.[3a-c,8] The two most effective ligands reported are hexadentate with two nitrogen and four oxygen donar atoms.[3a,c] Although ligands **1.4** and **1.5** are hexadentate and have the same donor atoms, they have different donor types and are structurally different (**Figure 1.1**).

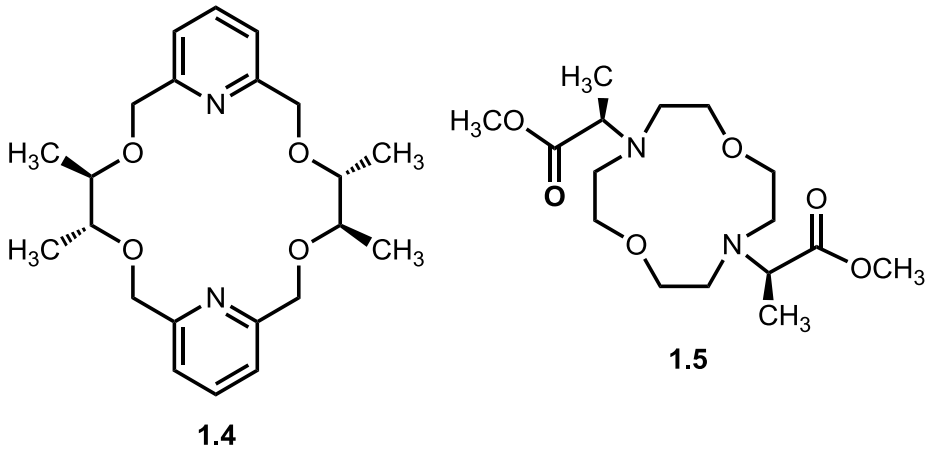

Figure 1.1. Chiral ligands used for lanthanide-catalyzed water-tolerant enantioselective Mukaiyama aldol reactions.

Precatalysts formed from lanthanide triflate salts using ligands **1.4** and **1.5** are able to stereospecifically form a range of β-hydroxy carbonyl compounds. Mukaiyama aldol reactions promoted by either **1.4** or **1.5** with $Ln(OTf)_3$ have a wide range of reactivities and selectivities. Ligand **1.4** with either $Ce(OTf)_3$ or $Pr(OTf)_3$ catalyzes a variety of Mukaiyama aldol reactions to produce different products (**Table 1.1**) with diastereoselectivities (*syn*:*anti*) ranging from 90:10 to 95:5 and enantioselectivities (*R*/*S*) ranging from 87.5:12.5 to 91.5:8.5 (**Table 1.1**). Ligand **1.5** with either $Eu(OTf)_3$ or

$Nd(OTf)_3$ was able to catalyze Mukaiyama aldol reactions with diastereoselectivities (*syn*:*anti*) ranging from 75:25 to 97.3:2.7 and enantioselectivities (*R*/*S*) ranging from 82:18 to 98:2.

Table 1.1. Aqueous enantioselective Mukaiyama aldol reaction results from reactions carried out in $EtOH/H_2O$ (9:1 v/v).

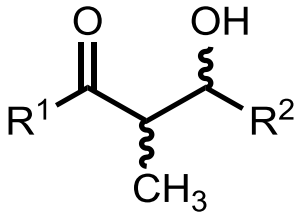

R^1	R^2	Ln^{3+}	ligand	dr[h]	er (*syn*)	T (°C)	ref
Ph	Ph	Ce^{3+a}	**1.4**[c]	93:7	91:9	0	4f
Ph	4-$CH_3OC_6H_4$	Pr^{3+b}	**1.4**[d]	92:8	87.5:12.5	0	3b
Ph	2-$CH_3OC_6H_4$	Pr^{3+b}	**1.4**[d]	95:5	91.5:8.5	0	3b
Ph	4-ClC_6H_4	Pr^{3+b}	**1.4**[d]	90:10	91.5:8.5	0	3b
Ph	1-napthyl	Pr^{3+b}	**1.4**[d]	91:9	90.5:9.5	0	3b
Ph	Ph	Eu^{3+a}	**1.5**[e]	97:3	96.5:3.5	–25	3c
Ph	4-ClC_6H_4	Eu^{3+a}	**1.5**[e]	95:5	95.5:4.5	–25	3c
Ph	4-$CH_3C_6H_4$	Eu^{3+a}	**1.5**[e]	96:4	95:5	–25	3c
Ph	$(CH_2)_5CH_3$	Eu^{3+a}	**1.5**[e]	96:4	98:2	–25	3c
Ph	Ph	Nd^{3+a}	**1.5**[c]	75:25	82:18	–25	3d
Ph	Ph	Nd^{3+a}	**1.5**[f]	95:5	95.6:4.4	–25	3d
Ph	Ph	Nd^{3+a}	**1.5**[g]	97:3	96:4	–25	3d
4-ClC_6H_4	Ph	Nd^{3+a}	**1.5**[g]	94:6	96:4	–25	3d
4-$CH_3C_6H_4$	Ph	Nd^{3+a}	**1.5**[g]	97:3	96:4	–25	3d
Ph	4-ClC_6H_4	Nd^{3+a}	**1.5**[g]	92:8	95:5	–25	3d
Ph	4-$CH_3C_6H_4$	Nd^{3+a}	**1.5**[g]	97:3	96:4	–25	3d

[a]20 mol %, [b]10 mol %, [c]24 mol %, [d]12 mol %, [e]48 mol %, [f]36 mol %, [g]42 mol %, [h](*syn*:*anti*)

An important feature of the Ln^{3+} series is the steady decrease in ionic radii from La^{3+} (103.2 pm) to Lu^{3+} (86.1 pm). This feature of the Ln^{3+} series was explored to identify the best suited Ln^{3+} ion to combine with ligands **1.4** or **1.5**.[3a,d] In a benchmark Mukaiyama aldol reaction (**Scheme 1.2**), ligand **1.4** with Ce^{3+} and ligand **1.5** with Nd^{3+} produced the highest enantioselectivites. With both ligands, small changes in Ln^{3+} size drastically affect reaction outcomes in terms of selectivity (**Figure 1.2** and **Table 1.2**). By comparison of selectivity with

Ln^{3+} ionic radius, ligand **1.4** appears to have a smaller binding pocket than ligand **1.5**, likely contributing to differences in selectivity based on substrate bulk.

Scheme 1.2. Ln^{3+}-catalyzed Mukaiyama aldol reaction used to monitor selectivity with precatalysts that use ligands **1.4** or **1.5**.

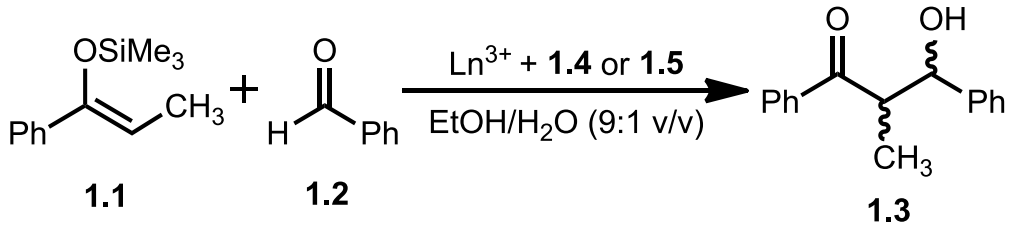

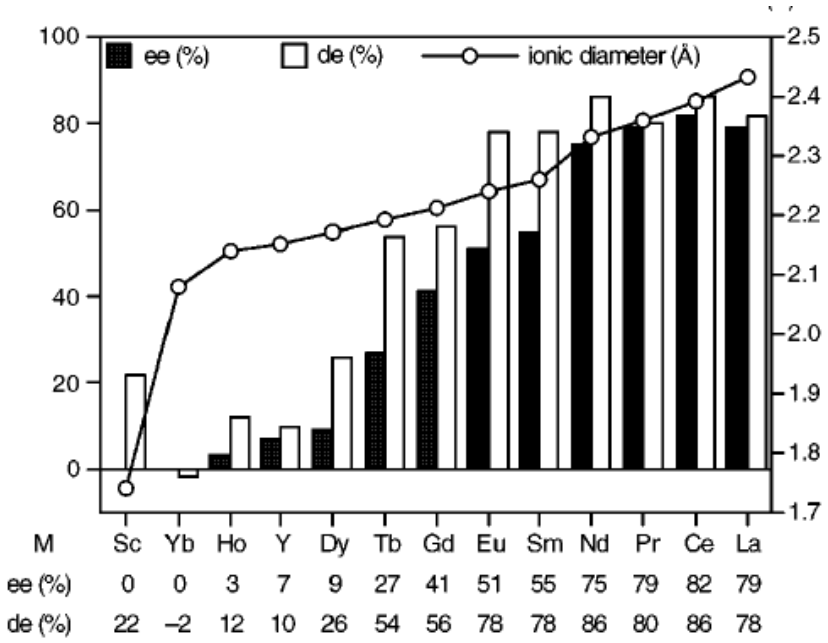

Figure 1.2. Graph of selectivity data for the reaction shown in **Scheme 1.2** using different Ln^{3+} ions and ligand **1.4**. Increased selectivity is observed as the ionic radii of Ln^{3+} increase from Yb^{3+} to Ce^{3+}. Adapted with permission from S. Kobayashi, T. Hamada, S. Nagayama and K. Manabe, *Org. Lett.*, 2001, **3**, 165. Copyright 2001 American Chemical Society.

Table 1.2. Selectivity data for the reaction shown in **Scheme 1.2** using different Ln^{3+} ions with ligand **1.5**. Selectivity is highest for ligand **1.5** and Nd^{3+}. A ligand-to-Ln^{3+} ratio of 1.2:1 was used instead of 2.4:1 so that a difference in selectivity could be observed for the different Ln^{3+} with ligand **1.5**.[3d]

Ln^{3+}	Ln^{3+} radius (pm)	*syn*:*anti*	er (*syn*)
La^{3+}	103.2	1.7:1	52:48
Ce^{3+}	102	1.8:1	60:40
Pr^{3+}	99	2.2:1	74:26
Nd^{3+}	98.3	3.0:1	82:18
Sm^{3+}	95.8	2.1:1	58:42
Eu^{3+}	94.7	2.4:1	75:25
Gd^{3+}	93.8	2.7:1	74:26
Tb^{3+}	92.3	2.5:1	72:28
Dy^{3+}	91.2	2.0:1	64:36
Ho^{3+}	90.1	1.9:1	59:41
Er^{3+}	89.0	1.8:1	58:42
Tm^{3+}	88.0	1.5:1	53:47
Yb^{3+}	86.8	1.3:1	50:50
Lu^{3+}	86.1	1.4:1	51:49

Although high enantio- and diastereoselectivities can be observed for the water-tolerant Mukaiyama aldol reaction using Ln^{3+} ions with ligands **1.4** or **1.5**, reaction times are long and high ligand loadings are required.[3a-d] These limitations have prompted structural investigations of Ln^{3+}-based precatalysts to learn more about the precatalysts and the mechanism of the reaction. Due to the labile nature of Ln^{3+} complexes in aqueous media, details about Ln^{3+}–ligand interactions, substrate–precatalyst interactions, and transition state modeling likely will assist in future development of Ln^{3+}-based precatalysts.

1.3 Part 2: Crystal structure determination of precatalysts.

X-ray crystal structures are useful for determining relative orientation of ligands that surround Ln^{3+} ions and information related to ligand–metal interactions.[3a,9] A crystal structure of ligand **1.4** with $Pr(NO_3)_3$ (**Figure 1.3**) was solved, and it was found that Pr^{3+} and **1.4** bind in a 1:1 ligand-to-metal stoichiometry and that Pr^{3+} is nearly in the plane of

the ring. Further, the structure revealed that the methyl groups are in the axial positions likely forcing the stereochemical outcomes of reactions performed with this precatalyst. Ligand-to-metal binding stoichiometries and geometries of a chiral Tb^{3+} complex were studied by solving crystal structures in the presence of excess citrate, lactate, glycinate, and serinate anions (**Figure 1.4**).[9b] The complex was used as a precatalyst for enantioselective nitroaldol reactions.[3e] Crystal structures are helpful for the development of precatalysts because they enable rational modifications to the geometry of precatalysts by changing ligands that surround the metal center.

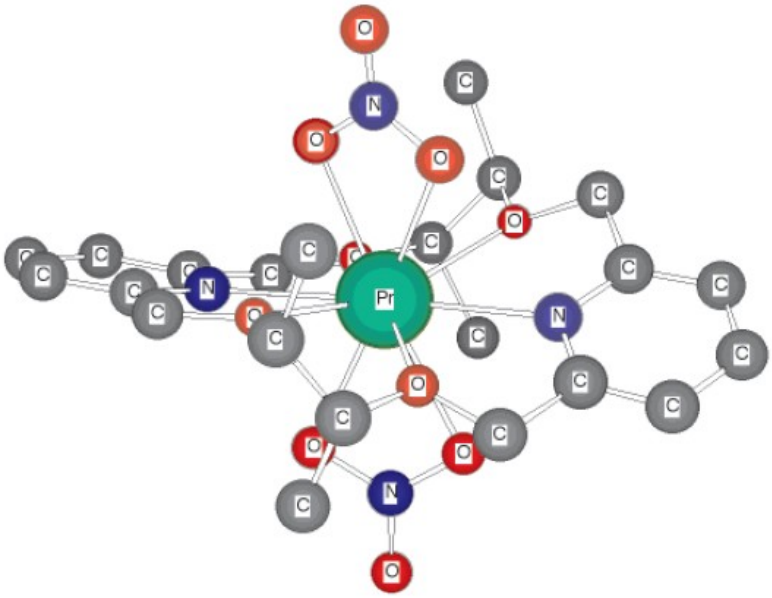

Figure 1.3. X-ray crystal structure of $[Pr(NO_3)_2 \cdot \mathbf{1.4}]^+$. Hydrogen atoms have been omitted for clarity. Adapted with permission from S. Kobayashi, T. Hamada, S. Nagayama and K. Manabe, *Org. Lett.*, 2001, **3**, 165. Copyright 2001 American Chemical Society.

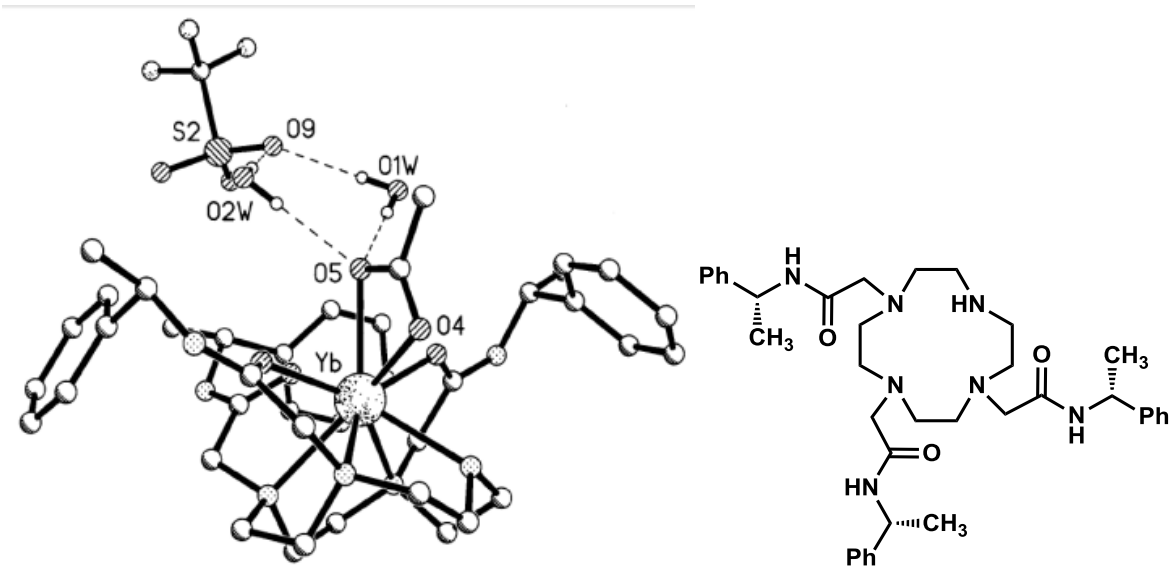

Figure 1.4. (left) X-ray crystal structure of Yb^{3+}-based precatalyst showing a distant triflate anion and chelated acetate moiety with its hydrogen bonding interactions to nearby water molecules. The macrocycle is 1, 4, 7, 10-tetraazacyclododecane, and it has methyl and phenyl substitutions on its three pendant sidearms that are coordinated to Yb^{3+}. Reprinted with permission from R. S. Dickens, S. Aime, A. S. Batsanov, A. Beeby, M. Botta, J. I. Bruce, J. A. K. Howard, C. S. Love, D. Parker, R. D. Peacock and H. Puschmann, *J. Am. Chem. Soc.* 2002; **124**, 12697. Copyright 2002 American Chemical Society. (right) Ligand used for Yb^{3+} complex shown on the left.

1.4 Part 3: Luminescence measurements to study Eu^{3+}-based precatalysts.

A widely used technique to study the number of metal-bound water molecules (q) of contrast agents for magnetic resonance imaging was adapted to study Eu^{3+}-based precatalysts in aqueous media.[10] The technique is based on a series of empirically derived equations, similar to **Eq 1.1**, that were derived by measuring the differences of luminescence-decay rates of crystalline Eu^{3+}-containing complexes with known q values.[11] Inner-sphere oscillators other than water are accounted for with correction constants where n_{OH} is the number of inner-sphere alcoholic O–H oscillators, n_{NH} is the number of inner-sphere amine N–H oscillators, and $n_{O=CNH}$ is the number of inner-sphere

amide N–H oscillators. The uncertainty of this equation is ±0.1 water molecules.[11a] A detailed review of the derivation and theory of these equations can be found elsewhere.[12]

Eq 1.1 $q = 1.11[\tau_{H_2O}^{-1} - \tau_{D_2O}^{-1} - 0.31 + 0.45\mathrm{n_{OH}} + 0.99\mathrm{n_{NH}} + 0.075\mathrm{n_{O=CNH}}]$

To gain mechanistic insight into the aqueous Ln^{3+}-catalyzed Mukaiyama aldol reaction, **Eq 1.1** was used to calculate the number of Eu^{3+}-bound water molecules at different stages of the catalytic cycle of the Mukaiyama aldol reaction (**Scheme 1.3**). The study was carried out in mixtures of THF and water. THF was chosen as a cosolvent because it does not have O–H or N–H oscillators that would complicate the measurements. By presynthesizing the reaction product, the coordination environment of Eu^{3+} was studied in four different scenarios: (1) $Eu(OTf)_3$ with no starting materials; (2) $Eu(OTf)_3$ with silyl enol ether; (3) $Eu(OTf)_3$ with benzaldehyde; and (4) $Eu(OTf)_3$ with product. Values of q were calculated q for Eu^{3+} in all four scenarios. The water-coordination number calculations revealed that benzaldehyde was able to displace coordinated water and that ability changes as a function of solvent composition. Additionally, neither the silyl enol ether nor the product was able to displace Eu^{3+}-coordinated water molecules, and consequently, product inhibition is not likely to occur for the reaction in question. These results are important because they provide mechanistic details about the aqueous lanthanide-catalyzed Mukaiyama aldol reaction and a route to study other reactions that use Eu^{3+}-based precatalysts.

Scheme 1.3. Proposed aqueous lanthanide triflate-catalyzed Mukaiyama aldol catalytic cycle. Adapted with permission from P. Dissanayake and M. J. Allen, *J. Am. Chem. Soc.*, 2009, **131**, 6342. Copyright 2009 American Chemical Society.

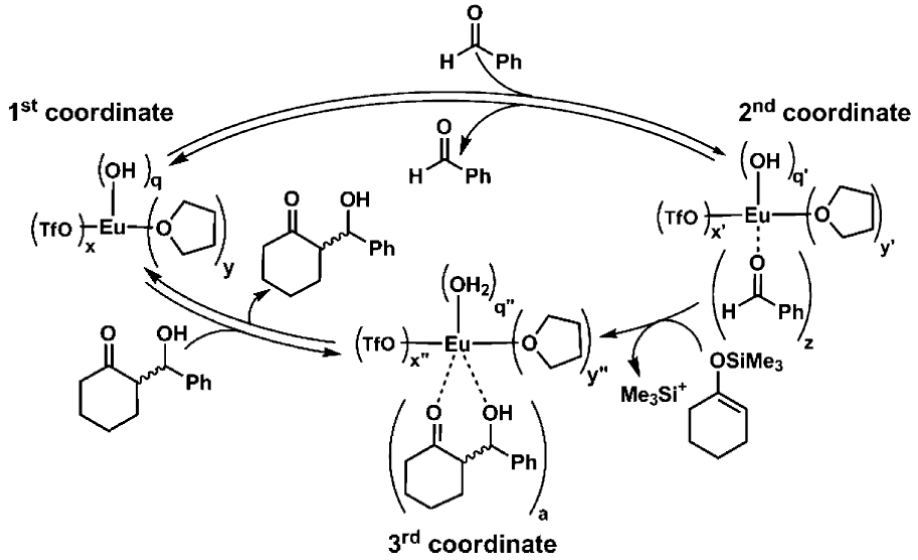

By measuring q and monitoring rates of Mukaiyama aldol reactions that use either $Eu(OTf)_3$ or $Eu(NO_3)_3$ precatalysts in solvent systems containing between 1 and 40% H_2O in THF (**Scheme 1.4**), We (Prabani Dissanayake, a graduate student in the Allen lab and I) found that reactivity increases with increased q (as a general trend, q increases with water concentration for $Eu(NO_3)_3$ and $Eu(OTf)_3$) for Eu^{3+}-based precatalysts (**Figure 1.5**).[13] More details about this discovery will be described in Chapter 2. This discovery is important because future Eu^{3+}-based precatalysts can be designed in a way that increases their reactivity by taking advantage of ligand features such as denticity and electron donating ability.

To gain insight into factors that affect the selectivity and reactivity of Ln^{3+}-based precatalysts, six variations of ligand **1.5** were combined with Eu^{3+} (**Figure 1.6**).[3c] Luminescence-decay measurements were used to study changes of q (Δq) of ligand–Eu^{3+} systems in the absence and presence of benzaldehyde. Additionally, reactivities of each precatalyst were compared by differences in isolated yields and enantiomeric ratios were determined by chiral high performance liquid chromatography analyses (**Table 1.3**).

Scheme 1.4. Mukaiyama aldol reaction used to study the influence of reaction rate by *q*.[13]

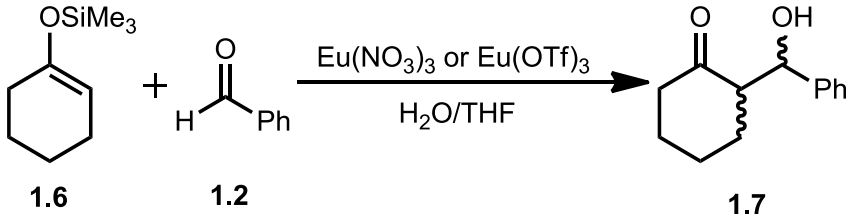

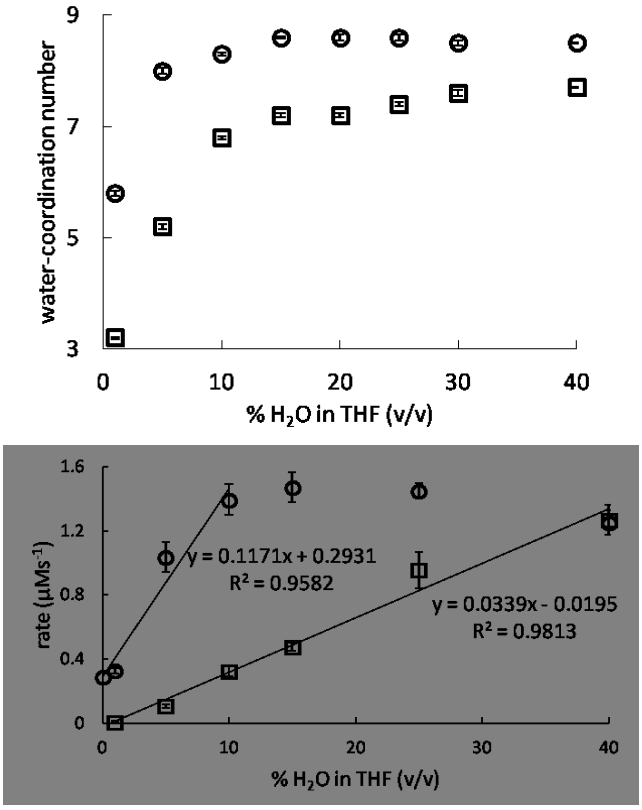

Figure 1.5. Top, Water-coordination number of $Eu(OTf)_3$ (○), and $Eu(NO_3)_3$ (□) as a function of % H_2O in THF (v/v). Error is represented by standard error of the mean of between 3 and 9 measurements. Bottom, Steady-state reaction rates of 7 mol % $Eu(OTf)_3$-(○) or $Eu(NO_3)_3$-catalyzed (□) Mukaiyama aldol reactions in 0–40% H_2O in THF (v/v). Regression lines represent the dependence of rate on solvent composition and anion identity. Reprinted with permission by Averill, D. J.; Dissanayake, P.; Allen, M. J. The Role of Water in Lanthanide-Catalyzed Carbon–Carbon Bond Formation. Molecules 2012, 17, 2073–2081. http://www.mdpi.com/1420-3049/17/2/2073.

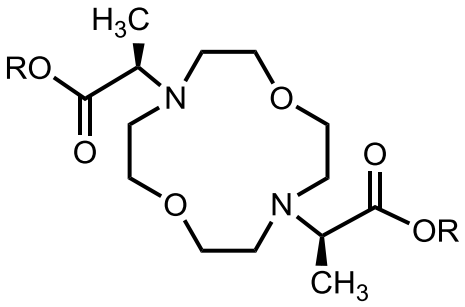

ligand	**1.5**	**1.8**	**1.9**	**1.10**	**1.11**	**1.12**	**1.13**
R	CH_3	C_2H_5	*n*-C_3H_7	*n*-C_4H_9	*i*-Pr	*t*-Bu	H

Figure 1.6. Hexadentate ligands used to study changes in selectivity and reactivity based on ligand identity.

Table 1.3. Selectivity, reactivity, and coordination changes among different Eu^{3+}-based precatalysts using the ligands from **Figure 1.6**.[3c]

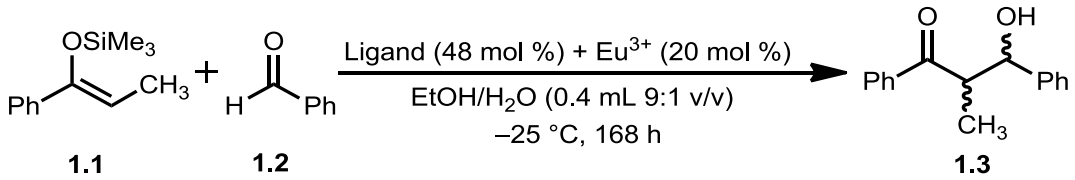

ligand	Δq	yield (%)	er (*syn*)
1.5	–0.68	92	96.5:3.5
1.8	–0.40	82	92.5:7.5
1.9	–0.45	83	93:7
1.10	–0.49	83	93.5:6.5
1.11	–0.19	20	90:10
1.12	–0.14	18	75.5:24.5
1.13	–0.09	8	0

Yields for Mukaiyama aldol reactions catalyzed by ligands **1.5** and **1.8**–**1.10** with Eu^{3+} were good (>80%) while ligands **1.11**–**1.13** with Eu^{3+} had low yields (≤20%).[3c] These results indicate that complexes with a greater propensity to exchange coordinated water for benzaldehyde, Δq, (**Figure 1.7**) are more reactive than complexes that are less influenced by benzaldehyde. Additionally, ligands with branched ester groups (R = *i*-Pr or *t*-Bu) gave low yields. These results are likely related to the reduced chance of

benzaldehyde displacing Eu^{3+}-coordinated water. Surprisingly, Eu^{3+} and ligand **1.13** (R = H) resulted in a low yield (8%) and a Δq of only –0.09. The reduction in reactivity and Δq are likely due to differences in Lewis acidity of Eu^{3+} caused by the carboxylic acid sidearms of **1.13** vs the ester sidearms of ligands **1.5** and **1.8–1.13**. Enantioselectivity was not observed for **1.13** with Eu^{3+} and that is not surprising because there is no bulky "R" group to selectively block incoming nucleophiles (**Figure 1.8**). Based on q and selectivity data, for selectivity to occur in Mukaiyama aldol reactions catalyzed by ligands **1.5** and **1.8–1.13** with Eu^{3+}, the ester sidearm must block the incoming nucleophilic attack at only one side of the coordinated aldehyde.

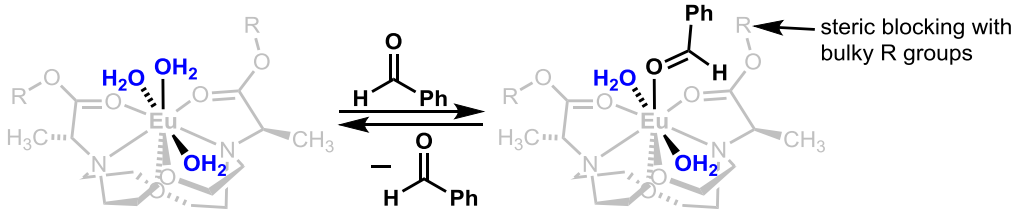

Figure 1.7. Proposed equilibrium leading to the activation and selective nucleophilic attack of benzaldehyde. Adapted with permission from Y. Mei, P. Dissanayake and M. J. Allen, *J. Am. Chem. Soc.* 2010, 132, 12871. Copyright 2010 American Chemical Society.

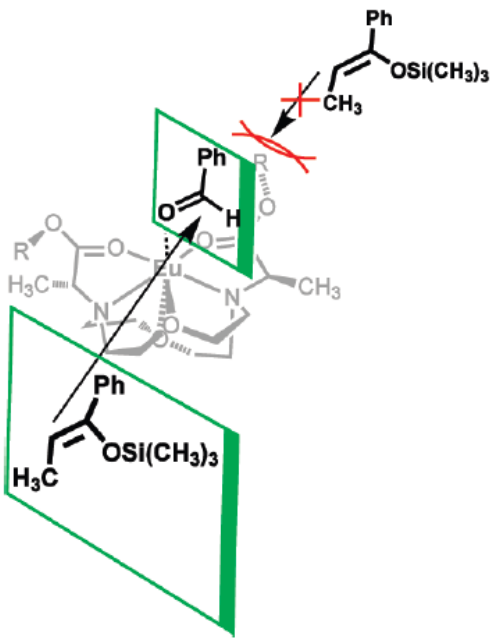

Figure 1.8. Proposed transition state for the asymmetric Mukaiyama aldol reaction using hexadentate ligands **1.5** and **1.8**–**1.13** and Eu^{3+} as a precatalyst. Adapted with permission from Y. Mei, P. Dissanayake and M. J. Allen, *J. Am. Chem. Soc.* 2010, 132, 12871. Copyright 2010 American Chemical Society.

We studied the interactions between six hexadentate ligands (**Figure 1.9**) and Eu^{3+} to learn about changes in relative Eu^{3+} binding strengths as a function of chiral center location, bulk, and sidearm donor type (ester, carboxylic acid, alcohol, and amide) using luminescence-decay measurements.[8b] Water-coordination numbers were measured at different ligand-to-metal ratios (**Table 1.4**), and it was found that Eu^{3+} is coordinatively saturated (**Figure 1.10**) in the presence of excess hexadentate ligands (q = 0). By comparing q data with yields, we concluded that binding Eu^{3+} with hexadentate ligands likely slows Mukaiyama aldol reactions. These observations are in agreement with earlier studies,[3a,13] and they are helpful for the future design of water-tolerant enantioselective Ln^{3+}-based precatalysts because ligands must minimize unbound Ln^{3+} while avoiding deactivation of Ln^{3+}. Chapter 3 contains a detailed description of these findings.

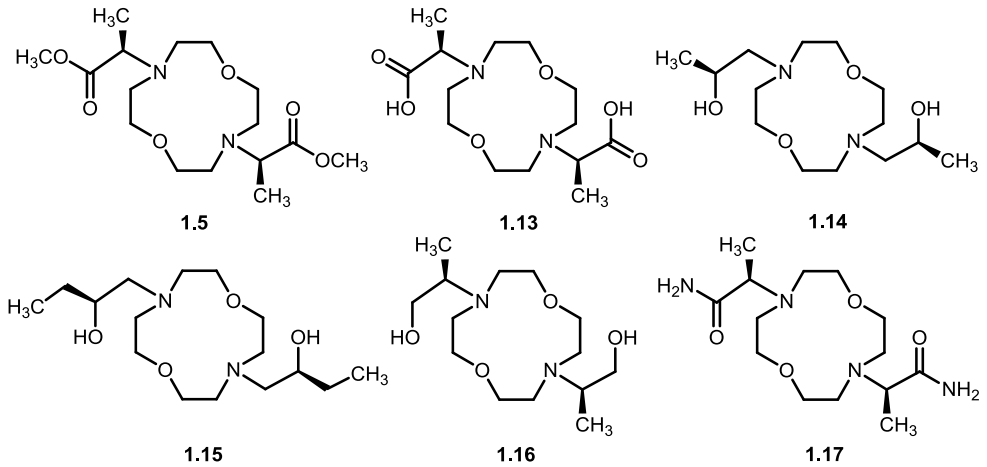

Figure 1.9. Hexadentate ligands studied in the presence of Eu^{3+}.[8b]

Table 1.4. Water-coordination numbers for Eu^{3+} with ligands **1.5** and **1.13**–**1.17**.[8b]

ligand	$q^{a,d,g}$	$q^{a,e,g}$	$q^{b,d,g}$	$q^{b,e,g}$	$q^{c,d,g}$	$q^{c,e,g}$
1.5[f]	3.5	3.5	2.1	2.1	1.4	1.4
1.13[f]	2.2	2.2	0.8	0.8	0.0	0.0
1.14	2.2	1.1	2.0	1.0	1.1	0.0
1.15	1.9	0.8	1.8	0.8	nd	nd
1.16	2.1	1.0	2.1	1.0	0.5	0.0
1.17	3.8	3.4	3.0	2.6	1.7	1.3

[a]Ligand-to-metal ratio of 1:1. [b]Ligand-to-metal ratio of 2:1. [c]Ligand-to-metal ratio of 6:1. [d]Calculated for complexes with Eu^{3+} coordination by one ligand. [e]Calculated for complexes with Eu^{3+} coordination by two ligands. [f]Ligands **1.5** and **1.13** do not have chelator-based inner-sphere O–H or N–H oscillators; therefore, $q^d = q^e$. nd = not determined. [g]The error associated with water-coordination number determination is ±0.1 water molecules.

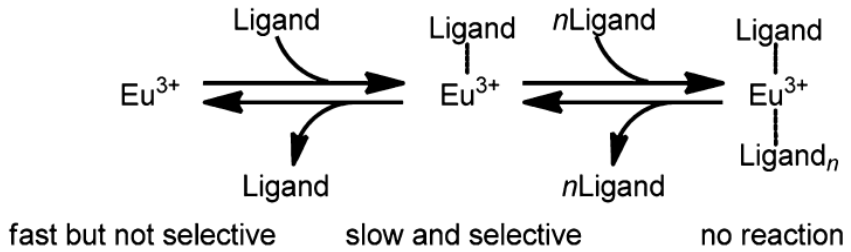

Figure 1.10. Proposed equilibria involving multiple Eu^{3+} species. Reprinted with permission from D. J. Averill and M. J. Allen, *Inorg. Chem.* 2014, **53**, 6257. Copyright 2014 American Chemical Society.

Steady-state luminescence measurements can be used as a supplemental technique to q measurements for the rapid (seconds) analysis of changes in Eu^{3+} coordination environments.[1d,1e,4a,4b] Eu^{3+} emission spectra can be highly sensitive to changes in

coordination environment (**Figure 1.11**). Therefore, luminescence measurements can be used to study changes in Eu^{3+} coordination environments. Comparison of the $^5D_0 \rightarrow {}^7F_1$ (~591 nm) and $^5D_0 \rightarrow {}^7F_2$ (~616 nm) transitions of Eu^{3+} is a useful tool for the ratiometric monitoring ligand-to-Eu^{3+} titrations.[14] Ligand-to-metal titrations were monitored by plotting the ratio of Eu^{3+} emission intensity at 616 nm divided by the emission intensity at 591 nm [($^5D_0 \rightarrow {}^7F_2$)/($^5D_0 \rightarrow {}^7F_1$)] as a function of ligand-to-metal ratio for ligands **1.5** and **1.13**–**1.17** (**Figure 1.12**). Steady-state luminescence measurements do not provide *q* values, but they enable monitoring changes in coordination environment by avoiding the need to obtain luminescence-decay rates in deuterated solvent systems. Chapter 3 has an in-depth description of the findings and methods used to study Eu^{3+} coordination. We found the use of steady-state luminescence measurements to be a great tool for studying changes in Eu^{3+} coordination during ligand-to-Eu^{3+} titrations.

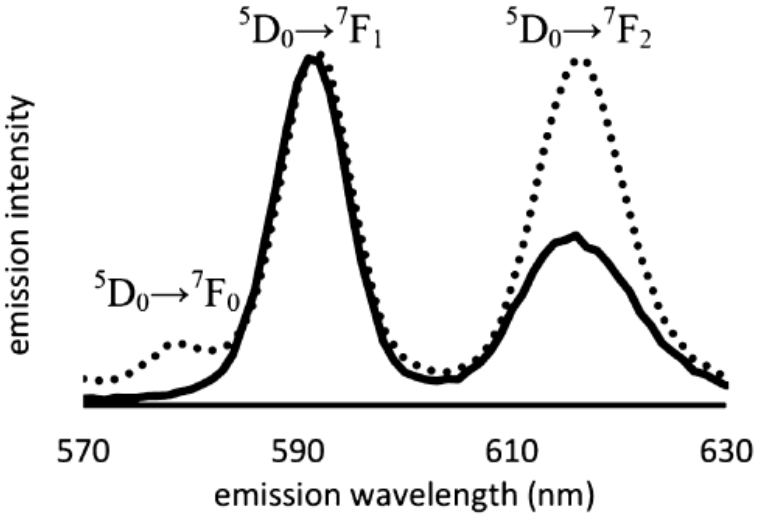

Figure 1.11. Emission spectra of $Eu(OTf)_3$ in 9:1 $EtOH/H_2O$ with (dotted line) and without (solid line) a hexadentate ligand. Adapted with permission from D. J. Averill and M. J. Allen, *Inorg. Chem*. 2014, **53**, 6257. Copyright 2014 American Chemical Society.

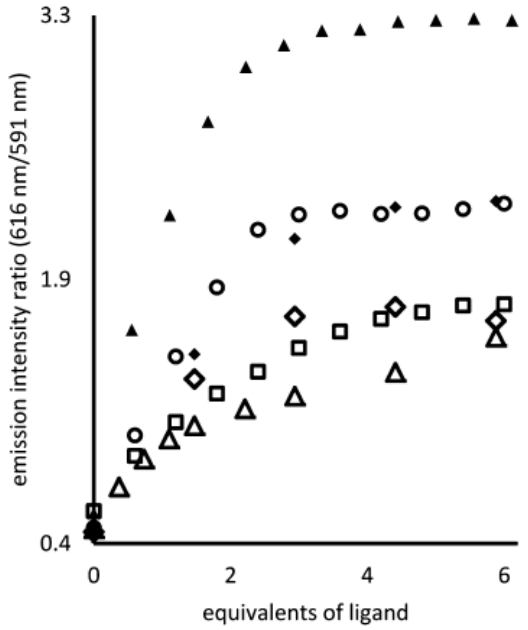

Figure 1.12. Emission intensity ratios of Eu^{3+} (616 nm/591 nm) versus equivalents of ligand for Eu^{3+} with **1.5** (△), **1.13** (▲), **1.14** (◆), **1.15** (◇), **1.16** (○), and **1.17** (□). Increases in magnitude of the emission intensity quotient (616 nm/591 nm) arise from increases in crystal field splitting of Eu^{3+}. Adapted with permission from D. J. Averill and M. J. Allen, *Inorg. Chem*. 2014, **53**, 6257. Copyright 2014 American Chemical Society.

1.5 Part 4: ^{1}H-NMR experiments to study Ln^{3+}-based precatalysts.

In addition to Eu^{3+} luminescence measurements for the study of structural features of Ln^{3+}-based precatalysts, ^{1}H-NMR studies have been used.[3a,e,8b] Changes in ligand environment can be found by monitoring ^{1}H-NMR spectra of ligands in the absence of Ln^{3+} and presence of varying amounts of Ln^{3+}. Kobayashi and co-workers used ^{1}H-NMR studies to investigate ligand **1.4** in the presence of $La(OTf)_3$. By changing ligand-to-metal stoichiometries and comparing ^{1}H-NMR spectra, they found that ligand **1.4** binds to La^{3+} tightly (only scarce amounts of free **1.4** were observed in the ^{1}H-NMR spectra).[3a] From ^{1}H-NMR experiments, it was found (details can be found in Chapter 3) that at least three distinct species can exist in solution when Eu^{3+} is combined with ligands **1.5**, **1.13**–**1.17** (**Figure 1.13**) and the ratio of these species is influenced by ligand-to-Eu^{3+} ratios.[8b] The

findings are important because Le Chatelier's principle can be followed to drive the equilibrium system towards selective precatalysts (one hexadentate ligand per Ln^{3+} ion). ^{1}H-NMR experiments have the ability to provide valuable information about ligand environments that compliment Eu^{3+} luminescence measurements.

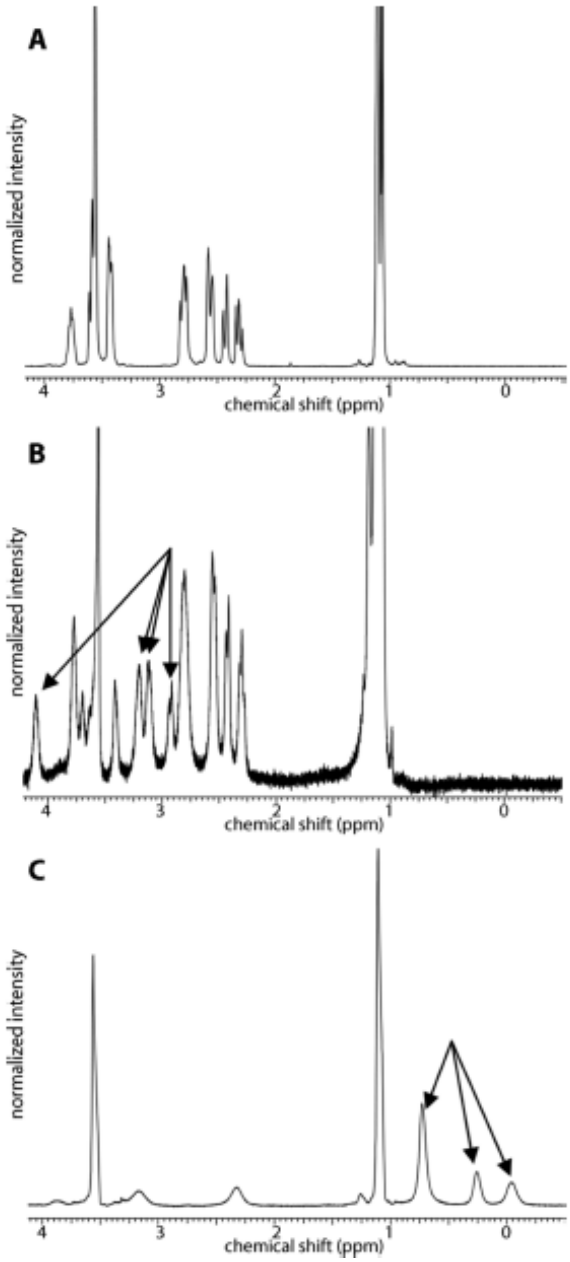

Figure 1.13. (A) ^{1}H-NMR spectrum of **1.14** in 9:1 EtOD/D_2O. (B) ^{1}H-NMR spectrum of **1.14** in 9:1 EtOD/D_2O at –40 °C with 0.25 equiv of $Eu(OTf)_3$. Arrows point to signals observed in the presence of excess ligand (the temperature of –40 °C was required to resolve the signals between 4 and 2 ppm). These new signals are attributed to a Eu^{3+}–L_n (n > 1) species. (C) ^{1}H-NMR spectrum of **1.14** in 9:1 EtOD/D_2O with 2 equiv of $Eu(OTf)_3$. Arrows point to signals observed in the presence of excess Eu^{3+}. The new upfield signals are attributed to $Eu^{3+}{}_n$–L ($n \geq 1$) species. Adapted with permission from D. J. Averill and M. J. Allen, *Inorg. Chem.* 2014, **53**, 6257. Copyright 2014 American Chemical Society.

1.6 Part 5: Computational studies of Mukaiyama aldol reactions.

Computational studies of Ln^{3+}-catalyzed Mukaiyama aldol reactions can provide details about the reaction mechanism that are not readily accessible by X-ray crystal structures, luminescence measurements, or NMR experiments. Recently, Morokuma and co-workers reported two computational studies that are based on the reaction in **Scheme 1.4**.[15] The studies were focused on transition states of the reaction to learn about diastereoselectivity and the changes in free energy of Eu^{3+} complexes depending on coordination environment. To study transition states of Mukaiyama aldol reactions, the Morokuma group used a computational technique called artificial force-induced reaction to explore approximate reaction pathways that start from dissociation limits or local minima.[15a] By studying the C–C–C–O dihedral angles (ϕ), they found that the reaction shown in **Scheme 1.4** may have as many as 17 different transition states that are within 2 kcal/mol of each other (**Table 1.5**). It is worth noting that four of the five most likely transition states are for reactions that result in *syn* products. The authors suggest that this low energy difference for transition states leads to the low diastereoselectivity of Mukaiyama aldol reactions.

Table 1.5. Relative free energies, key structural parameters, and existence probability of lower transition states, with ΔΔG less than 2 kcal/mol.[15a]

transition states	ΔΔ*G* (kcal/mol)	ϕ (deg)	product	existence probability (%)
1	0.00	180.6	*syn*	20.85
2	0.28	180.6	*syn*	12.94
3	0.40	53.1	*anti*	10.59
4	0.45	49.0	*syn*	9.73
5	0.85	161.3	*syn*	4.96
6	0.86	180.2	*syn*	4.89
7	0.97	55.0	*syn*	4.02
8	1.16	298.2	*syn*	2.92
9	1.27	51.2	*anti*	2.46
10	1.28	174.5	*anti*	2.41
11	1.28	291.1	*anti*	2.41
12	1.28	176.0	*anti*	2.38
13	1.30	178.1	*syn*	2.32
14	1.44	166.4	*syn*	1.84
15	1.56	59.2	*syn*	1.50
16	1.58	161.6	*syn*	1.44
17	1.73	182.9	*anti*	1.12

In addition to investigating factors that affect selectivity of Mukaiyama aldol reactions, the Morokuma group studied factors that affect reactivity.[15b] By dissecting the reaction into fragments (**Figure 1.14**), they were able to calculate the free energy of transition states that are likely to take place during the course of the reaction (**Figure 1.15**). These results are helpful because they support a reaction mechanism that is based on minimal energy pathways. The Morokuma group reported that the reaction begins with a Eu^{3+}-coordinated benzaldehyde followed by C–C bond formation between the silyl enol ether (**1.6**) and the coordinated aldehyde (**1.2**). They calculated that a series of proton transfers occurs after the C–C bond formation and finally the silyl group dissociates after nucleophilic attack from a water molecule as shown in **Figure 1.15**. The computational studies reviewed here contribute to the further understanding of factors that influence rates and selectivity of Mukaiyama aldol reactions. Studies of this nature can be used in

the future to aid in the development of selective catalysts for Ln^{3+}-catalyzed bond forming reactions.

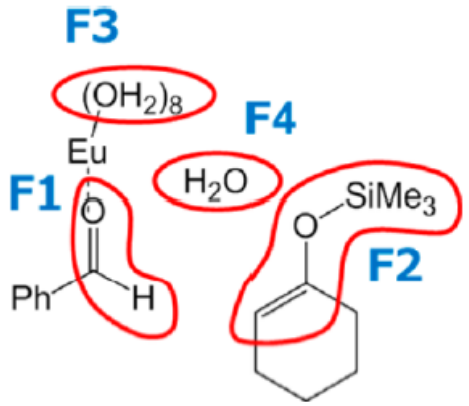

Figure 1.14. Fragments F1, F2, F3, and F4 used by Morokuma and co-workers to study the Mukaiyama aldol reaction by the artificial force-induced reaction method. Reprinted with permission from M. Hatanaka and K. Morokuma, *J. Am. Chem. Soc.* 2013, **135**, 13972.

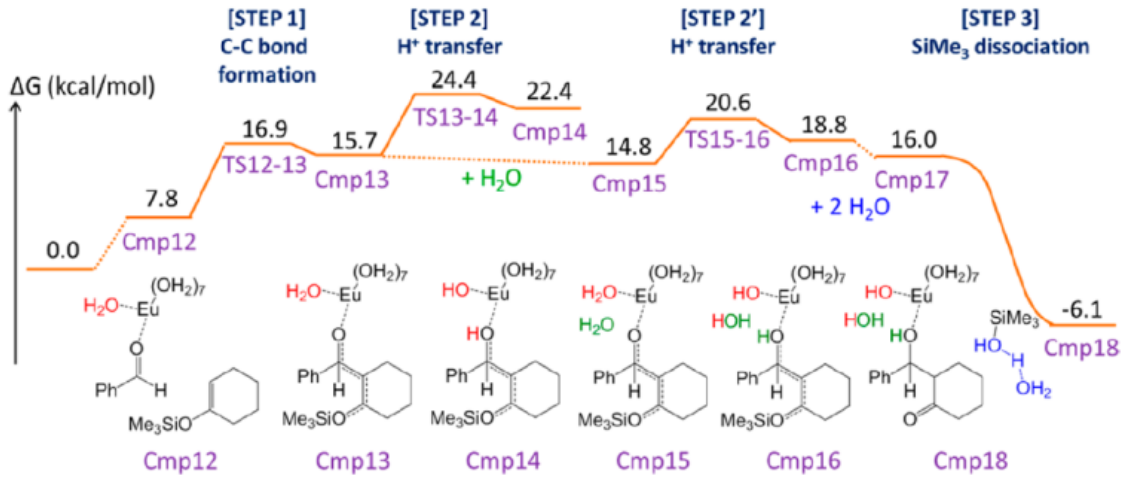

Figure 1.15. Reaction pathway as calculated by the artificial force-induced reaction method. Reprinted with permission from M. Hatanaka and K. Morokuma, *J. Am. Chem. Soc.* 2013, **135**, 13972.

1.7 Thesis context

Chapter 1 served to put our studies into context with respect to prior and current work in the field of precatalyst development for stereospecific water-tolerant lanthanide-catalyzed bond-forming reactions. As pointed out in this chapter, chapters 2 and 3 of this dissertation are detailed accounts of the studies that were performed with respect to studying lanthanide-catalyzed reactions. Finally, Chapter 4 will begin with a brief summary of our findings and end with the future outlook of this project. The recent developments that were outlined in this chapter have made the study of Ln^{3+} precatalysts more accessible, and tools like luminescence and NMR spectroscopy have made these developments possible.

CHAPTER TWO

The Role of Water in Lanthanide-Catalyzed Carbon–Carbon Bond Formation.

Portions of chapter two have been adapted or reprinted with permission from Averill, D. J.; Dissanayake, P.; Allen, M. J. The Role of Water in Lanthanide-Catalyzed Carbon–Carbon Bond Formation. *Molecules*, **2012**, *17*, 2073–2081.

2.1 Introduction

Some of the most important transformations in organic chemistry result in the formation of carbon–carbon and carbon–heteroatom bonds, and both of these bonds can be formed using lanthanide triflate [$Ln(OTf)_3$]-containing precatalysts.[1j,3b,3c,16] Lanthanide triflates are reusable, easy-to-handle, and can function as strong Lewis acids in both aqueous and non-aqueous solvent mixtures.[1j] Water-tolerant Lewis acid catalysts are advantageous relative to water-sensitive catalysts because water-tolerant Lewis acids eliminate the need to rigorously dry solvents before use. Consequently, the Lewis-acidic and water-tolerant features of lanthanide(III) salts have aroused much interest in aqueous lanthanide-catalyzed bond-forming reactions.[1j,3b,3c,16a–16c] The Mukaiyama aldol reaction between a silyl enol ether and an aldehyde was studied because the reaction can be both water-tolerant and stereoselective, making it an important carbon–carbon bond-forming reaction (**Figure 2.1**).[3b,3c,6d,17]

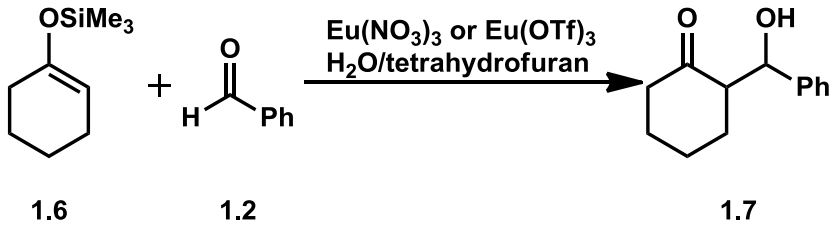

Figure 2.1. The water-tolerant Mukaiyama aldol reaction between silyl enol ether **1.6**, and benzaldehyde **1.2**, studied in this work.

We hypothesized that the water-coordination numbers of lanthanide-based precatalysts influenced the reaction rate and final yield of this reaction. In aqueous solution, lanthanide(III) ions have relatively fast inner-sphere water-exchange rates (~10^8 s^{-1}),[18] and each site of exchanging water represents a potential site for benzaldehyde coordination. We hypothesized that a larger water-coordination number would result in greater probability for aldehyde coordination and, consequently, a faster reaction rate because bound aldehyde, **1.2**, is activated for nucleophilic attack by enol ether, **1.6** (**Figure 2.1**). The Allen lab has previously reported the use of luminescence-decay measurements to monitor the average water-coordination number of $Eu(OTf)_3$ in mixtures of water with organic co-solvents in the presence and absence of substrates.[10,11c] This chapter contains a description of efforts to contribute to the mechanistic understanding of the aqueous lanthanide-catalyzed Mukaiyama aldol reaction by correlating the water-coordination numbers of europium-based precatalysts with steady state reaction rates. Further, a description of the influence of europium counteranions on reaction yields and steady state reaction rates is included.

2.2 Results and Discussion

Water-coordination numbers were determined using measured luminescence-decay rates with **Equation 2.1**, where ${\tau_{H_2O}}^{-1}$ and ${\tau_{D_2O}}^{-1}$ represent the measured decay rates in H_2O and

D_2O, respectively; q represents the average water-coordination number; and α accounts for the influence of non-coordinated molecules on luminescence decay.[11c] We found the average water-coordination numbers of the studied europium salts in H_2O/THF mixtures ranging from 1 to 40% H_2O in THF (v/v) to be between 3.2 and 8.6 water molecules (**Figure 2.2**, **Table 2.1**). These values are in agreement with previous lanthanide-coordination studies which show a maximum coordination number between 8 and 9.[1f,10,11c]

Eq 2.1 $q = 1.2\left[\left(\tau_{H_2O}{}^{-1} - \tau_{D_2O}{}^{-1}\right) - \alpha\right]$

We hypothesized that $Eu(NO_3)_3$ should have lower catalytic activity than $Eu(OTf)_3$, an effective Lewis acid precatalyst, because of its lower water-coordination numbers. By studying $Eu(OTf)_3$ and $Eu(NO_3)_3$, we were able to assess the effects of counteranions on the catalytic activity of europium. These precatalysts were chosen because the water-coordination numbers of europium ions in aqueous solutions are influenced by the composition of the solvent and the identity of the counteranions (**Figure 2.2**). Due to the limited water solubility of **1.6**, we were unable to study **1.6** at water percentages of greater than 40% H_2O in THF (v/v). To test our hypothesis that water-coordination numbers influence the steady state reaction rate and final yield of this reaction, the yields of $Eu(OTf)_3$- and $Eu(NO_3)_3$-catalyzed Mukaiyama aldol reactions were measured after 48 h in solvent mixtures ranging from 1 to 40% H_2O in THF (v/v) (**Figure 2.3**). Yields were measured after 48 h because $Eu(NO_3)_3$-catalyzed reactions in 1, 5, and 10% H_2O in THF (v/v) required longer than 24 h to reach completion. As shown in **Figure 2.3**, $Eu(OTf)_3$- and $Eu(NO_3)_3$-catalyzed Mukaiyama aldol reactions afforded the highest yields at 5 and 15% H_2O in THF (v/v), respectively. Interestingly, 5 and 15% H_2O in THF (v/v) roughly correspond to the solvent composition at which increasing the H_2O concentration has the least effect on the water-coordination number for both $Eu(OTf)_3$ and $Eu(NO_3)_3$ (**Figure 2.2**).

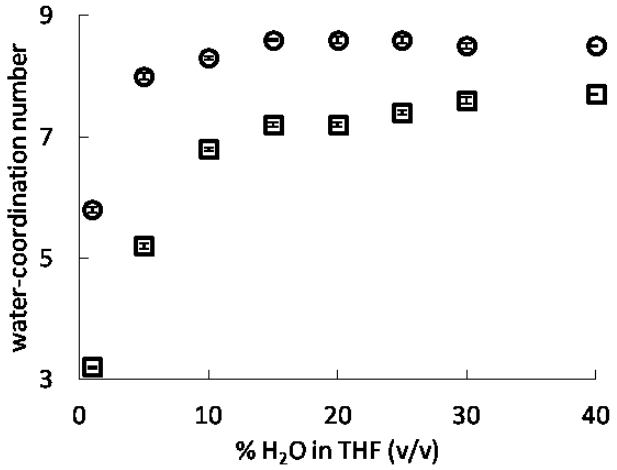

Figure 2.2. Water-coordination numbers as a function of solvent ratio for $Eu(OTf)_3$ (○) and $Eu(NO_3)_3$ (□) in mixtures of H_2O and THF. Water-coordination numbers of $Eu(OTf)_3$ (○) in 5, 10, 20, 30, and 40% H_2O in THF (v/v) are from reference.[11c] Error bars represent the standard error of the mean of between three and nine independent measurements. A list of *q* values and standard error of the mean can be found in **Appendix A**.

Table 2.1. Mean water-coordination numbers (*q*) of (a) $Eu(OTf)_3$ and (b) $Eu(NO_3)_3$ in mixtures of H_2O/THF. Error represents standard error of the mean of between 3 and 9 measurements.

(a)		(b)	
% H_2O in THF (v/v)	***q***	**% H_2O in THF (v/v)**	***q***
1	5.8 ± 0.1	1	3.2 ± 0.02
5	8.0 ± 0.1 *	5	5.2 ± 0.04
10	8.3 ± 0.03 *	10	6.8 ± 0.03
15	8.6 ± 0.02	15	7.2 ± 0.03
20	8.6 ± 0.1 *	20	7.2 ± 0.04
25	8.6 ± 0.1	25	7.4 ± 0.04
30	8.5 ± 0.04 *	30	7.6 ± 0.1
40	8.5 ± 0.01 *	40	7.7 ± 0.01

nd = not determined, * from reference [10]

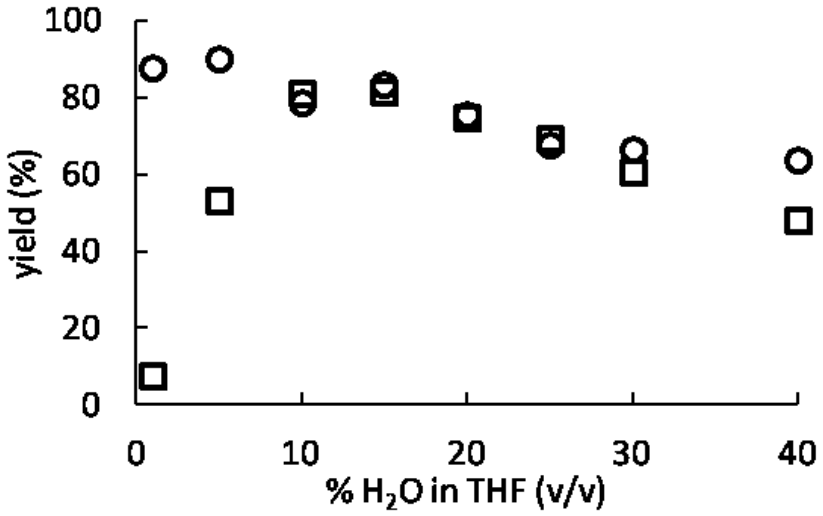

Figure 2.3. Yields of the reaction shown in **Figure 2.1** catalyzed by $Eu(OTf)_3$ or $Eu(NO_3)_3$ after 48 h as a function of solvent composition. Conditions: solvent mixtures of 1 to 40% H_2O in THF (v/v) containing 7 mol % $Eu(OTf)_3$ (○) or $Eu(NO_3)_3$ (□).

We also investigated the relationship between the water-coordination numbers of europium precatalysts and the steady state reaction rates of the Mukaiyama aldol reaction shown in **Figure 2.1**. For these studies, $Eu(OTf)_3$ or $Eu(NO_3)_3$ was used in solvent mixtures ranging from 1 to 40% H_2O in THF (v/v) and $Eu(OTf)_3$ in THF. These europium-containing precatalysts and solvent mixtures were used because of the wide range of water-coordination numbers (3.2 to 8.6) accessible under these conditions (**Figure 2.2**). We expected that this range of water-coordination numbers would allow us to observe changes in reactivity to test our hypothesis regarding the relationship between steady state reaction rate and water-coordination number. The concentration of product **1.7** at 2, 18, 34, 50, and 66 min was determined using HPLC to find the steady state reaction rates of $Eu(NO_3)_3$- and $Eu(OTf)_3$-catalyzed Mukaiyama aldol reactions (**Figure 2.4**).

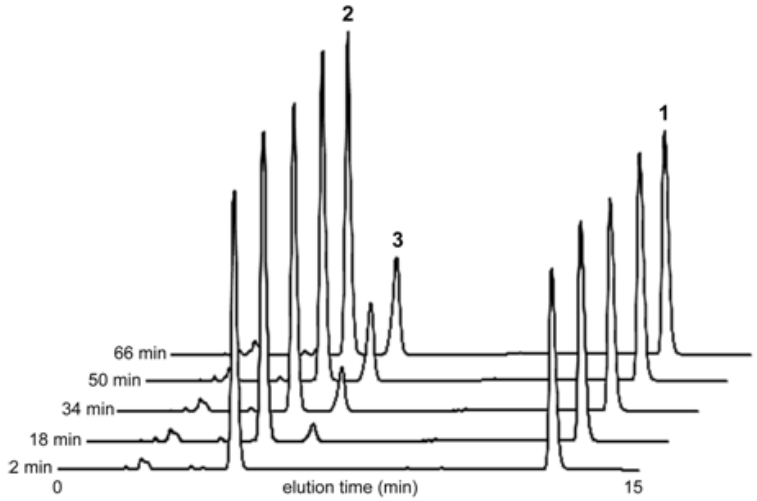

Figure 2.4. HPLC traces of 7 mol % $Eu(OTf)_3$-catalyzed Mukaiyama aldol reaction in 10% H_2O/THF (v/v) after 2, 18, 34, 50, and 66 min. The increase in peak 3 with time corresponds to an increase in product concentration. Peaks 1 and 2 are due to **1.6** and **1.2** respectively. The y-axis shows absorbance at 210 nm in arbitrary units.

From these HPLC traces and a calibration curve for **1.7** produced using the same conditions, the area under the peaks was used to determine concentration. An example of the resulting data is plotted in **Figure 2.5**, which exemplifies the linear increase of product concentration as a function of time for the conditions studied between 18 and 66 min. By monitoring the linear increase in product, **1.7**, concentration as a function of time we were able to calculate the steady state reaction rates as the slope of the best fit line in **Figure 2.5**.[19] **Table 2.2** contains a complete list of steady state reaction rates.

From the data in **Figure 2.5** and data from similar experiments using $Eu(OTf)_3$ or $Eu(NO_3)_3$ in a range of solvents [0–40% H_2O in THF (v/v)], a relationship was observed between the steady state reaction rates of europium-catalyzed Mukaiyama aldol reactions and solvent composition (**Figure 2.6**). Reactions catalyzed by $Eu(OTf)_3$ had faster steady state reaction rates than reactions catalyzed by $Eu(NO_3)_3$ in every solvent composition studied. This observation can be rationalized based upon relative binding affinities of the anions for Eu^{3+}, which affect the

water-coordination numbers of the precatalysts: triflate has a lower binding affinity for lanthanide(III) ions than nitrate.[20]

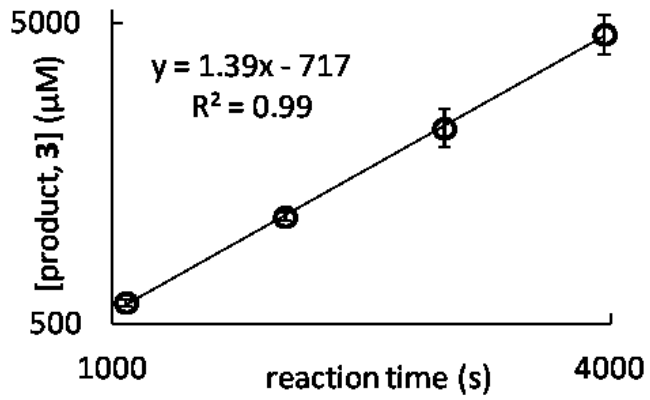

Figure 2.5. Plot of the formation of product, **1.7**, as a function of time. Conditions: 7 mol % $Eu(OTf)_3$ in 10% H_2O/THF (v/v) after 1080, 2040, 3000, and 3960 s. The steady state reaction rate derived from this plot is the slope of the best fit line and is 1.39 μM s^{-1}. Error bars represent the standard error of the mean of three independently prepared samples.

Table 2.2. Mean steady state reaction rates of 7 mol % $Eu(OTf)_3$ (a) or 7 mol % $Eu(NO_3)_3$ (b) catalyzed Mukaiyama aldol reactions. Error represents standard error of the mean of 3 independent samples.

(a) % H_2O in THF (v/v)	steady state reaction rate (μM s^{-1})	(b) % H_2O in THF (v/v)	steady state reaction rate (μM s^{-1})
0	0.29 ± 0.06	0	nd
1	0.33 ± 0.03	1	0.008 ± 0.001
5	1.0 ± 0.2	5	0.11 ± 0.02
10	1.4 ± 0.2	10	0.33 ± 0.06
15	1.5 ± 0.2	15	0.48 ± 0.04
20	nd	20	nd
25	1.45 ± 0.08	25	1.0 ± 0.2
30	nd	30	nd
40	1.3 ± 0.1	40	1.3 ± 0.2

nd = not determined

This difference in europium binding affinities between triflate and nitrate results in higher water-coordination numbers for $Eu(OTf)_3$ compared to $Eu(NO_3)_3$ and, ultimately, corresponds to higher europium accessibility because each water molecule coordinated to Eu^{3+} represents a

potential site for benzaldehyde coordination and activation for reaction. In general, increasing water percentages resulted in faster steady state reaction rates, but the steady state reaction rates of $Eu(OTf)_3$-catalyzed reactions reached a maximum and remained constant at solvent mixtures containing greater than 10% H_2O in THF (v/v) (**Figure 2.6**).

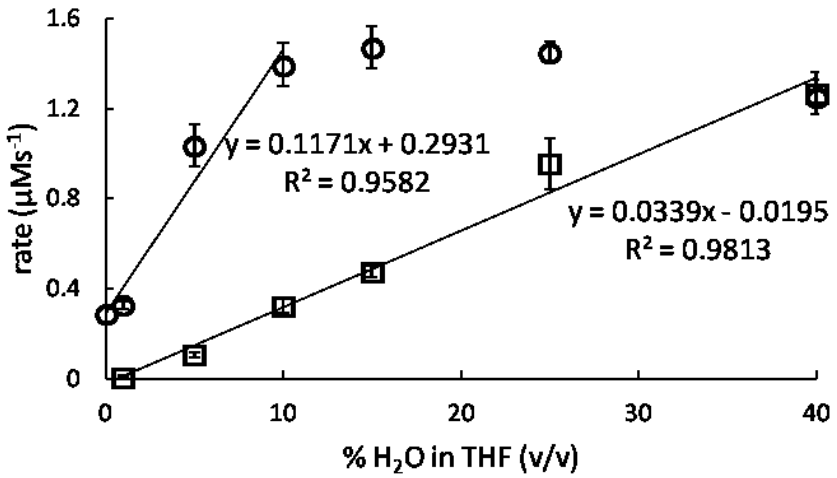

Figure 2.6. Steady state reaction rates of 7 mol % $Eu(OTf)_3$- (○) or $Eu(NO_3)_3$- catalyzed (□) Mukaiyama aldol reactions in 0–40% H_2O/THF mixtures (v/v). Regression lines represent the rate dependence on anion identity and solvent composition. Note: 10% H_2O in THF (v/v) corresponds to the solvent composition at which $Eu(OTf)_3$ is saturated with water (**Figure 2.2**). Error bars represent the standard error of the mean of three independently prepared samples.

This solvent composition [10% H_2O in THF (v/v)] corresponds to the lowest H_2O concentration at which the water-coordination number is at a maximum value (**Figure 2.2**). The increase of steady state reaction rates of $Eu(NO_3)_3$-catalyzed reactions over the entire range of solvents in this study can be attributed to the water-coordination number of $Eu(NO_3)_3$ that increases without reaching a maximum with increasing H_2O in THF from 1 to 40%. An alternative explanation for our observations with $Eu(NO_3)_3$ is the determination of rate by a dynamic involvement of NO_3^- in the inner-sphere of the lanthanide ion. However, the slower steady state reaction rates of $Eu(NO_3)_3$-catalyzed Mukaiyama aldol reactions relative to

$Eu(OTf)_3$-catalyzed reactions support our hypothesis that larger water-coordination numbers and less strongly binding counteranions enable faster reaction rates.

2.3 Experimental Section

General

Unless otherwise noted, purchased chemicals were used as supplied. THF was purified using a solvent purification system (Vacuum Atmospheres Company), and water was purified using a PURELAB Ultra Mk2 (ELGA) water purification system. 2-(Hydroxyphenylmethyl)-cyclohexanone (**1.7**), was synthesized according to a published procedure.[1j] Flash chromatography was performed using silica gel 60, 230–400 mesh (EMD Chemicals). TLC was performed on silica gel 60 coated ASTM TLC plates F_{254} (250 μm thickness). TLC visualization was accomplished using a hand-held UV lamp followed by staining with potassium permanganate (2 g $KMnO_4$, 20 g K_2CO_3, 5 mL 5% w/v aqueous NaOH, 300 mL H_2O). HPLC analyses were performed on a Shimadzu HPLC system equipped with a C18 column (Zorbax Eclipse XDB-C18, 3.5 μm, 4.6 × 150 mm). Detection of eluent was carried out with a photodiode array detector at 210 nm. HPLC analyses used a binary gradient method (pump A: water, pump B: acetonitrile; 40–90% B over 15 min; flow rate: 1 mL/min). Europium concentrations were verified using xylenol orange according to a published procedure.[21]

Mukaiyama Aldol Protocol

Mukaiyama aldol reactions were carried out at ambient temperature in 0, 1, 5, 10, 15, 20, 25, 30, or 40% H_2O in THF (v/v) (3.0 mL) containing either $Eu(OTf)_3$ or $Eu(NO_3)_3$ (1.2 mM); to each solution, **1.6** (20.0 μL, 0.100 mmol) and **1.2** (5.0 μL, 0.050 mmol) were added using gas tight syringes. Immediately after preparation, each reaction mixture was vigorously shaken for 10 s and passed through a 0.20 μm syringe filter into an HPLC autosampler vial. Analyses were performed to determine product concentration using HPLC. Compounds **1.6**, **1.2**, and **1.7** eluted in the order **1.2**, **1.7**, and **1.6**. For the quantitative determination of products, a calibration curve of **1.7** from 0.0 to 4.0 mg/mL in 1:1 H_2O/THF (v/v) was made from peak integrations using the same HPLC conditions.

Luminescence-Decay Measurements

Water-coordination numbers were determined by acquiring luminescence-decay measurements using a HORIBA Jobin Yvon Fluoromax-4 spectrofluorometer in decay-by-delay scan mode using the phosphorescence lifetime setting. Experimental details and data analyses were performed according to previously described methods.[11c]

2.4 Conclusions

This chapter describes the dynamic luminescence-decay measurements of $Eu(NO_3)_3$ and $Eu(OTf)_3$ in binary solvent mixtures. In addition to monitoring the water-coordination numbers of these europium-containing precatalysts, we found the yields and measured steady state reaction rates of the Mukaiyama aldol reaction catalyzed by these salts in solvent mixtures from 1 to 40% H_2O in THF (v/v), and the steady state rate of the $Eu(OTf)_3$-catalyzed Mukaiyama aldol in THF. From these measurements, we found a correlation between steady state reaction rate and water-coordination number as well as between yield and solvent composition. The use of luminescence-decay measurements to probe the coordination environment of europium-based precatalysts in solution enabled the study of the influence of precatalyst coordination-environment on steady state reaction rate. These results are useful in the design of new precatalysts to be used for aqueous, enantioselective, lanthanide-catalyzed bond forming reactions because they suggest that faster rates of catalysis will require lower ligand coordination numbers. Further, the methodology described here can be applied to other lanthanide-catalyzed bond-forming reactions in aqueous media to gain a better understanding of the influence of water on the structure–activity relationship between precatalysts and rates of catalysis.

CHAPTER THREE

Synthesis, Spectroscopic Characterization, and Reactivity of Water-Tolerant Eu^{3+}-Based Precatalysts.

Portions of Chapter three have been adapted or reprinted with permission from Averill, D. J.; Allen, M. J. Synthesis, Spectroscopic Characterization, and Reactivity of Water-Tolerant Eu^{3+}-Based Precatalysts. *Inorg. Chem.*, **2014**, *53*, 6257–6263.

3.1 Introduction

Many pharmaceuticals and natural products contain β-hydroxy carbonyl moieties, making the synthesis of this functional group an active area of research.[5,22a,22b] The Mukaiyama aldol reaction is a Lewis-acid-catalyzed, carbon–carbon bond-forming reaction that produces β-hydroxy carbonyls (**Scheme 3.1**), and this reaction requires chiral precatalysts to induce stereoselectivity. Due to precatalyst instability towards hydrolysis, anhydrous solvents are used commonly,[2d,23a,23b] but recent efforts have focused on aqueous versions of the enantioselective Mukaiyama aldol reaction because of the financial and environmental benefits of using aqueous media.[1j] Several examples of enantioselective precatalysts that function in the presence of water exist: $Cu(OTf)_2$, $Pb(OTf)_2$, and $Ln(OTf)_3$ with crown ethers, where OTf^- is trifluoromethanesulfonate;[3a,3b,6a–6c] Trost-type semicrowns with $Ga(OTf)_3$;[17,24] and $Zn(OTf)_2$ and $FeCl_2$ with pybox-type ligands.[6d,25]

Scheme 3.1 Aqueous Mukaiyama aldol reaction.

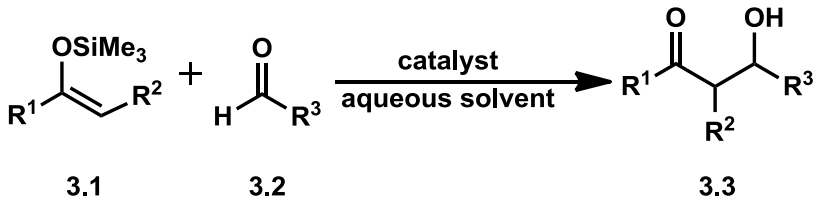

Previously, the Allen lab reported the synthesis and application of water-tolerant Eu^{3+}-based precatalysts for aqueous, enantioselective Mukaiyama aldol reactions using ligands **1.5** and **1.13** shown in **Figure 3.1**.[3c,3d] The use of ligand **1.5** with $Eu(OTf)_3$ at a ligand-to-metal ratio of 2.4:1 resulted in high enantiomeric ratios (95:5–99:1) for Mukaiyama aldol reaction products but required long (168 h) reaction times. The excess of ligand was required to achieve high stereoselectivity, but reaction times were slower in the presence of excess ligand, suggesting that excess ligand slows the reaction. Because of these observations, we hypothesized that equilibria exist between uncomplexed Eu^{3+} (racemic precatalyst), ligand-bound Eu^{3+} (stereoselective precatalyst), and Eu^{3+} encapsulated by more than one ligand (deactivated precatalyst) and that an understanding of the ligand features that influence this equilibrium would enable rational ligand variations to improve reactivity and selectivity.

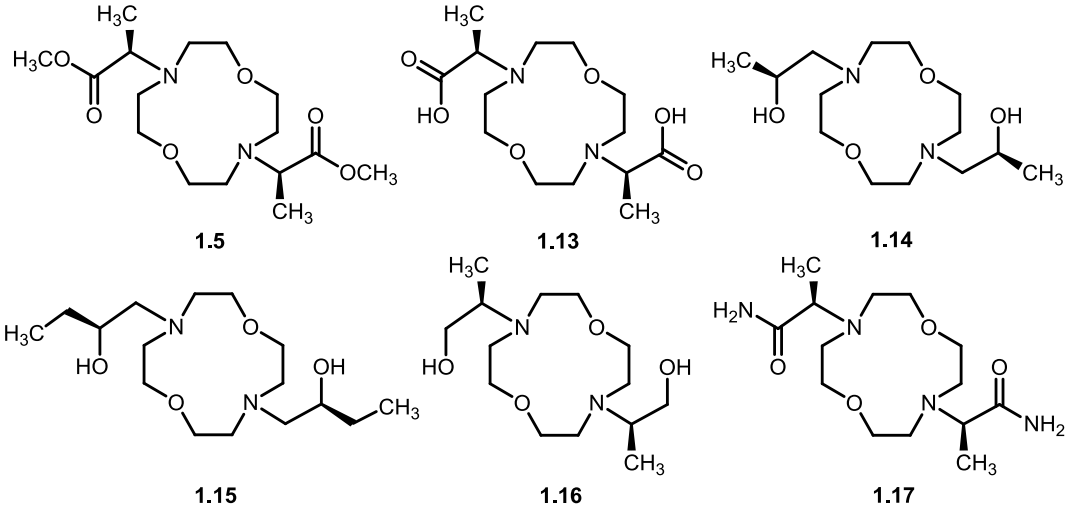

Figure 3.1. C_2-symmetric ligands used to prepare Eu^{3+}-based precatalysts.

To test our hypothesis, we studied a variety of ligand features that we suspected could affect reactivity and selectivity. To investigate the influence of ligand donor type, chiral center location, and chiral center bulk on reactivity we synthesized ligands **1.14–1.17** and combined them with Eu^{3+}. Eu^{3+} was chosen over other trivalent lanthanides because it can act as an optical

probe to provide feedback regarding its coordination environment via luminescence-decay and steady-state luminescence measurements. Additional information about the Eu^{3+} coordination environment was obtained from NMR spectroscopy, and the enantioselectivities and diastereoselectivities of reaction products formed in the presence of ligands **1.14–1.17** with Eu^{3+} were determined using chiral columns with HPLC for the aqueous, enantioselective, Mukaiyama aldol reaction. This chapter contains a description of the relationships between ligand structure and precatalyst activity with regard to efficiency and coordination.

3.2 Results and Discussion

Ligands 1.5, **1.13–1.17** With ligands **1.5**, **1.13–1.17** and Eu^{3+}, we were able to study the influence of ligand structure on reactivity, selectivity, and complex formation. The functional groups that bind to the metal were changed as part of this strategy to incorporate esters (**1.5**), carboxylic acids (likely carboxylates under reaction conditions) (**1.13**), alcohols (**1.14**, **1.15**, and **1.16**), and amides (**1.17**). These functional groups were chosen because esters, carboxylic acids, alcohols, and amides have different Lewis basicities that affect the ability of ligands to bind Eu^{3+}. In addition to functional groups, the location and size of the chiral center on the ligand sidearms were investigated with ligands **1.14**, **1.15**, and **1.16** to study the influence of structural features on reactivity and selectivity.

The syntheses of ligands **1.14–1.17** are shown in **Scheme 3.2**. Briefly, **1.14** and **1.15** were synthesized by the ring opening of epoxides with macrocycle **3.4** in MeOH. Ligand **1.16** was prepared by reducing **1.5** with lithium aluminum hydride. The reduction of **1.5** to produce **1.16** was chosen instead of preparing a chiral-alcohol sidearm to react with **3.4** because the stereoisomers of starting material **1.5** can be readily purified by HPLC. Ligand **1.17** was synthesized by functionalizing **3.4** using (*S*)-amino-1-oxypropan-2-yl-4- methylbenzenesulfonate

(**3.7**). Ligands **1.14**–**1.17** were all synthesized in good yields (74–91%) in one step from commercially available or reported starting materials.

Scheme 3.2. Syntheses of ligands **1.14**–**1.17**.

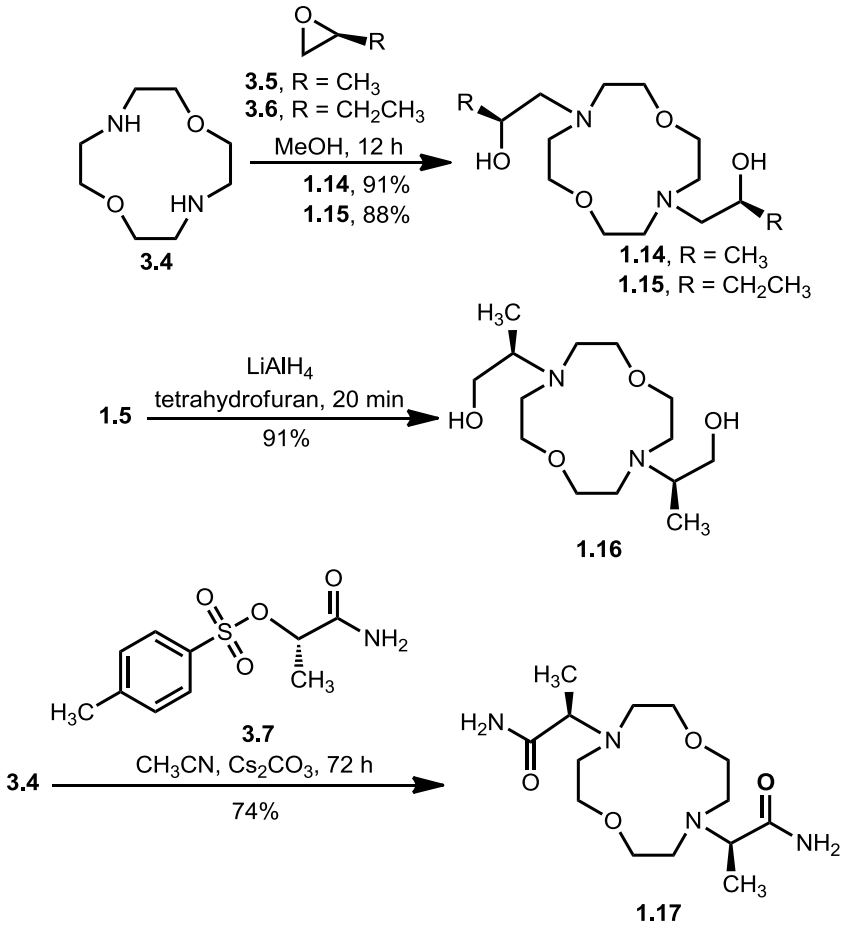

3.3 Luminescence measurements for the study of Eu^{3+} coordination environment.

Luminescence measurements were performed to study the interaction of Eu^{3+} with ligands **1.5**, **1.13–1.17**. Eu^{3+} is a useful optical probe for studying coordination environments because of its coordination-environment sensitive luminescence-lifetime[1f,10,11a,12,13] and the hypersensitivity of the $^5D_0 \rightarrow {}^7F_2$ transition (emission at ~616 nm) to perturbations of symmetry.[14b,27] Consequently, luminescence-lifetime measurements were used to determine water-coordination numbers (*q*), and steady-state luminescence measurements were used to monitor changes in the crystal field of Eu^{3+} during ligand-to-metal titrations.

To calculate q for Eu^{3+} in each mixture, we used **Eq. 3.1**, where 1.2 and 0.1927 are empirically derived constants;[11a,11c] ${\tau_{H_2O}}^{-1}$and ${\tau_{D_2O}}^{-1}$are the measured luminescence-decay rates of Eu^{3+} in EtOH/H_2O and EtOD/D_2O, respectively (decay rates are in APPENDIX B); and *n*OH and *n*NH are the number of non-water-based inner-sphere alcohol (O–H) or amide (N–H) oscillators, respectively. Water-coordination numbers of Eu^{3+} were measured in mixtures of EtOH/H_2O 9:1 (v/v) with ligand-to-Eu^{3+} ratios of 1:1, 2:1, and 6:1 (**Table 3.1**). This solvent composition was chosen because it is commonly used for lanthanide-catalyzed Mukaiyama aldol reactions.[3c,3d,6c] Also, ligand-to-Eu^{3+} ratios of 1:1, 2:1, and 6:1 were chosen to determine if more than one equivalent of ligand can bind Eu^{3+}. Due to the possibility of more than one equivalent of ligand being coordinated to Eu^{3+}, q values for both 1 and 2 equivalents of ligand bound to Eu^{3+} were calculated (We did not calculate q values for greater than 2 equivalents of ligand bound to Eu^{3+} because this type of binding is unlikely to occur based on sterics and entropy) assuming that all N–H or O–H oscillators on each ligand would be in the innersphere of the metal ion. This assumption allowed us to obtain maximum and minimum q values with ratios of 1:1 ligand-to-Eu^{3+} (maximum) and 2:1 ligand-to-Eu^{3+} (minimum). For example, maximum and minimum q values for Eu^{3+} with ligand **1.17** were calculated for one equivalent of ligand (2 amides or 4 N–H oscillators) for a maximum q value and for 2 equivalents of ligand (4 amides or 8 N–H oscillators) for a minimum q value.

Eq 3.1: $q = 1.2[({\tau_{H_2O}}^{-1} - {\tau_{D_2O}}^{-1}) - 0.1927 - 0.45n\mathrm{OH} - 0.075n\mathrm{NH}]$

Eu^{3+} usually has a coordination number between 8 and 9; therefore, because q determinations represent the average of all species in solution, water-coordination numbers greater than 3 in the presence of hexadentate ligands suggest the presence of uncomplexed Eu^{3+} (**Figure 3.2**) or incomplete coordination by the ligands. By measuring the water-coordination

numbers of Eu^{3+} at different ligand-to-metal ratios, we were able to monitor the complexation of Eu^{3+} with ligands **1.5**, **1.13–1.17**. Mixtures of Eu^{3+} with ligands **1.5** and **1.17** at ligand-to-metal ratios of 1:1 have Eu^{3+} water-coordination numbers greater than 3, indicating incomplete complexation of Eu^{3+}. This observation suggests that ligands **1.5** and **1.17** form labile complexes with Eu^{3+} under these conditions. Ligands **1.13–1.16** with Eu^{3+} at ligand-to-metal ratios of 1:1 have q values between 0.9 and 2.3. These values of q suggest that ligands **1.13–1.16** (ligands with sidearms that have functional groups with the ability to become deprotonated) chelate Eu^{3+} more strongly than **1.5** and **1.17** (ligands with sidearms that have functional groups that lack the ability to become deprotonated).

Average values of q are lower at ligand-to-metal ratios of 2:1 compared to 1:1 mixtures prepared from the same ligands. This observation is a demonstration of Le Chatelier's principle where the equilibrium system shown in **Figure 3.2** can be driven to the right (increased chelation of Eu^{3+}) in the presence of excess ligand. Water-coordination numbers were lower than 3 at ligand-to-Eu^{3+} ratios of 6:1 in the presence of ligands **1.5, 1.13**, **1.14**, **1.16**, and **1.17** indicating that Eu^{3+} can be bound by more than one ligand at a time. Mixtures of **1.15** and Eu^{3+} at a ligand-to-Eu^{3+} ratio of 6:1 became turbid in EtOD/D_2O; therefore, q was not calculated for Eu^{3+} with **1.15** at this ratio. Interestingly, Eu^{3+} in the presence of six equivalents of ligand **1.13** had a q value of 0.1, the most reasonable explanation for such a low q is complete encapsulation of Eu^{3+} by two or more equivalents of ligand **1.13**. These observations of q at different ligand-to-Eu^{3+} ratios support our hypothesis that an equilibrium system with multiple species occurs with ligands **1.5**, **1.13–1.17** and Eu^{3+}.

Table 3.1. Water-coordination numbers for Eu^{3+} with ligands **1.5** and **1.13–1.17**.

ligand	$q^{a,d,g}$	$q^{a,e,g}$	$q^{b,d,g}$	$q^{b,e,g}$	$q^{c,d,g}$	$q^{c,e,g}$
1.5[f]	3.5	3.5	2.1	2.1	1.4	1.4
1.13[f]	2.2	2.2	0.8	0.8	0.0	0.0
1.14	2.2	1.1	2.0	1.0	1.1	0.0
1.15	1.9	0.8	1.8	0.8	nd	nd
1.16	2.1	1.0	2.1	1.0	0.5	0.0
1.17	3.8	3.4	3.0	2.6	1.7	1.3

[a]Ligand-to-metal ratio of 1:1. [b]Ligand-to-metal ratio of 2:1. [c]Ligand-to-metal ratio of 6:1. [d]Calculated for complexes with Eu^{3+} coordination by one ligand. [e]Calculated for complexes with Eu^{3+} coordination by two ligands. [f]Ligands **1.5** and **1.13** do not have chelator-based inner-sphere O−H or N−H oscillators; therefore, $q^d = q^e$. nd = not determined. [g]The error associated with water-coordination number determination is ±0.1 water molecules.[11a]

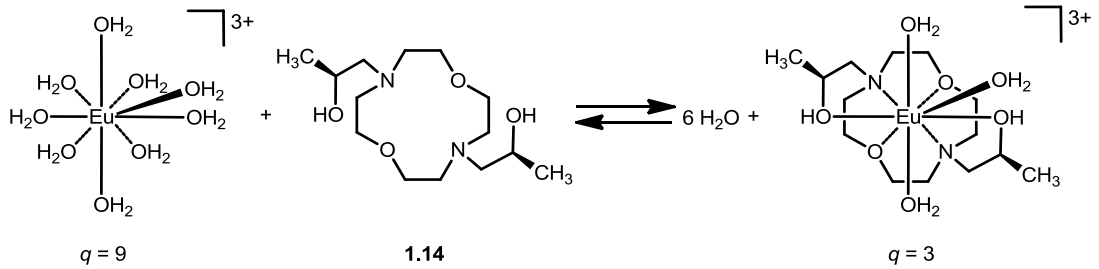

Figure 3.2. Representation of unchelated Eu^{3+} and a Eu^{3+}-containing complex of **1.14** with q values of 9 and 3, respectively (counteranions have been omitted for clarity). One complex is shown on the right of the equilibrium to demonstrate the point of the figure, but multiple species are likely in the actual solution.

To gain a better understanding of the Eu^{3+} equilibrium system, we titrated solutions of ligand into solutions containing Eu^{3+} and monitored the changes in coordination by steady-state luminescence measurements. Monitoring changes in steady-state luminescence intensity as a function of ligand-to-Eu^{3+} ratio allows the determination of end points for ligand-to-Eu^{3+} binding stoichiometries for ligands **1.5**, **1.13–1.17** with Eu^{3+}. To monitor changes in luminescence intensities, the $^5D_0 \rightarrow {}^7F_1$ and $^5D_0 \rightarrow {}^7F_2$ transitions of Eu^{3+} were compared. **Figure 3.3** illustrates the sensitivity of the $^5D_0 \rightarrow {}^7F_2$ transition to changes in coordination environment (with and

without 0.6 equiv of multidentate ligand **1.14**). The emission spectrum of Eu^{3+} in the presence of ligand **1.14** was normalized to the magnetic-dipole ($^5D_0 \rightarrow {}^7F_1$) band at 591 nm (relatively insensitive to changes in coordination environment) for visual comparison of the $^5D_0 \rightarrow {}^7F_2$ emission intensities.

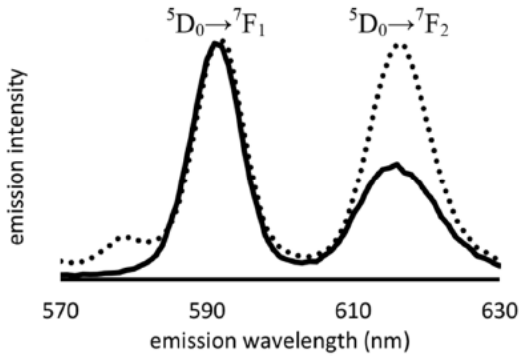

Figure 3.3. Normalized emission spectra (λex = 395 nm) of $Eu(OTf)_3$ in $EtOH/H_2O$ 1:9 with (dotted line) and without (solid line) 0.6 equiv of ligand **1.14**. The bands at 591 and 616 nm arise from the $^5D_0 \rightarrow {}^7F_1$ and hypersensitive $^5D_0 \rightarrow {}^7F_2$ transitions, respectively. Similar spectra were observed for the other ligands in this chapter.

The sensitivity of the $^5D_0 \rightarrow {}^7F_2$ transition combined with the less sensitive $^5D_0 \rightarrow {}^7F_1$ transition makes Eu^{3+} a useful ratiometric sensor for concentration-independent sensing of changes in coordination [($^5D_0 \rightarrow {}^7F_2$)/($^5D_0 \rightarrow {}^7F_1$) emission intensity ratios are independent of concentration]. The intensity ratio increase is expected upon ligand coordination to Eu^{3+} because the $^5D_0 \rightarrow {}^7F_2$ emission intensity is highly sensitive to perturbations of the Eu^{3+} crystal field by coordinated ligands.[14b,27b,28,29] Compared to $Eu(OTf)_3$ in the absence of hexadentate ligands, the intensity of the $^5D_0 \rightarrow {}^7F_2$ transition relative to the $^5D_0 \rightarrow {}^7F_1$ transition increased in the presence of every hexadentate ligand in this study. Changes in Eu^{3+} coordination environments were monitored by plotting the emission intensity ratios vs ligand-to-Eu^{3+} ratios (**Figure 3.4**). Ligand-to-Eu^{3+} titrations with **1.5**, **1.13–1.17** caused an increase in the intensity ratio of the $^5D_0 \rightarrow {}^7F_2$ to $^5D_0 \rightarrow {}^7F_1$ transitions of Eu^{3+} between 1 and 3 equiv of ligand (indicating change in Eu^{3+}

coordination). Ester functionalized ligand **1.5** does not have titration endpoints in the range studied, indicating weak interactions between ligand and Eu^{3+}. Lastly, the titration of ligand **1.17** and Eu^{3+} has an apparent endpoint near 6 equiv of ligand, which indicated weak interactions between ligand and Eu^{3+}. Based on the titration data in **Figure 3.4**, ligand donor type affects coordination more than chiral center location and size. The relative strengths of interactions with Eu^{3+} for these ligands is carboxylate > alcohol > amide > ester. This stability trend is in agreement with other studies of macrocyclic ligands with Eu^{3+}.[1g,30]

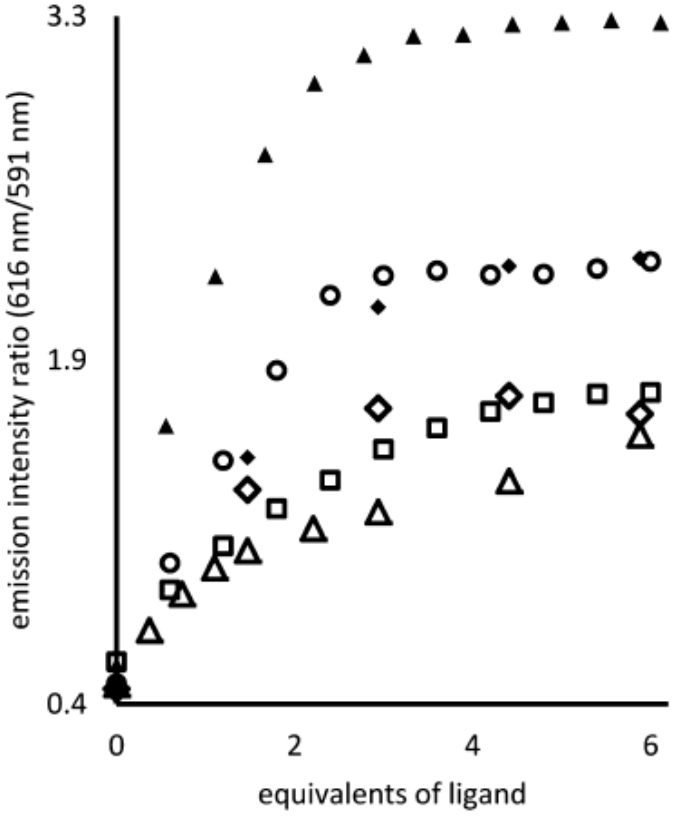

Figure 3.4. Emission intensity ratios of Eu^{3+} (616 nm/591 nm) versus equiv of ligand for Eu^{3+} with **1.5** (△), **1.13** (▲), **1.4** (◆), **1.15** (◇), **1.16** (○), and **1.17** (□). Increases in magnitude of the emission intensity quotient (616 nm/591 nm) arise from increases in crystal field splitting of Eu^{3+}.[14b]

3.4 ^{1}H-NMR characterization of ligands with Eu^{3+}.

In addition to luminescence measurements, we used NMR spectroscopy to investigate the interactions between ligands and Eu^{3+}. By monitoring changes in the ^{1}H-NMR spectra of ligands in the presence of Eu^{3+} at different ligand-to-Eu^{3+} ratios, we found that at least three different species can exist in solution. **Figure 3.5** contains ^{1}H-NMR spectra of ligand **1.14** that were acquired at ligand-to-Eu^{3+} ratios of 1:0, 4:1, and 0.5:1. These ligand-to-Eu^{3+} ratios were chosen because they allowed me to investigate **1.14** without Eu^{3+} (1:0), with a subsess of Eu^{3+} (4:1), and with an excess of Eu^{3+} (0.5:1). The NMR spectra were different at each ratio, indicating the presence of different ligand environments.

With a ligand-to-Eu^{3+} ratio of 4:1 and an acquisition temperature of –40 °C, new downfield signals were observed compared to the signals arising from only ligand. We attribute the downfield signals to a Eu^{3+}-Ln (n > 1) species because an excess of ligand increases the probability for multiple ligands to bind Eu^{3+}. The NMR spectral evidence for the presence of a Eu^{3+}-Ln (n > 1) species is also consistent with q measurements for Eu^{3+} in the presence of excess **1.14**. At a ligand-to-metal ratio of 0.5:1, upfield signals were observed relative to signals arising from the ligand. We attribute the upfield signals to a 1:1 Eu^{3+}-to-ligand complex because an excess of metal will shift the equilibrium towards 1:1 ligand-to-metal complexes and unchelated Eu^{3+}, or possibly a Eu^{3+} n-L ($n \geq 1$) species. From the ^{1}H-NMR spectra of ligands **1.5**, **1.13–1.17** with Eu^{3+} at different ligand-to-metal ratios, it was found that at least three different species of Eu^{3+} exist depending on the ligand-to-Eu^{3+} ratio, and these findings corroborate the luminescence observations.

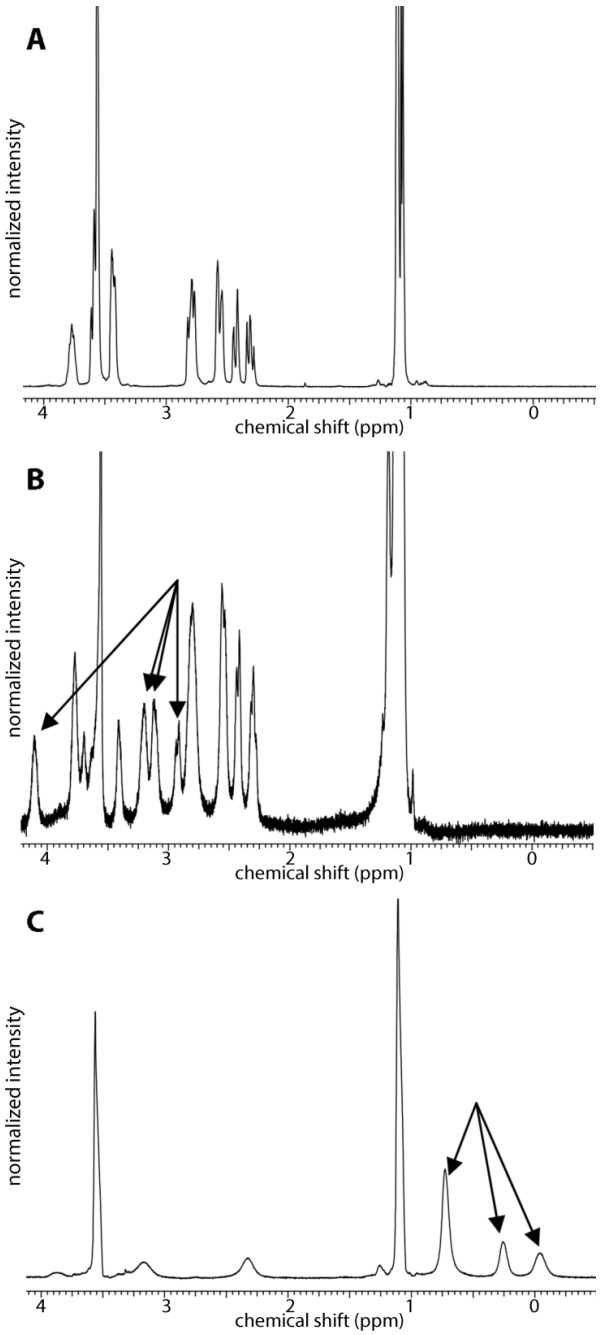

Figure 3.5. A. ^{1}H-NMR spectrum of **1.14** in 9:1 EtOD/D_2O. **B**. ^{1}H-NMR spectrum of **1.14** in 9:1 EtOD/D_2O at –40 °C with 0.25 equiv of $Eu(OTf)_3$. Arrows point to signals observed in the presence of a subsess of Eu^{3+} (the temperature of –40 °C was required to resolve the signals between 4 and 2 ppm). These new signals are attributed to a Eu^{3+}-L*n* (*n* > 1) species. **C**. ^{1}H-NMR spectrum of **1.14** in 9:1 EtOD/D_2O with 2 equiv of $Eu(OTf)_3$. Arrows point to signals observed in the presence of excess Eu^{3+}. The new upfield signals are attributed to a Eu^{3+} *n*-L (*n* ≥ 1) species.

3.5 Testing of precatalyst reactivity and selectivity in the aqueous enantioselective Mukaiyama aldol reaction.

The reactivities and selectivities of mixtures of Eu^{3+} with ligands **1.5**, **1.13–1.17** in the aqueous Mukaiyama aldol reaction shown in **Scheme 3.3** were tested. The reaction in **Scheme 3.3** was chosen because it has been previously used for testing of precatalysts for Mukaiyama aldol reactions;[1i,1k,31] therefore, the results can be compared to results obtained using other precatalysts. Because reactivity and selectivity of Mukaiyama aldol reactions depends on ligand-to-metal ratios,[3a,3c,3d] the reactions in this study were performed at ligand-to-Eu^{3+} ratios of 1.2:1 and 2.4:1 (**Table 3.3**) to enable comparison to published values.[3d,17]

Scheme 3.3. Aqueous Mukaiyama aldol reaction performed with ligands **1.5**, **1.13–1.17**.

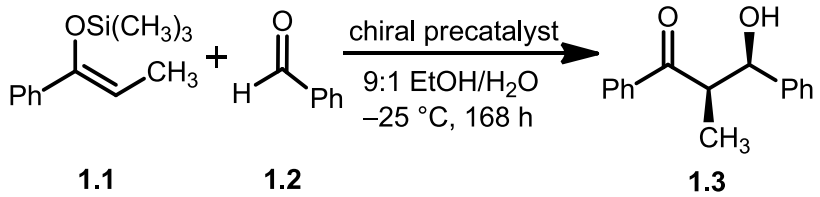

Table 3.2. Aqueous Mukaiyama aldol yields and selectivities catalyzed by $Eu(OTf)_3$ with ligands **1.5** and **1.13–1.17**.

	1.5	**1.13**	**1.14**	**1.15**	**1.16**	**1.17**
yield[a,b] (%)	96[c]	8	17	12	5	20
yield[b,d] (%)	92[c]	0	0	0	0	6
dr[a,f] (syn:anti)	2.1:1[c]	0.72:1	1.3:1	1.1:1	1.1:1	0.93:1
dr[d,f] (syn:anti)	32:1[e]	nd	nd	nd	nd	0.55:1
er[a,f] (syn)	2:1[c]	1.03:1	1.2:1	1:1	1:1	0.78:1
er[d,f] (syn)	96:1[e]	nd	nd	nd	nd	0.66:1

[a]24 mol % ligand, 20 mol % $Eu(OTf)_3$; [b]isolated yield; [c]reference 17; [d]48 mol % ligand, 20 mol % $Eu(OTf)_3$; [e]reference 3d; [f]determined by chiral HPLC analysis; nd = not determined.

Ligand **1.5** with Eu^{3+} was previously reported to give 96 and 92% yields at ligand-to-Eu^{3+} ratios of 1.2:1 and 2.4:1 with respective diastereomeric ratios of 2.1:1 and 32:1 and enantiomeric ratios of 2:1 and 96:1.[3c,3d] In this study, ligand **1.13** with Eu^{3+} gave an 8% yield at a ligand-to-Eu^{3+} ratio of 1.2:1 with a diastereomeric ratio of 0.72:1 and an enantiomeric ratio of 1.03:1 with no products being formed at the 2.4:1 ligand-to-Eu^{3+} ratio. We hypothesize that in the presence of excess **1.13**, the inner-coordination sphere of Eu^{3+} nears saturation and cannot act as a precatalyst for Mukaiyama aldol reactions, which is consistent with observed *q* numbers for Eu^{3+} in the presence of excess **1.13**. Chiral alcohol ligands **1.14–1.16** with Eu^{3+} gave low yields (5–17%) and low diasteriomeric (1.1:1–1.3:1) and enantiomeric (1:1–1.2:1) ratios at ligand-to-Eu^{3+} ratios of 1.2:1. The low selectivity is likely due to the lack of steric bulk on the ligand sidearms. A lack of steric bulk near the coordinated atom might not allow the ligand to block nucleophilic attack at either the *re* or *si* face of the aldehyde from the incoming silyl enol ether (**Figure 3.6**, left). This blocking is the suspected mechanism that imparts selectivity.[3c] No products were observed for mixtures of 2.4:1 ligand-to-Eu^{3+} with ligands **1.14–1.16**, and this lack of reactivity is likely due to an equilibrium system that involves displacement of innersphere water by a second equivalent of ligands **1.14–1.16** (**Figure 3.7**). Saturation of Eu^{3+} by more than one equivalent of ligand could inhibit the reaction by preventing aldehyde coordination to Eu^{3+} to become activated for nucleophilic attack. The *q* data for Eu^{3+} with ligands **1.14–1.16** support our hypothesis that excess ligand prevents the aldehyde from becoming activated for nucleophilic attack.

Amide functionalized ligand **1.17** with $Eu(OTf)_3$ at ligand-to-Eu^{3+} ratios of 1.2:1 and 2.4:1 gave low yields (20 and 6%, respectively) and low diasteriomeric and enantiomeric

selectivity. It is likely that excess **1.17** slowed the Mukaiyama aldol reaction by decreasing the Lewis acidity at the metal center. These findings suggest that amide sidearms deactivate the metal center compared to ester sidearms. The reduced reactivity of Eu^{3+} in the presence of **1.17** is likely explained by the resonance structure of amides that place electron density on the carbonyl oxygen, lowering the Lewis acidity of Eu^{3+}. Because low selectivity was observed with $Eu(OTf)_3$ in the presence of **1.17**, we hypothesized that the steric bulk of the primary amide ligand is not large enough to selectively block the nucleophilic attack by the incoming silyl enol ether (**Figure 3.6**).

From Mukaiyama aldol reactions, it was found that substitution at the carbonyl carbon and the carbon adjacent to the macrocycle nitrogen is required for high stereoselectivity in the products (**Figure 3.7**). Finally, it was found that carboxylic acid, alcohol, and amide functionalized ligands (**1.13**, **1.14**–**1.16**, and **1.17**, respectively) cause a reduction in reactivity compared to **1.5**.

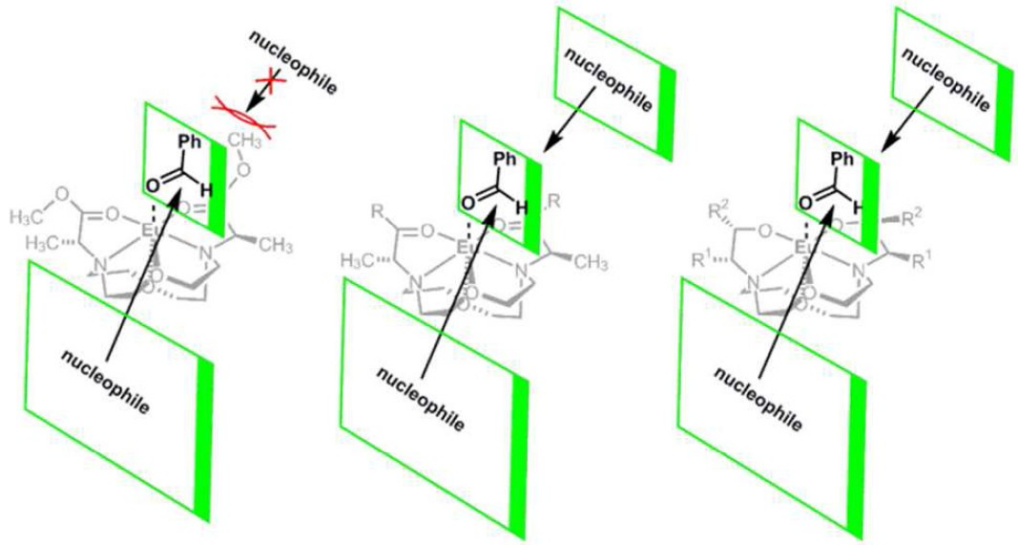

Figure 3.6. (left) Proposed selective nucleophilic attack at the *si* face of benzaldehyde (high selectivity and reactivity is observed). (middle) Precatalysts are non-selective when R is OH or NH_2. (right) Ligands **1.14**–**1.16** with Eu^{3+} are unable to block nucleophilic attack at either face of benzaldehyde likely due to the stereochemistry at the position of R^2 causing less blocking than with ligand **1.5**. Coordinated water has been omitted for clarity, additionally ligand **1.13** has been

drawn in the carboxylic acid form although it likely exists in the deprotonated state while coordinated to Eu^{3+} in aqueous media.

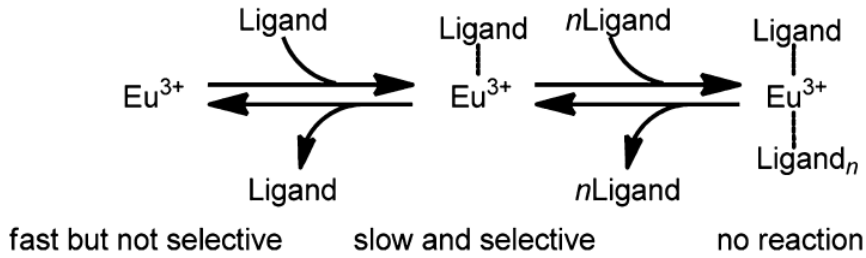

Figure 3.7. Proposed equilibria involving multiple Eu^{3+} species with reactivity summarized under the species. This equilibria is based on luminescence-decay, steady-state luminescence measurements, and ^{1}H-NMR data with reactivity and selectivity from Mukaiyama aldol reaction results.

3.6 Experimental section

Materials. Commercially available chemicals were used without further purification. Water was purified using a PURELAB Ultra Mk2 (ELGA) water purification system. (2*R*,2'*R*)-Dimethyl-2,2'- (1,7-dioxa-4,10-diazacyclododecane-4,10-diyl)dipropanoate (**1.5**),[3d] (2*R*,2'*R*)-2,2'-(1,7-dioxa-4,10-diazacyclododecane-4,10-diyl)dipropanoic acid (**1.13**),[3c] and (*Z*)-trimethyl(1-phenylpropyl-1-enyloxy)- trimethylsilane (**1.1**) (*Z*/*E* = 12:1)[17] were synthesized according to previously published procedures.

Characterization. Flash chromatography was performed using silica gel 60, 230–400 mesh.[26] Analytical TLC was carried out on TLC plates precoated with silica gel 60 F254 (250 μm layer thickness). TLC visualization was accomplished using a UV lamp. NMR spectra were obtained in the Lumigen Instrumentation Center at Wayne State University. ^{1}H-NMR and correlation spectroscopy (COSY) spectra were obtained using a Varian Mercury 400 (400 MHz) spectrometer, a Varian MR400 (400 MHz) spectrometer, or a Varian 500-S (500 MHz) spectrometer. ^{13}C-NMR, distortionless enhancement by polarization transfer (DEPT), and heteronuclear multiple quantum coherence (HMQC) spectra were obtained using a Varian Mercury 400 (100 MHz) spectrometer, a Varian MR400 (100 MHz) spectrometer, or a Varian

500-S (125 MHz) spectrometer. DEPT, COSY, and HMQC spectra were used to assign spectral peaks. Data for ^{1}H-NMR spectra are reported as follows: chemical shift (ppm) relative to residual $CHCl_3$ in $CDCl_3$ (7.27 ppm) or CHD_2OD in CD_3OD (3.31 ppm); multiplicity ("s" = singlet, "d" = doublet, "t" = triplet, "q" = quartet, "m" = multiplet, and "brs" = broad singlet); coupling constant, *J*, (Hz); assignment (italicized elements are responsible for the shifts); and integration. Data for ^{13}C-NMR spectroscopy are reported as ppm relative to CDCl3 (77.23 ppm) or CD_3OD (49.15 ppm) followed by assignment (italicized elements are responsible for the shifts). High-resolution electrospray ionization mass spectrometry (HRESIMS) was used to obtain high-resolution mass spectra on a Waters Micromass LCT Premier XE mass spectrometer electrospray time-of-flight high-resolution mass spectrometer. HPLC analyses were carried out on a Shimadzu instrument equipped with a Chiralpak AS-H column (Chiral Technologies Inc, 250 × 4.6 mm) using a binary isocratic method (pump A: 2-propanol; pump B: hexanes, flow rate 1.0 mL/min, isocratic, 90% A, 10% B, λ = 254 nm). Luminescence-decay measurements[1f,10,13] for the determination of water-coordination number, *q*, and steady-state luminescence measurements were performed using a HORIBA Jobin Yvon Fluormax-4 spectrofluorometer. Titration mixtures were vortexed using a Fisher Scientific vortex mixer before each measurement. Centrifugation was performed using a CentrificTM Centrifuge at 7000 rotations per minute (04-978-50, Fisher Scientific). Optical rotations were recorded using an Autopol III automatic polarimeter.

Synthesis and characterization of chiral ligands 1.14–1.17.

(2*S*,2'*S*)-1,1'-(1,7-dioxa-4,10-diazacyclododecane-4,10-diyl)bis(propan-2-ol) (1.14): To a stirring solution of 1,7-dioxa-4,10-diazacyclododecane (**3.4**) (0.040 g, 0.23 mmol) in methanol (2 mL) was added (*S*)-(–)-propylene oxide (**3.5**) (0.41 g, 7.0 mmol) at ambient temperature. After

12 h, the reaction mixture was filtered and concentrated under reduced pressure to yield a clear, colorless oil. Yield 61 mg, 91%: ^{1}H NMR (400 MHz, $CDCl_3$, δ): 5.33 (brs, O*H*, 2H), 3.78–3.67 (m, C*H*, 2H), 3.58–3.47 (m, CH_2, ring, 4H), 3.43–3.33 (m, CH_2 ring, 4H), 2.79–2.66 (m, CH_2 ring, 4H), 2.60–2.50 (m, CH_2 ring, 4H), 2.44–2.35 (m, CH_2 arm, 2H), 2.31–2.19 (m, CH_2 arm, 2H), 1.05 (d, CH_3, 6H). ^{13}C NMR (100 MHz, $CDCl_3$, δ): 69.5 (*C*H_2 ring), 64.3 (*C*H_2 arm) 64.2 (*C*H), 55.3 (*C*H_2 ring), 19.8 (*C*H_3). HRESIMS (*m*/*z*): $[M + H]^+$ calcd for $C_{14}H_{31}N_2O_4$, 291.2284; found 291.2289. $[\alpha]_D^{23}$+1.48 (*c* 1.35, CH_3OH).

(2*S*,2'*S*)-1,1'-(1,7-dioxa-4,10-diazacyclododecane-4,10-diyl)bis(butan-2-ol) (1.15): To a stirring solution of 1,7-dioxa-4,10-diazacyclododecane (**3.4**) (0.040 g, 0.23 mmol) in methanol (2 mL) was added (*S*)-(–)-1,2-epoxybutane (**3.6**) (0.51 g, 7.0 mmol) at ambient temperature. After 12 h, the reaction mixture was filtered and concentrated under reduced pressure to yield a clear, colorless oil. Yield 64 mg, 88%: ^{1}H NMR (400 MHz, $CDCl_3$, δ): 5.3 (s, O*H*, 2H), 3.61–3.37 (m, C*H* and CH_2, 10H), 2.83–2.71 (m, CH_2, 4H), 2.59–2.50 (m, CH_2, 4H), 2.48–2.40 (m, CH_2, 2H), 2.36–2.26 (m, CH_2, 2H), 1.51–1.28 (m, CH_3CH_2, 4H), 0.96 (t, *J* = 7.3Hz, CH_3, 6H). ^{13}C NMR (100 MHz, $CDCl_3$, δ): 70.0 (*C*H), 69.5 (*C*H_2), 62.6 (*C*H_2), 55.5 (*C*H_2), 27.5 (CH_3*C*H_2), 10.5 (*C*H_3). HRESIMS (*m*/*z*): $[M + H]^+$ calcd for $C_{16}H_{35}N_2O_4$, 319.2597; found 319.2596. $[\alpha]_D^{23}$ +1.28 (*c* 1.34, CH_3OH).

(2*R*,2'*R*)-2,2'-(1,7-dioxa-4,10-diazacyclododecane-4,10-diyl)bis(propan-1-ol) (1.16): To a stirring solution of **1.5** (0.038 g, 0.11 mmol) in tetrahydrofuran (1 mL) was added lithium aluminum hydride in tetrahydrofuran (0.27 mL, 2.0 M, 0.54 mmol) at ambient temperature. After 20 min of stirring, methanol (5 mL) was added followed by water (5 mL). The mixture was washed with CH_2Cl_2 (3 × 15 mL). Volatiles were removed under reduced pressure; water was added; the mixture was filtered; and water was removed under reduced pressure to yield a clear,

colorless oil. Yield 28 mg, 91%: ^{1}H NMR (400 MHz, $CDCl_3$, δ): 5.01–4.90 (m, O*H*, 2H), 3.60–3.52 (m, CH_2 ring, 4H), 3.45–3.24 (m, CH_2 ring and HOCH_2, 8H), 2.98–2.87 (m, C*H*, 2H), 2.83–2.74 (m, CH_2, ring, 4H), 2.56–2.47 (m, CH_2 ring, 4H), 0.82 (d, J = 6.5 Hz, CH_3, 6H). ^{13}C NMR (100 MHz, $CDCl_3$, δ): 69.9 (CH$_2$ ring), 64.1 (HOCH$_2$), 56.9 (CH), 49.5 (CH$_2$ ring), 9.34 (CH$_3$). HRESIMS (*m*/*z*): $[M + H]^+$ calcd for $C_{14}H_{31}N_2O_4$, 291.2284; found 291.2275. $[\alpha]_D^{23}$ +0.881 (*c* 0.267, CH_3OH).

(2*R*,2'*R*)-2,2'-(1,7-dioxa-4,10-diazacyclododecane-4,10-diyl)dipropanamide (1.17): To a mixture of 1,7-dioxa-4,10-diazacyclododecane (**3.4**) (0.050 g, 0.29 mmol) and Cs_2CO_3 (1.0 g, 3.1 mmol) in acetonitrile (4 mL) was added (*S*)-amino-1-oxypropan-2-yl-4-methylbenzenesulfonate (**3.7**) (0.21 g, 0.86 mmol), and the resulting mixture was stirred for 72 h at ambient temperature then centrifuged for 10 min. The supernatant was concentrated under reduced pressure and washed with diethyl ether (6 × 15 mL) to yield a white solid. Yield 67 mg, 74%: ^{1}H NMR (400 MHz, $CDCl_3$, δ): 8.16 (brs, NH_2, 2H), 5.44 (brs, NH_2, 2H), 3.70 (t, CH_2 J = 11.3 Hz, 4H), 3.44–3.31 (m, CH_2, C*H*, 6H), 2.94– 2.80 (m, CH_2, 4H), 2.60–2.48 (m, CH_2, 4H), 1.25 (d, CH_3, J = 7.5 Hz, 6H). ^{13}C NMR (100 MHz, $CDCl_3$, δ): 177.7 (CONH$_2$), 68.0 (CH$_2$), 59.1 (CH), 49.9 (CH$_2$), 8.6 (CH$_3$). HRESIMS (*m*/*z*): $[M + H]^+$ calcd for $C_{14}H_{29}N_4O_4$, 317.2189; found 317.2198. $[\alpha]_D^{23}$ +0.349 (*c* 1.16, CH_3OH).

(*S*)-amino-1-oxypropan-2-yl-4-methylbenzenesulfonate (3.7): To a stirring solution of (*S*)-2-hydroxypropanamide (1.00 g, 0.0112 mol) in a mixture of triethylamine and dichloromethane 1:5 v/v, 10 mL) was added 4-methylbenzene-1-sulfonyl chloride (2.35 g, 0.0123 mol) at ambient temperature. After 96 h, the crude reaction mixture was concentrated under reduced pressure and purified using flash chromatography (1:1 ethyl acetate/hexanes) to afford a fluffy white solid. Yield 704 mg, 26%: TLC *Rf* = 0.2 (1:1 ethyl acetate/hexanes). ^{1}H NMR (400 MHz, CD_3OD, δ): 7.83 (d, *J* = 8.3 Hz, C*H*, 2H), 7.45 (d, *J* = 8.3 Hz, C*H*, 2H), 4.82–4.73 (m, C*H*, 1H), 2.46 (s, C*H*3, 3H), 1.39 (d, *J* = 6.9 Hz, CH_3, 3H). ^{13}C NMR (100 MHz, CD_3OD, δ): 174.2 (*C*ONH_2), 147.1, 134.7, 131.3 (*C*H), 129.3 (*C*H), 77.4 (*C*H), 21.8 (*C*H_3), 19.4 (*C*H_3). HRESIMS (*m*/*z*): [M + H]$^+$ calcd for $C_{10}H_{14}NO_4S$, 244.0599; found 244.0644.

Titration experiment general procedure: Ligand-to-metal titrations were performed in a cuvette by adding solutions of ligand (11.0 mM in 9:1 EtOH/H_2O) to solutions of $Eu(OTf)_3$ (0.834 mM in 9:1 EtOH/H_2O). The resulting solutions were vigorously shaken using a vortex mixer for 20 s then allowed to stand for 5 min before acquiring emission spectra. Emission spectra were obtained by exciting at 395 nm (excitation and emission slit widths were set to 5 nm).

Mukaiyama aldol reaction general procedure: To a mixture of ligand and $Eu(OTf)_3$ in 9:1 ethanol/water (0.4 mL) at –25 °C was added benzaldehyde (**1.2**) (3.2 µL, 32 µmol, 1.0 equiv) followed by (*Z*)-trimethyl-(1-phenylpropyl-1-enyloxy)trimethylsilane (**1.1**) (11 µL, 48 µmol, 1.5 equiv). The mixture was stirred for 168 h at –25 °C. The mixture was then purified using silica gel chromatography (1:9 ethyl acetate/hexanes, R_f = 0.2), and volatiles were removed under

reduced pressure. The enantiomeric and diastereomeric ratios of the products were determined by HPLC.[23a]

3.7 Conclusions

We synthesized a series of new, chiral, Eu^{3+}-binding ligands. By spectroscopically characterizing the ligands and Eu^{3+} interactions using luminescence-decay, steady-state luminescence, and NMR spectroscopies, evidence suggesting that saturation of the Eu^{3+} coordination sphere by multiple hexadentate ligands occurs in the presence of excess ligand was found. A comparison of ligand functional groups and chiral center location and bulk provided insight into the factors that affectreactivity and selectivity of water-tolerant chiral precatalysts. It was found that the reactivity of Eu^{3+}-based precatalysts depends on the type of coordinating functional groups on the ligands, and that the selectivity of Eu^{3+}-based precatalysts depends on chiral center location and functional group size. The selectivity, reactivity, and spectroscopic characterizations described here contribute to the understanding of lanthanide-based precatalysts, and we expect these findings to be useful in the design of new precatalysts with high activity and selectivity for asymmetric carbon–carbon bond-forming reactions in aqueous media.

CHAPTER FOUR

Summary and Future Direction

4.1 Introduction

Chapter four begins with a summary of the findings that are described in detail in chapters two and three. Also, Chapter four contains a description of the implications of these results to the future use of enantioselective lanthanide-based precatalysts for bond-forming reactions. This chapter will conclude with a discussion of future efforts that can be carried out in an attempt to synthesize and study a reusable enantioselective tethered Ln^{3+}-based precatalyst for bond-forming reactions.

4.2 Summary of results from chapters two and three.

Chapters two and three are focused on the results from our contributions towards the development of Ln^{3+}-based precatalysts by monitoring changes in coordination, reactivity, and selectivity of Eu^{3+}-based precatalysts for Mukaiyama aldol reactions in aqueous media.[3d,8b,13] By studying the coordination and reactivity of Eu^{3+}-based precatalysts that used different anions (NO_3^- and OTf^-) in multiple solvent systems (Chapter two), we found that reactivity increases with increasing water-coordination numbers. The reactivity and *q* trends for precatalysts formed by $Eu(OTf)_3$ in different concentrations of water are quite similar (**Figure 1.5**), while precatalysts formed by $Eu(NO_3)_3$ continued to become more reactive (reactivity was proportional to H_2O content) at higher water concentrations even though *q* values did not reach a maximum. This result is likely due to differences in binding ability of $NO3^-$ verses OTf^-, based on *q* data it is likely that a NO_3^- ligand remains bound to Eu^{3+}. The study contributes toward the future design

of Ln^{3+}-based precatalysts in aqueous media because a correlation between reactivity and *q* has been discovered.

As described in Chapter three, it was found that the reactivity and selectivity of Mukaiyama aldol reactions are highly dependent on ligand identity and that an excess of hexadentate ligand can greatly slow Mukaiyama aldol reactions (**Figure 1.10**). Further, we found that hexadentate ligands with the ability to become negatively charged drastically reduce the reactivity of Ln^{3+}-based precatalysts in Mukaiyama aldol reactions (**Table 3.2**). These findings are important for future studies because the reactivity and stereospecific outcome of bond-forming reactions depends on ligand features such as donor type, denticity, stoichiometry (compared to Ln^{3+}), and chiral center location and bulk.

4.3 Future Direction

If implemented properly, water-tolerant Ln^{3+} ions have the ability to be highly reactive, enantioselective, and recoverable precatalysts for bond-forming reactions. These features make Ln^{3+} ions useful in organic synthesis because they can catalyze a variety of organic reactions such as the aldol, Mukaiyama aldol, nitro aldol, epoxide opening, Mannich, Michael, Friedel–Crafts, and Diels–Alder reactions. A limiting factor for the use of Ln^{3+} ions in the field of organic synthesis is the implementation and recovery.

Our research was primarily focused on Eu^{3+}-catalyzed Mukaiyama aldol reactions so that we could study changes in reactivity and selectivity while using luminescence measurements to monitor the coordination environments of Eu^{3+}. However, other reactions (aldol, nitro aldol, epoxide opening, Mannich, Michael, Friedel–Crafts, and Diels–Alder reactions) have the ability to be catalyzed by Ln^{3+} ions and should be investigated with precatalysts made from Ln^{3+} with

ligands similar to **1.5**. In general Ln^{3+}-based precatalysts would be more useful if they could be rapidly recovered by simply washing away substrates, and products.

A tethered (ligand covalently attached to a solid support) precatalyst may help to make Ln^{3+}-based precatalysts more sustainable and easy to use because the precatalyst can likely be recovered by washing the solid support. Attachment of a hexadentate ligand to a solid support could be achieved by converting ligand **1.13** into an activated diester using *N*-hydroxysuccinimide and combining the activated diester with an amine functionalized resin.

Monitoring reactivity of precatalysts can be carried out using HPLC analyses similar to the work described in Chapter two. Enantioselectivity of reactions could be studied using chiral HPLC analyses and any Ln^{3+} leaching could be monitored by analyzing the resin washings using inductively coupled plasma mass spectrometry. Finally, it will be useful to monitor any changes in reactivity and selectivity as a function of reuse cycle number, this can be accomplished by washing the resin and reusing the resin-bound precatalyst. The ideas presented here are likely to contribute toward the development of easy to use, highly selective and reusable precatalysts.

APPENDIX A

Page	Contents
58	Table of Contents
59	Tabulated *q* values and steady-state reaction rates for $Eu(OTf)_3$ and $Eu(NO_3)_3$ catalyzed Mukaiyama aldol reactions.

Table A1. Mean water-coordination numbers (q) of $Eu(OTf)_3$ in mixtures of H_2O/THF and steady-state reaction rates of 7 mol % $Eu(OTf)_3$ catalyzed Mukaiyama aldol reactions in mixtures of H_2O/THF.[1] Error represents standard error of the mean of between 3 and 9 measurements.

% H_2O in THF (v/v)	q	error	steady-state reaction rate (μMs^{-1})	error
0	nd		0.289	0.062
1	5.8	0.05	0.327	0.033
5	8.0	0.05	1.04	0.158
10	8.3	0.03	1.39	0.167
15	8.6	0.02	1.47	0.164
20	8.6	0.05	nd	
25	8.6	0.05	1.45	0.082
30	8.5	0.04	nd	
40	8.5	0.01	1.25	0.135

nd = not determined

Table A2. Mean water-coordination numbers (q) of $Eu(NO_3)_3$ in mixtures of H_2O/THF and steady-state reaction rates of 7 mol % $Eu(NO_3)_3$ catalyzed Mukaiyama aldol reactions in mixtures of H_2O/THF. Error represents standard error of the mean of between 3 and 9 measurements.

% H_2O in THF (v/v)	q	error	steady-state reaction rate (μMs^{-1})	error
1	3.2	0.02	0.0084	0.001
5	5.2	0.04	0.107	0.024
10	6.8	0.03	0.325	0.058
15	7.2	0.03	0.476	0.042
20	7.2	0.04	nd	
25	7.4	0.04	0.954	0.192
30	7.6	0.05	nd	
40	7.7	0.01	1.27	0.162

nd = not determined

APPENDIX B

Page	Contents
60	Table of Contents
61–64	^{1}H- and ^{13}C-NMR spectra for ligands **1.14–1.17**
65	^{1}H- and ^{13}C-NMR spectra for **3.7**
66–68	Chiral HPLC chromatograms for Mukaiyama aldol products
69–68	Tabulated emission intensity ratios from titrations
74–75	Tabulated luminescence-decay rates
76–83	^{1}H-NMR spectra of ligands **1.5**, **1.13**–**1.17** with and without Eu^{3+}

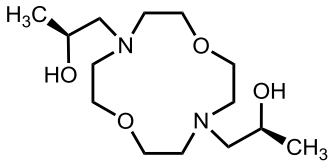
H3C
HO
N
O
OH
O
N
CH3

1.14

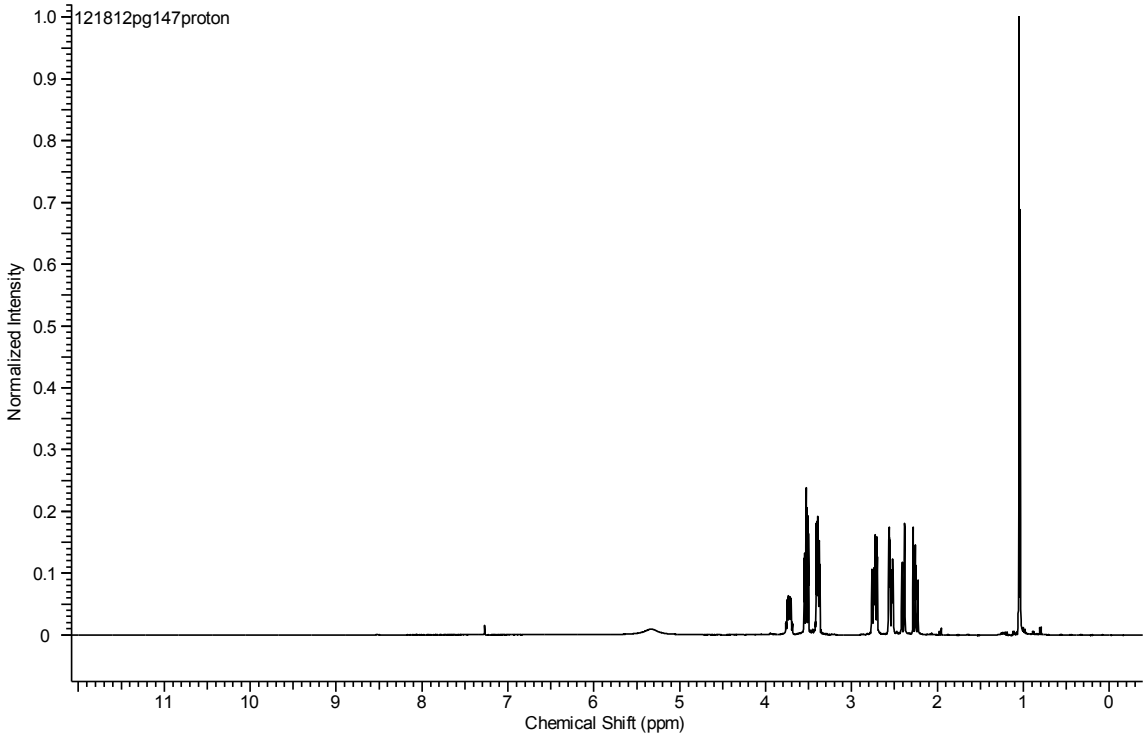
121812pg147proton
Normalized Intensity
Chemical Shift (ppm)

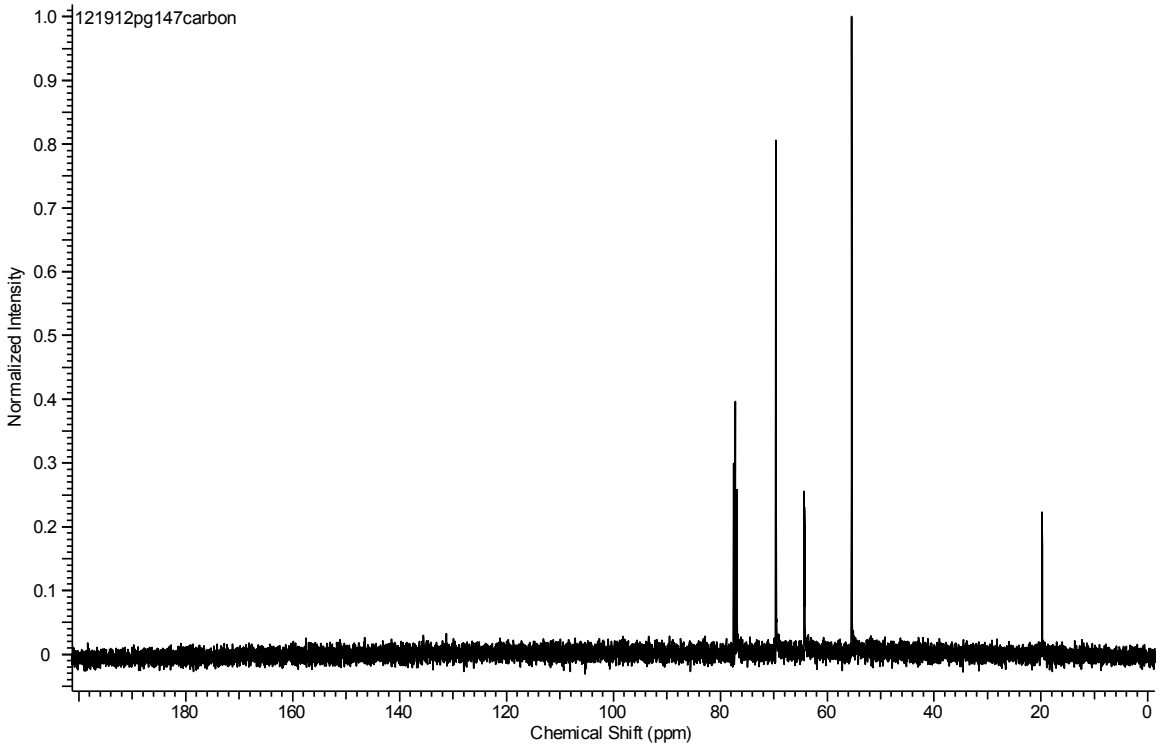
121912pg147carbon
Normalized Intensity
Chemical Shift (ppm)

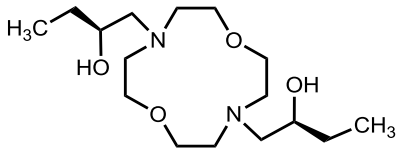
H3C
HO
N
O
O
N
OH
CH3

1.15

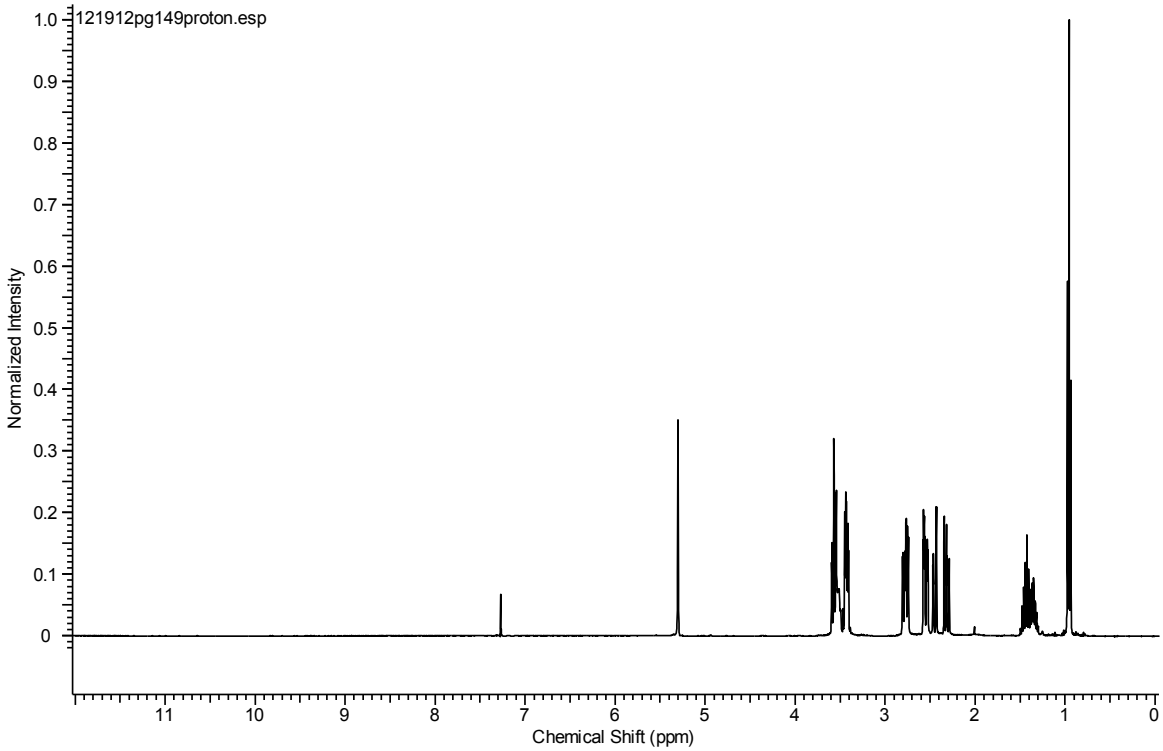
121912pg149proton.esp
Normalized Intensity
Chemical Shift (ppm)

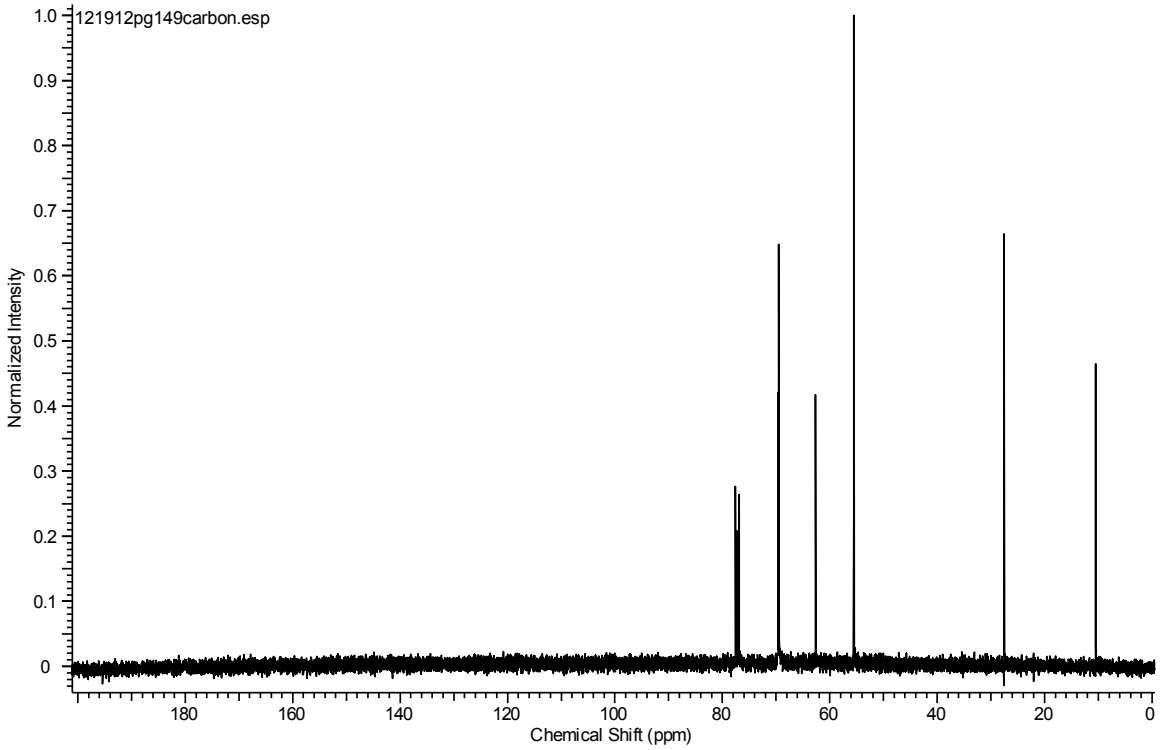
121912pg149carbon.esp
Normalized Intensity
Chemical Shift (ppm)

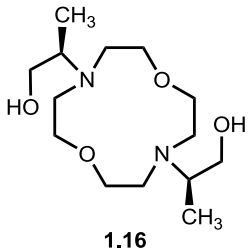
CH3
N
O
HO
OH
O
N
CH3

1.16

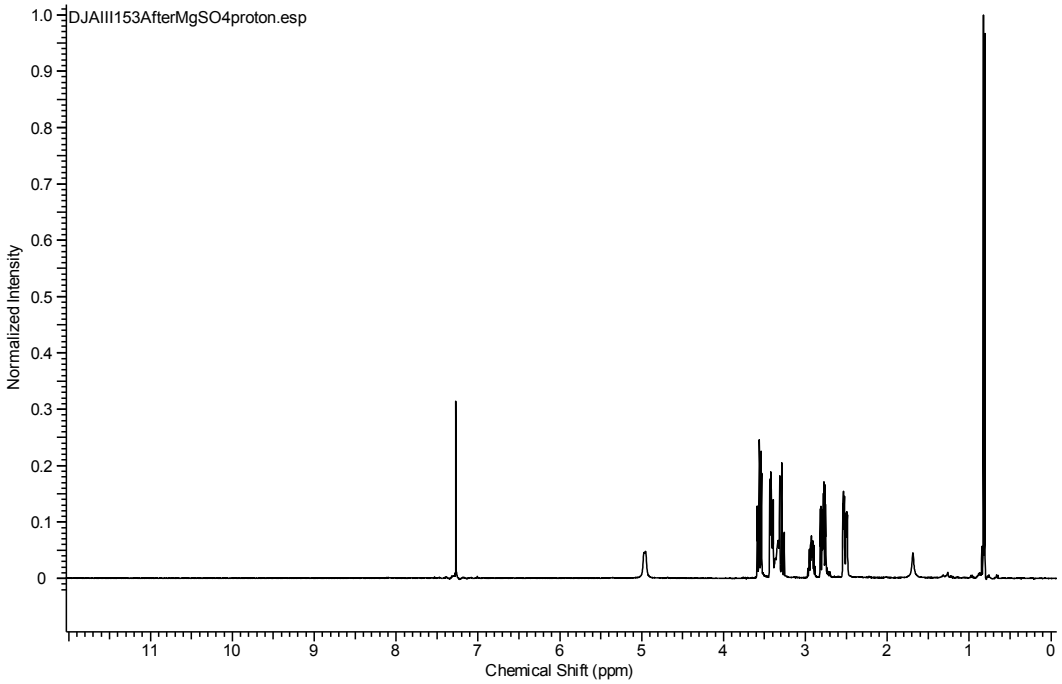
DJAIII153AfterMgSO4proton.esp
Normalized Intensity
Chemical Shift (ppm)

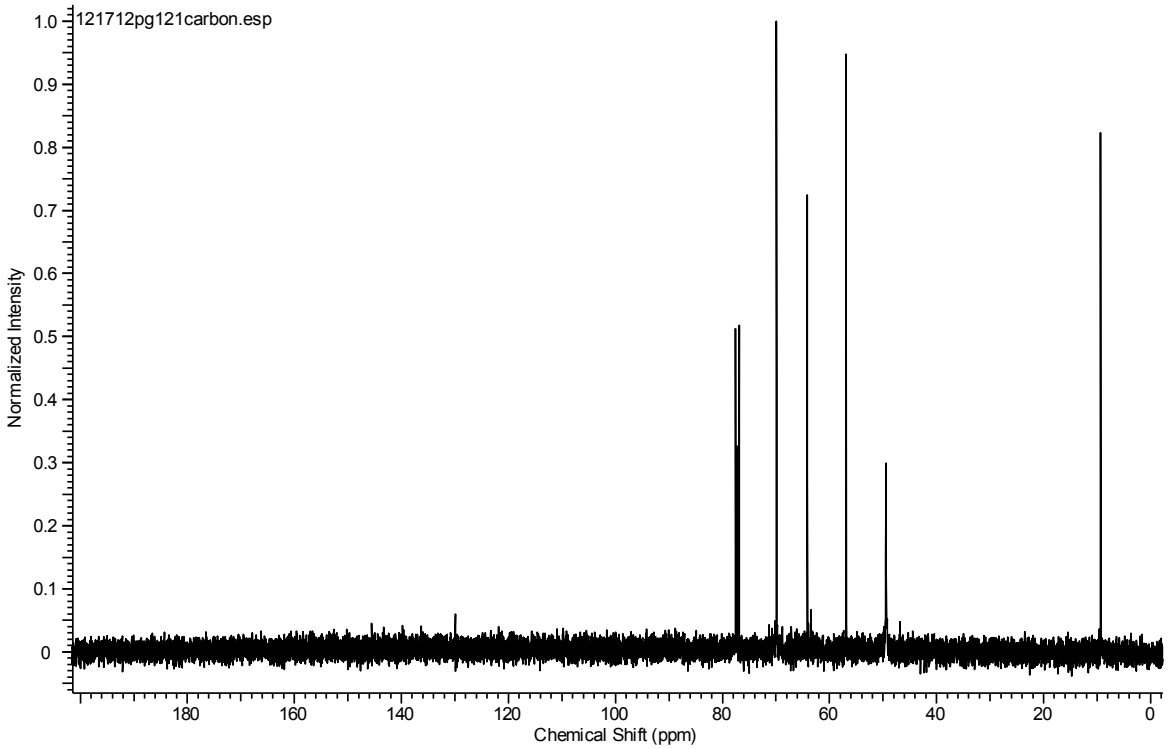
121712pg121carbon.esp
Normalized Intensity
Chemical Shift (ppm)

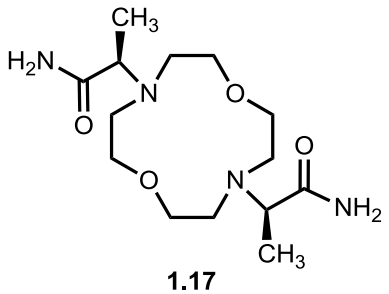
CH3
H2N
N
O
O
O
O
N
NH2
CH3

1.17

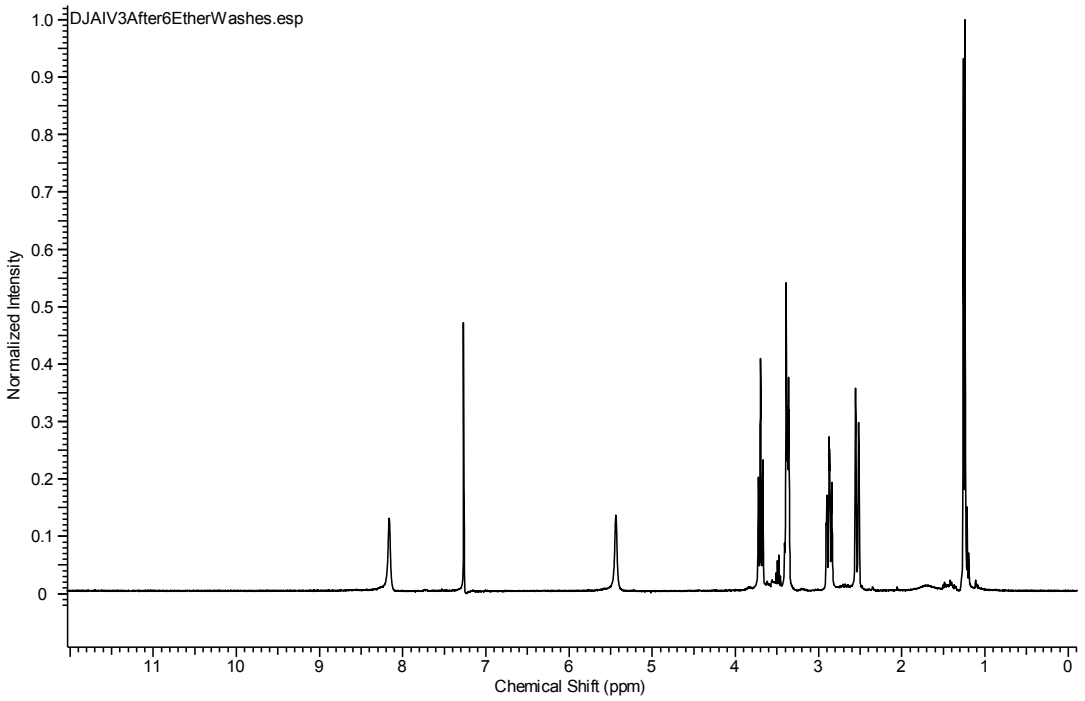
DJAIV3After6EtherWashes.esp
Normalized Intensity
Chemical Shift (ppm)

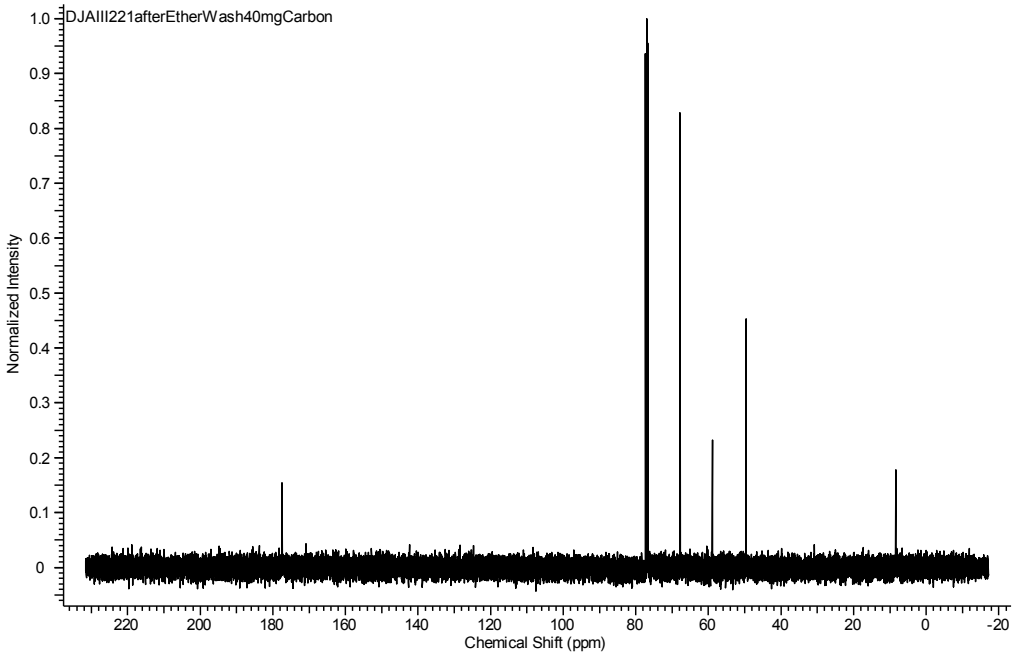
DJAIII221afterEtherWash40mgCarbon
Normalized Intensity
Chemical Shift (ppm)

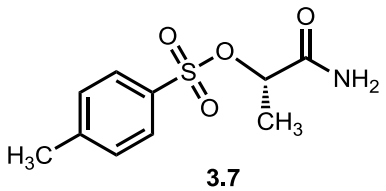
O
O
S
O
O
NH2
CH3
H3C

3.7

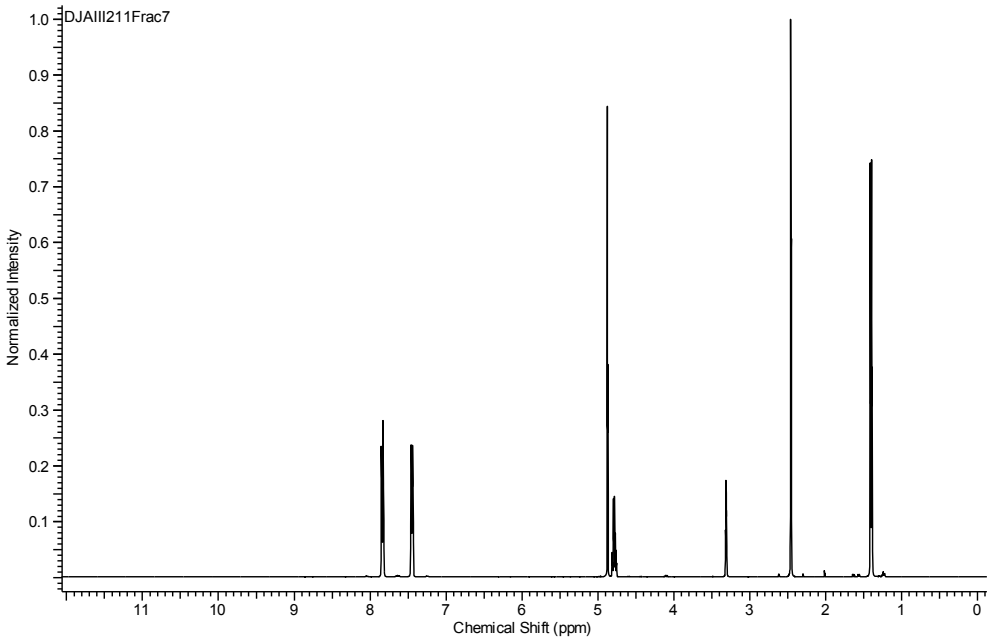
DJAIII211Frac7
Normalized Intensity
Chemical Shift (ppm)

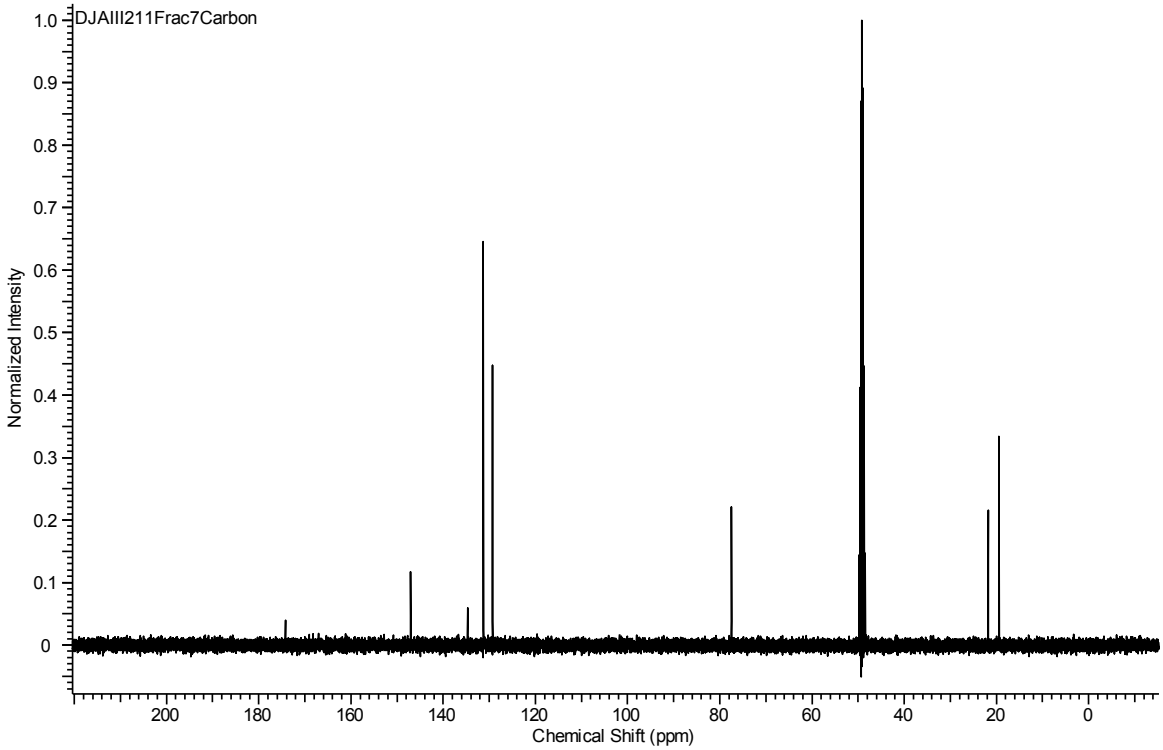
DJAIII211Frac7Carbon
Normalized Intensity
Chemical Shift (ppm)

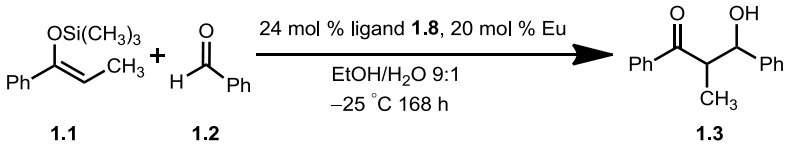
OSi(CH3)3
Ph
CH3
O
H
Ph
24 mol % ligand 1.8, 20 mol % Eu
EtOH/H2O 9:1
–25 °C 168 h
O
OH
Ph
Ph
CH3
1.1
1.2
1.3

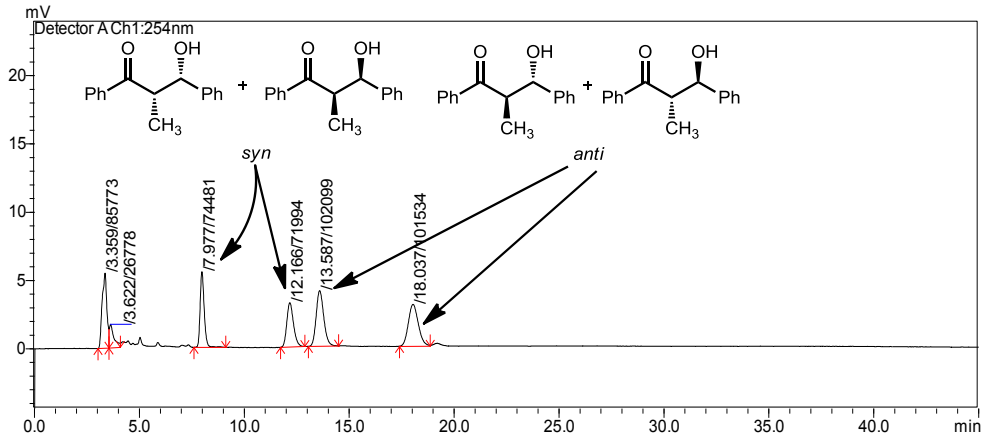
mV
Detector A Ch1:254nm
syn
anti
/3.359/85773
/3.622/26778
/7.977/74481
/12.166/71994
/13.587/102099
/18.037/101534
min

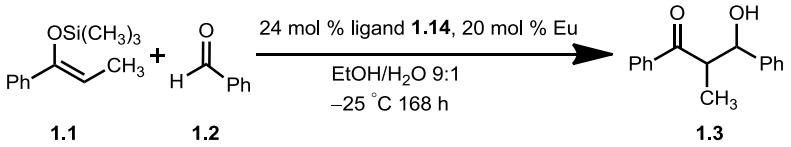
OSi(CH3)3
Ph
CH3
O
H
Ph
24 mol % ligand 1.14, 20 mol % Eu
EtOH/H2O 9:1
–25 °C 168 h
O
OH
Ph
Ph
CH3
1.1
1.2
1.3

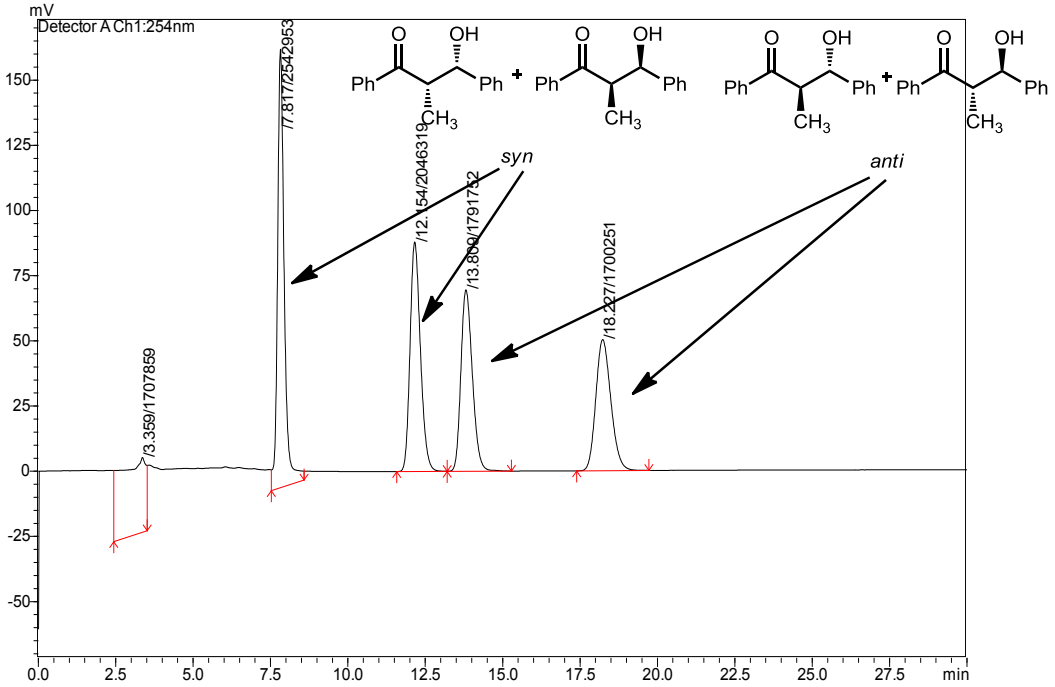
mV
Detector A Ch1:254nm
syn
anti
/3.359/1707859
/7.817/2542953
/12.154/2046319
/13.809/1791752
/18.227/1700251
min

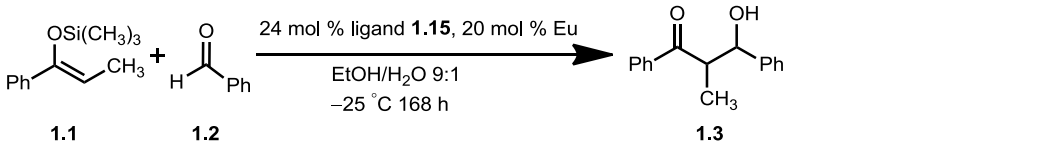

1.1 **1.2** **1.3**

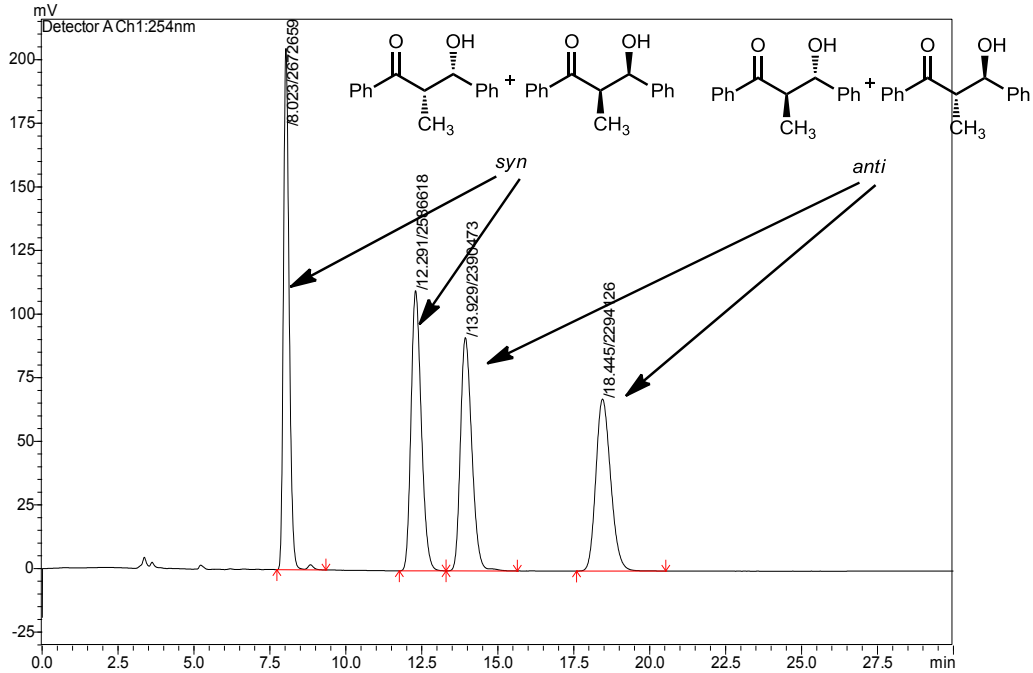

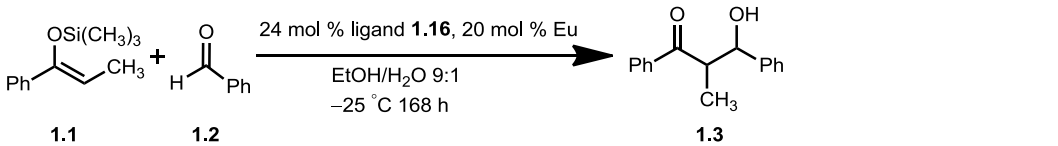

1.1 **1.2** **1.3**

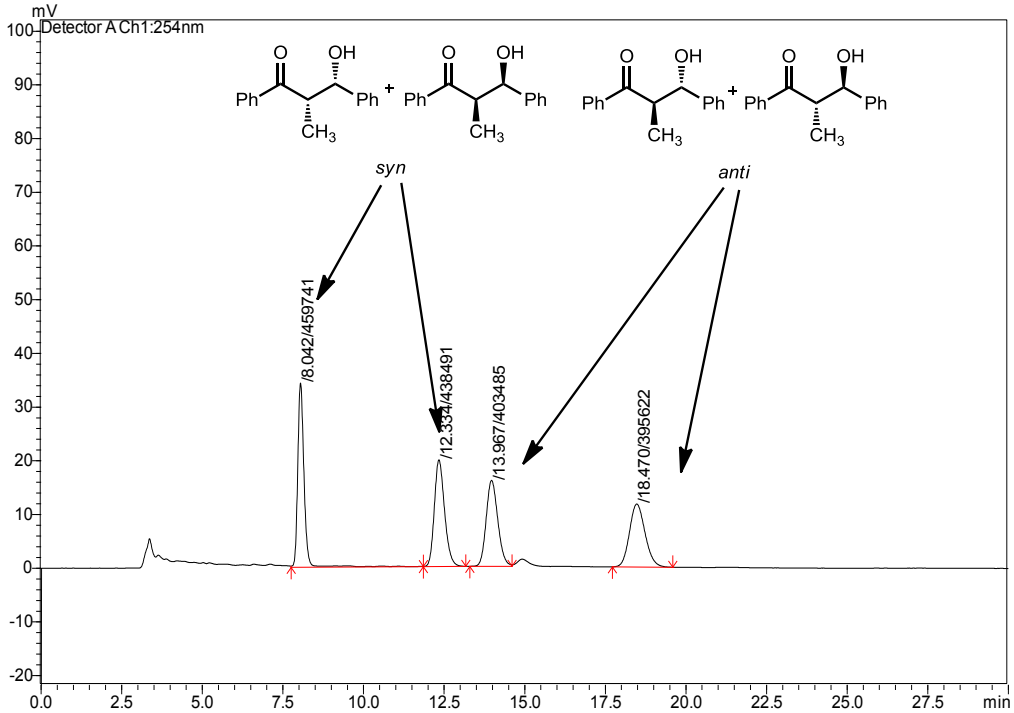

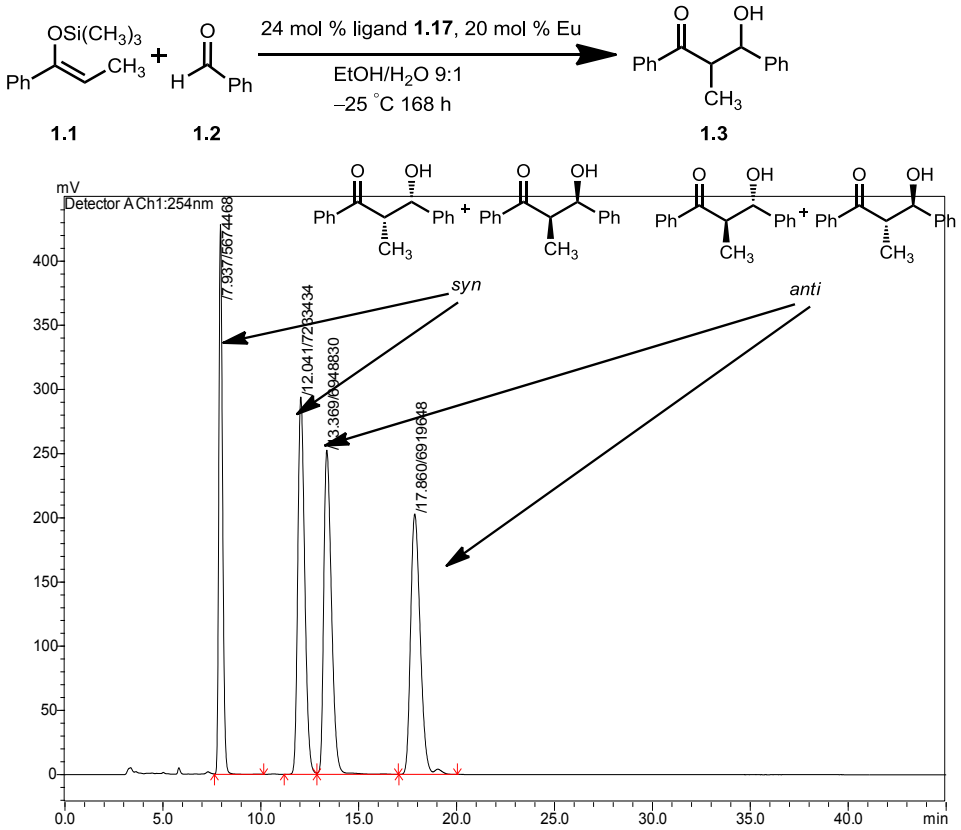
24 mol % ligand 1.17, 20 mol % Eu
EtOH/H2O 9:1
–25 °C 168 h
1.1
1.2
1.3
mV
Detector A Ch1:254nm
syn
anti
min

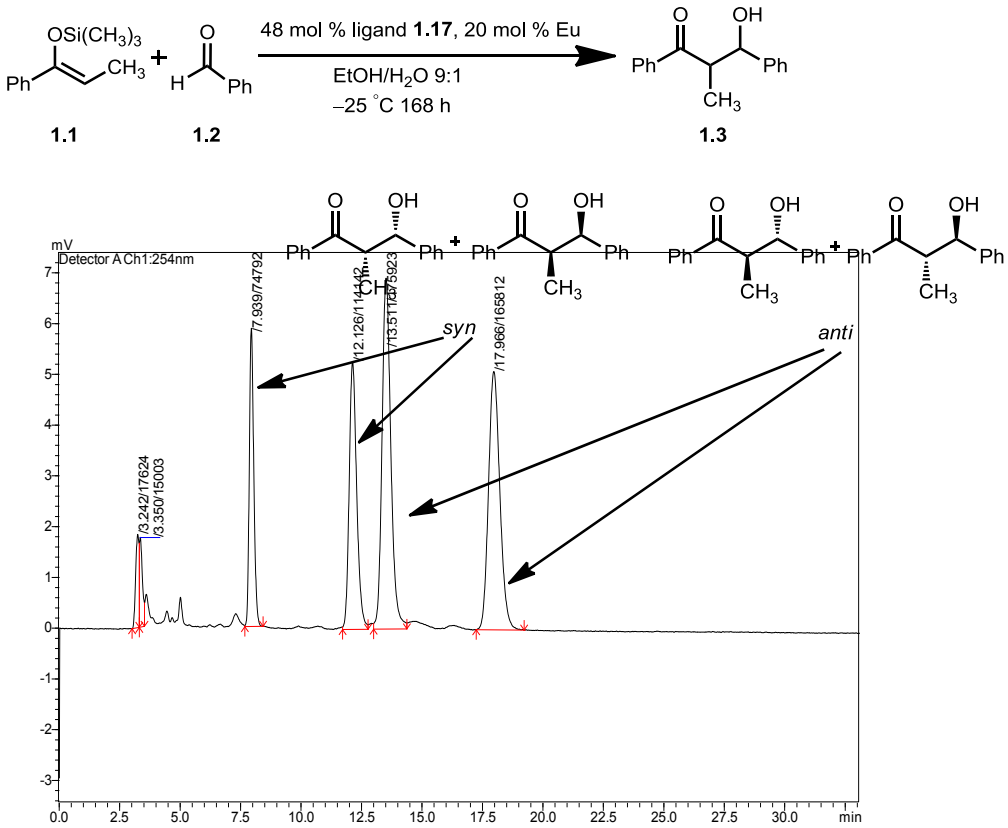
48 mol % ligand 1.17, 20 mol % Eu
EtOH/H2O 9:1
–25 °C 168 h
1.1
1.2
1.3
mV
Detector A Ch1:254nm
syn
anti
min

Ligand **1.5** and $Eu(OTf)_3$ titrations monitored by Eu^{3+} emission intensity ratio of 616 nm/591 nm.

ligand-to-Eu^{3+} ratio	**emission intensity ratio 616 nm/591 nm average of 3 titrations**	**standard error of the mean**
0:1	0.58	0.01
0.37:1	0.71	0.01
0.74:1	0.86	0.01
1.1:1	0.97	0.01
1.5:1	1.05	0.01
2.2:1	1.14	0.01
2.9:1	1.21	0.01
4.4:1	1.34	0.01
5.9:1	1.53	0.02
7.4:1	1.72	0.01

Ligand **1.13** and $Eu(OTf)_3$ titrations monitored by Eu^{3+} emission intensity ratio of 616 nm/591 nm.

ligand-to-Eu^{3+} ratio	**emission intensity ratio 616 nm/591 nm average of 3 titrations**	**standard error of the mean**
0:1	0.58	0.01
0.56:1	1.57	0.01
1.1:1	2.20	0.04
1.7:1	2.72	0.04
2.2:1	3.02	0.03
2.8:1	3.14	0.02
3.3:1	3.22	0.02
3.9:1	3.22	0.01
4.5:1	3.27	0.01
5.0:1	3.27	0.02
6.1:1	3.28	0.01
6.7:1	3.29	0.02
7.2:1	3.30	0.02

Ligand **1.14** and $Eu(OTf)_3$ titrations monitored by Eu^{3+} emission intensity ratio of 616 nm/591 nm.

ligand-to-Eu^{3+} ratio	**emission intensity ratio 616 nm/591 nm average of 3 titrations**	**standard error of the mean**
0:1	0.58	0.00
1.5:1	1.44	0.03
2.9:1	2.07	0.02
4.4:1	2.25	0.02
5.9:1	2.28	0.02
7.4:1	2.31	0.01

Ligand **1.15** and $Eu(OTf)_3$ titrations monitored by Eu^{3+} emission intensity ratio of 616 nm/591 nm.

ligand-to-Eu^{3+} ratio	**emission intensity ratio 616 nm/591 nm average of 3 titrations**	**standard error of the mean**
0:1	0.58	0.00
1.5:1	1.30	0.01
2.9:1	1.65	0.01
4.4:1	1.70	0.01
5.9:1	1.62	0.02
7.4:1	1.57	0.03

Ligand **1.16** and $Eu(OTf)_3$ titrations monitored by Eu^{3+} emission intensity ratio of 616 nm/591 nm.

ligand-to-Eu^{3+} ratio	**emission intensity ratio 616 nm/591 nm average of 3 titrations**	**standard error of the mean**
0:1	0.58	0.00
0.6:1	0.99	0.00
1.2:1	1.43	0.02
1.8:1	1.81	0.02
2.4:1	2.12	0.01
3.0:1	2.21	0.02
3.6:1	2.23	0.01
4.2:1	2.21	0.02
4.8:1	2.21	0.02
5.4:1	2.24	0.01
6.0:1	2.27	0.02

Ligand **1.17** and $Eu(OTf)_3$ titrations monitored by Eu^{3+} emission intensity ratio of 616 nm/591 nm.

ligand-to-Eu^{3+} ratio	**emission intensity ratio 616 nm/591 nm average of 3 titrations**	**standard error of the mean**
0:1	0.58	0.00
0.6:1	0.88	0.01
1.2:1	1.07	0.01
1.8:1	1.22	0.01
2.4:1	1.34	0.01
3.0:1	1.47	0.02
3.6:1	1.56	0.01
4.2:1	1.63	0.02
4.8:1	1.67	0.01
5.4:1	1.71	0.01
6.0:1	1.71	0.01

Eu^{3+} luminescence-decay rates in the presence of 1, 2, or 6 equivalents of ligand (average of three independently prepared samples).

Ligand **1.5**

ligand-to-Eu^{3+} ratio	**mean luminescence-decay rate (ms^{-1}) ± standard error in H_2O**	**mean luminescence-decay rate (ms^{-1}) ± standard error in D_2O**
1:1	–3.75 ± 0.07	–0.62 ± 0.01
2:1	–2.69 ± 0.01	–0.68 ± 0.01
6:1	–1.96 ± 0.03	–0.59 ± 0.00

Ligand **1.13**

ligand-to-Eu^{3+} ratio	**mean luminescence-decay rate (ms^{-1}) ± standard error in H_2O**	**mean luminescence-decay rate (ms^{-1}) ± standard error in D_2O**
1:1	–2.75 ± 0.03	–0.69 ± 0.00
2:1	–1.53 ± 0.01	–0.60 ± 0.00
6:1	–0.83 ± 0.00	–0.57 ± 0.00

Ligand **1.14**

ligand-to-Eu^{3+} ratio	**mean luminescence-decay rate (ms^{-1}) ± standard error in H_2O**	**mean luminescence-decay rate (ms^{-1}) ± standard error in D_2O**
1:1	–3.80 ± 0.03	–0.88 ± 0.00
2:1	–3.82 ± 0.03	–1.01 ± 0.01
6:1	–3.11 ± 0.01	–1.09 ± 0.03

Ligand **1.15**

ligand-to-Eu^{3+} ratio	**mean luminescence-decay rate (ms^{-1}) ± standard error in H_2O**	**mean luminescence-decay rate (ms^{-1}) ± standard error in D_2O**
1:1	–3.53 ± 0.01	–0.84 ± 0.01
2:1	–3.84 ± 0.01	–1.22 ± 0.01

Ligand **1.16**

ligand-to-Eu^{3+} ratio	**mean luminescence-decay rate (ms^{-1}) ± standard error in H_2O**	**mean luminescence-decay rate (ms^{-1}) ± standard error in D_2O**
1:1	–3.61 ± 0.01	–0.77 ± 0.00
2:1	–3.85 ± 0.02	–0.99 ± 0.01
6:1	–2.26 ± 0.02	–0.71 ± 0.00

Ligand **1.17**

ligand-to-Eu^{3+} ratio	**mean luminescence-decay rate (ms^{-1}) ± standard error in H_2O**	**mean luminescence-decay rate (ms^{-1}) ± standard error in D_2O**
1:1	–4.25 ± 0.02	–0.59 ± 0.00
2:1	–3.61 ± 0.01	–0.62 ± 0.01
6:1	–2.64 ± 0.02	–0.72 ± 0.00

Ligand 1.5, ^{1}H-NMR spectrum at –25 °C in 9:1 CD_3CD_2OD–D_2O with 1,1,1,2,2-pentachloroethane standard

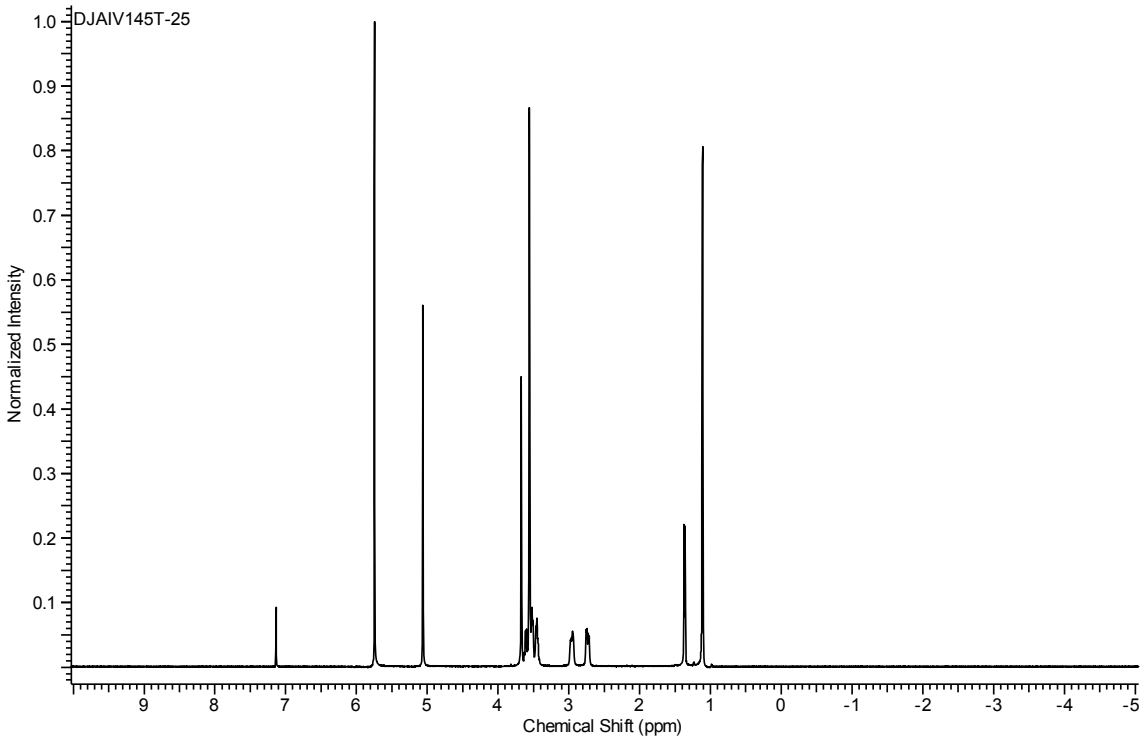

3-to-1 Ligand 1.5 to $Eu(OTf)_3$, ^{1}H-NMR spectrum at –40 °C in 9:1 CD_3CD_2OD–D_2O with 1,1,1,2,2-pentachloroethane standard

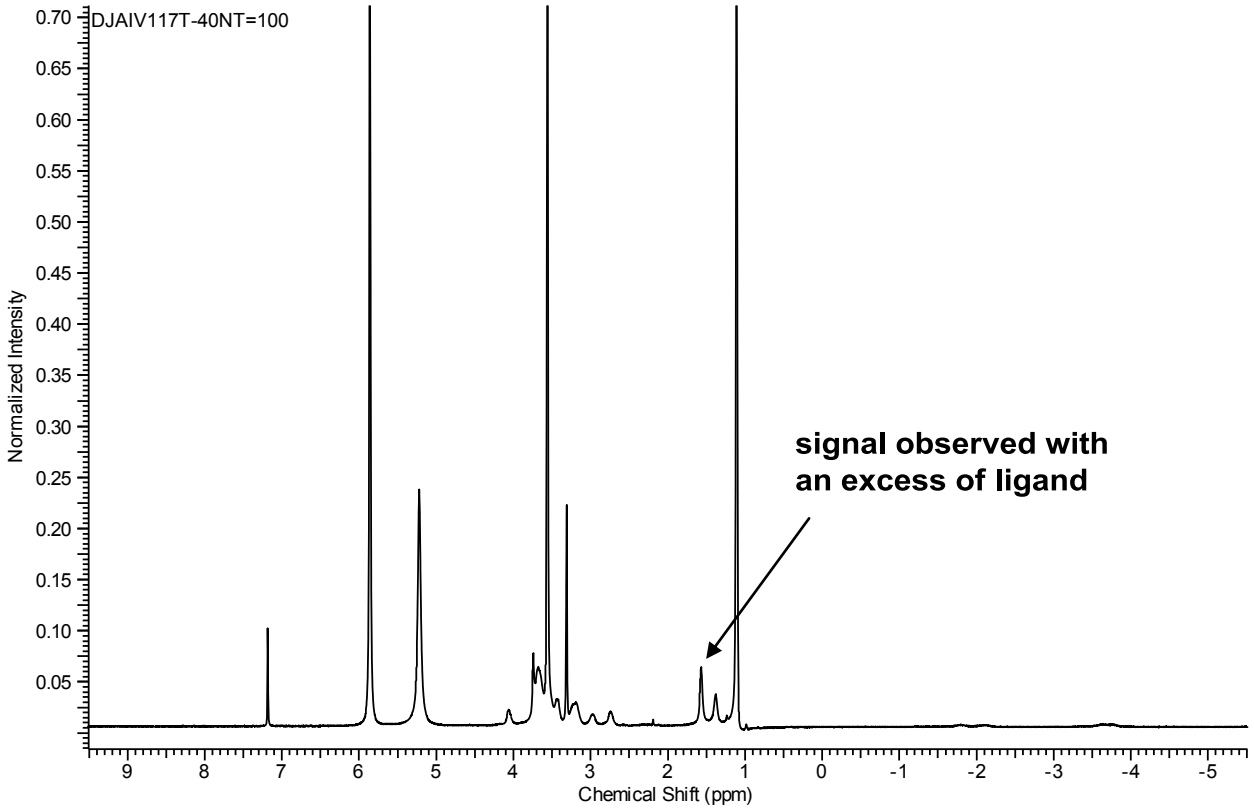

0.6-to-1 ligand 1.5 to $Eu(OTf)_3$, ^{1}H-NMR spectrum at –25 °C in 9:1 CD_3CD_2OD–D_2O with 1,1,1,2,2-pentachloroethane standard

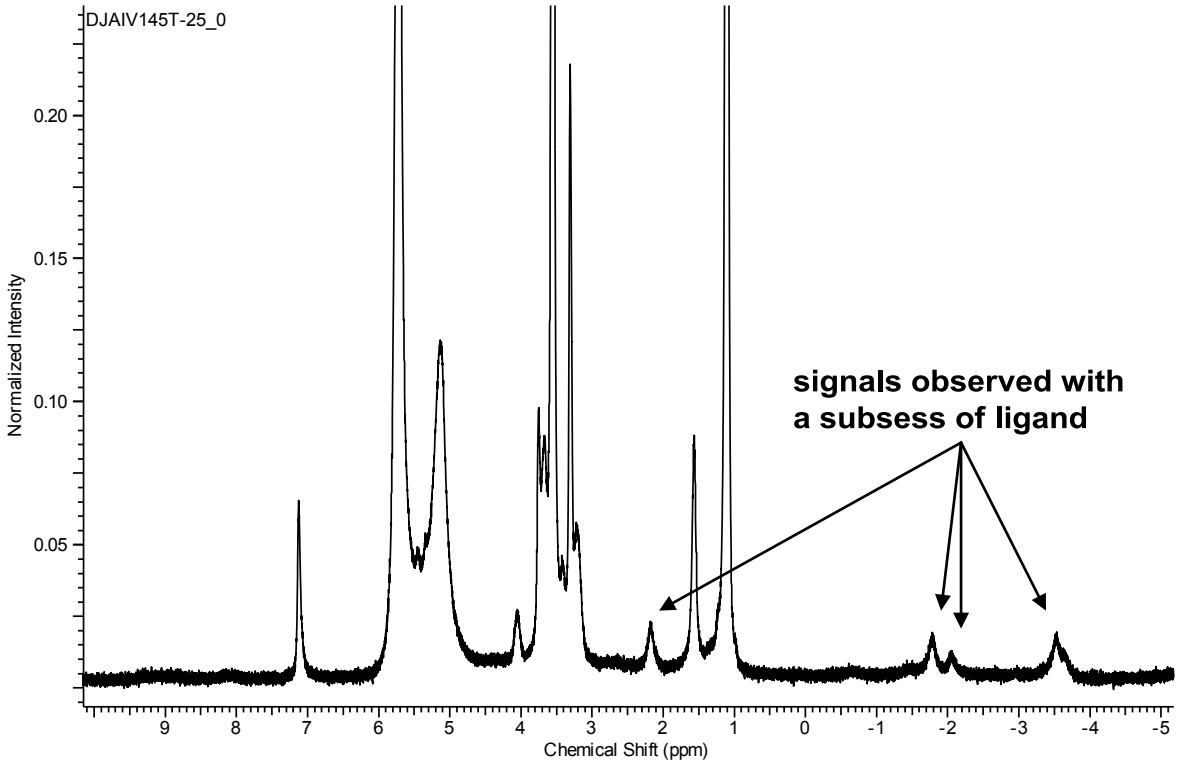

Ligand 1.13, ^{1}H-NMR spectrum at 4 °C in D_2O

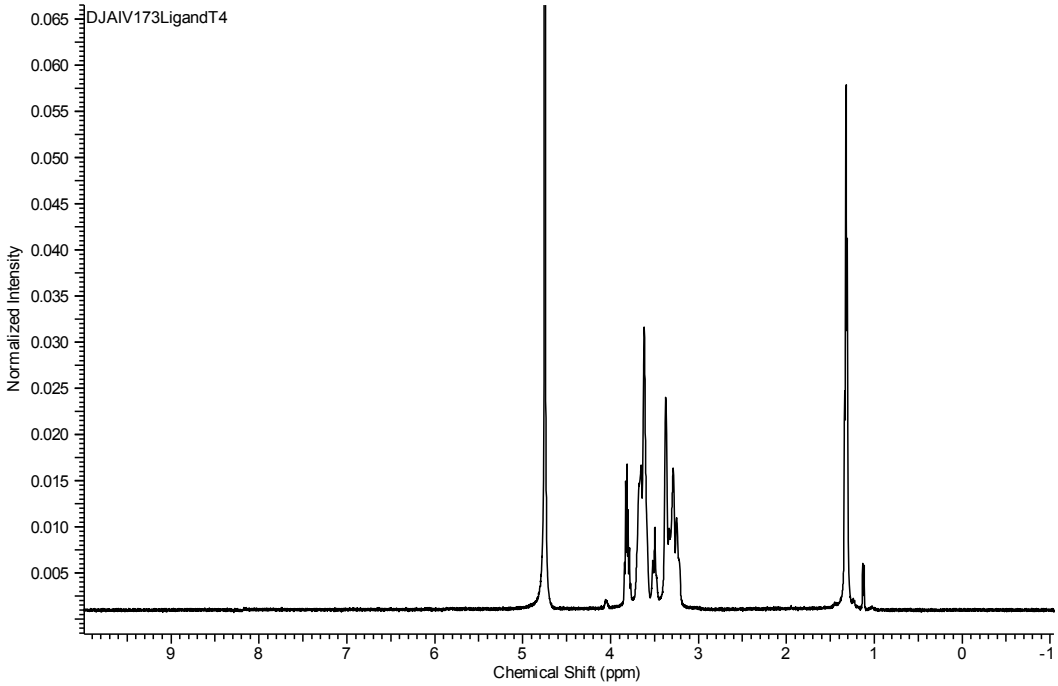

4-to-1 ligand 1.13 to $Eu(OTf)_3$, ^{1}H-NMR spectrum at 4 °C in 9:1 $CD_3CD_2OD–D_2O$

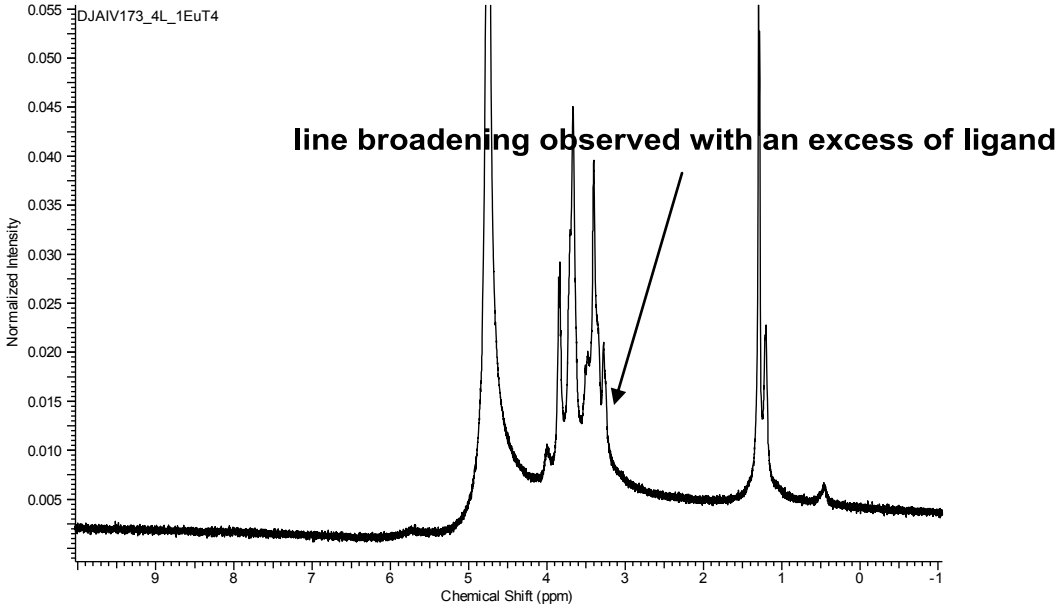

0.6-to-1 ligand 1.13 to $Eu(OTf)_3$, ^{1}H-NMR spectrum at –25 °C in 9:1 $CD_3CD_2OD–D_2O$

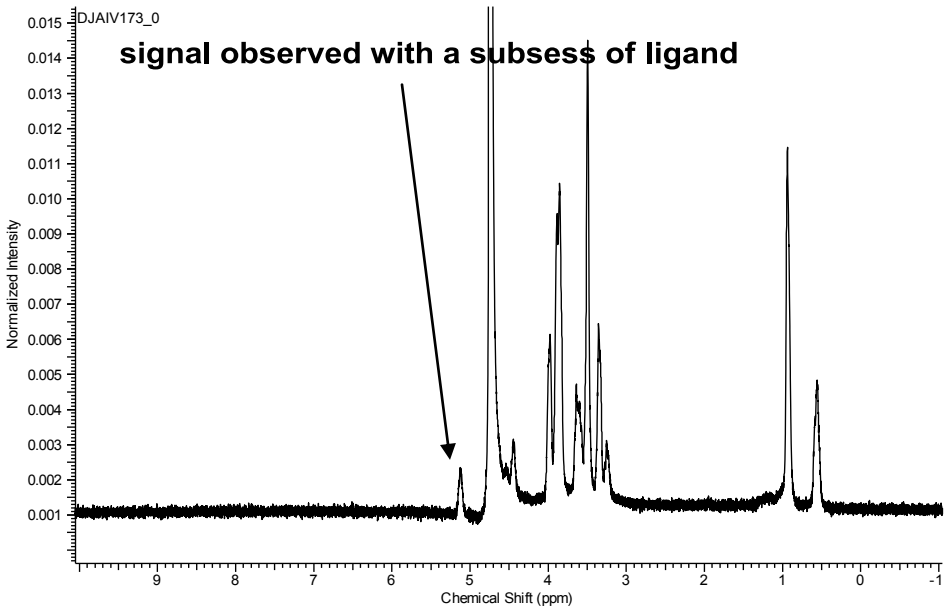

Ligand 1.15, ^{1}H-NMR spectrum at –25 °C in 9:1 CD_3CD_2OD–D_2O with 1,1,1,2,2-pentachloroethane standard

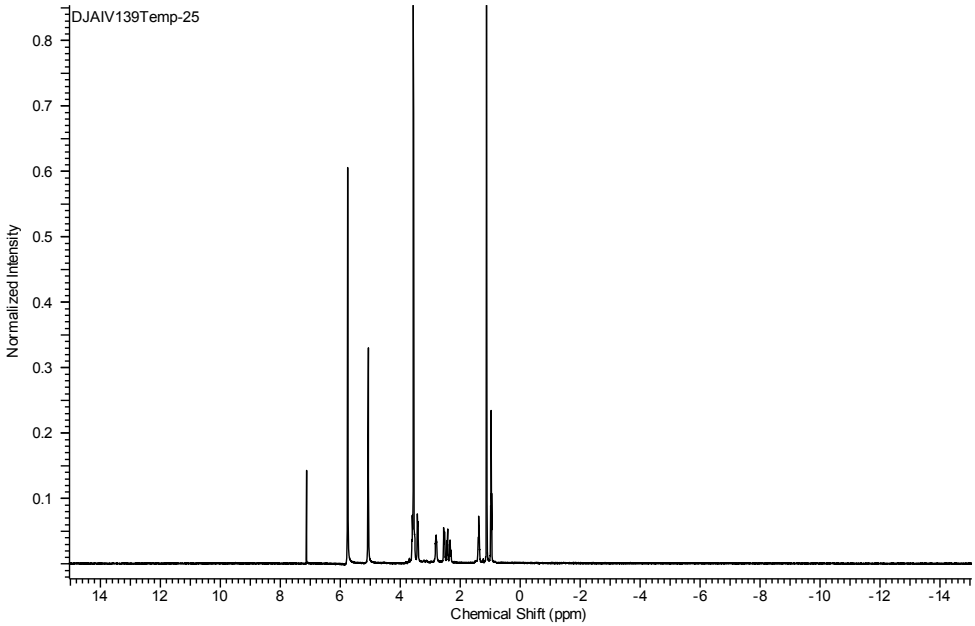

3-to-1 ligand 1.15 to $Eu(OTf)_3$, ^{1}H-NMR spectrum at –25 °C in 9:1 CD_3CD_2OD–D_2O with 1,1,1,2,2-pentachloroethane standard

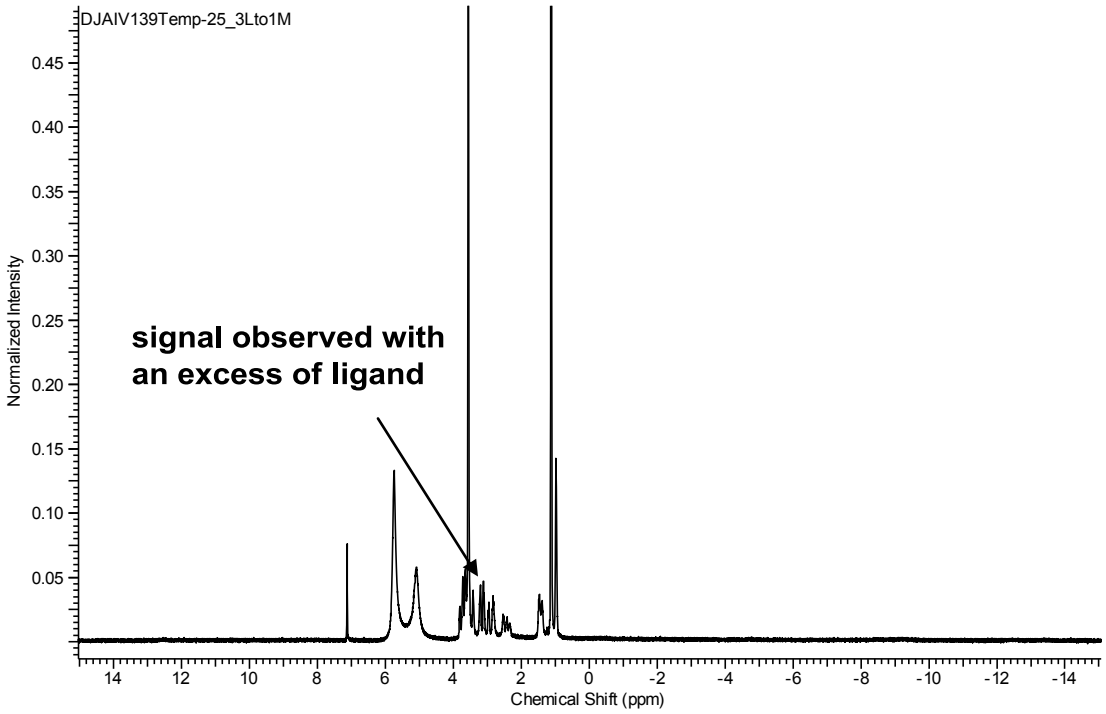

0.6-to-1 ligand 1.15 to $Eu(OTf)_3$, ^{1}H-NMR spectrum at –25 °C in 9:1 CD_3CD_2OD–D_2O with 1,1,1,2,2-pentachloroethane standard

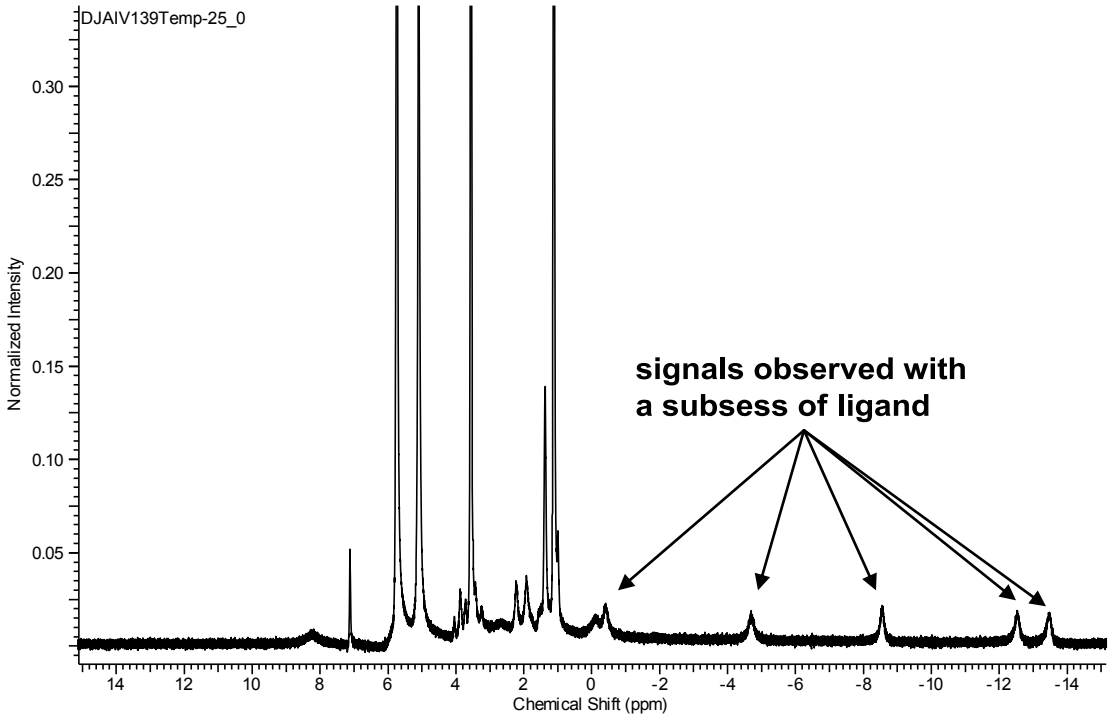

Ligand 1.16, ^{1}H-NMR spectrum at –25 °C in 9:1 CD_3CD_2OD–D_2O with 1,1,1,2,2-pentachloroethane standard

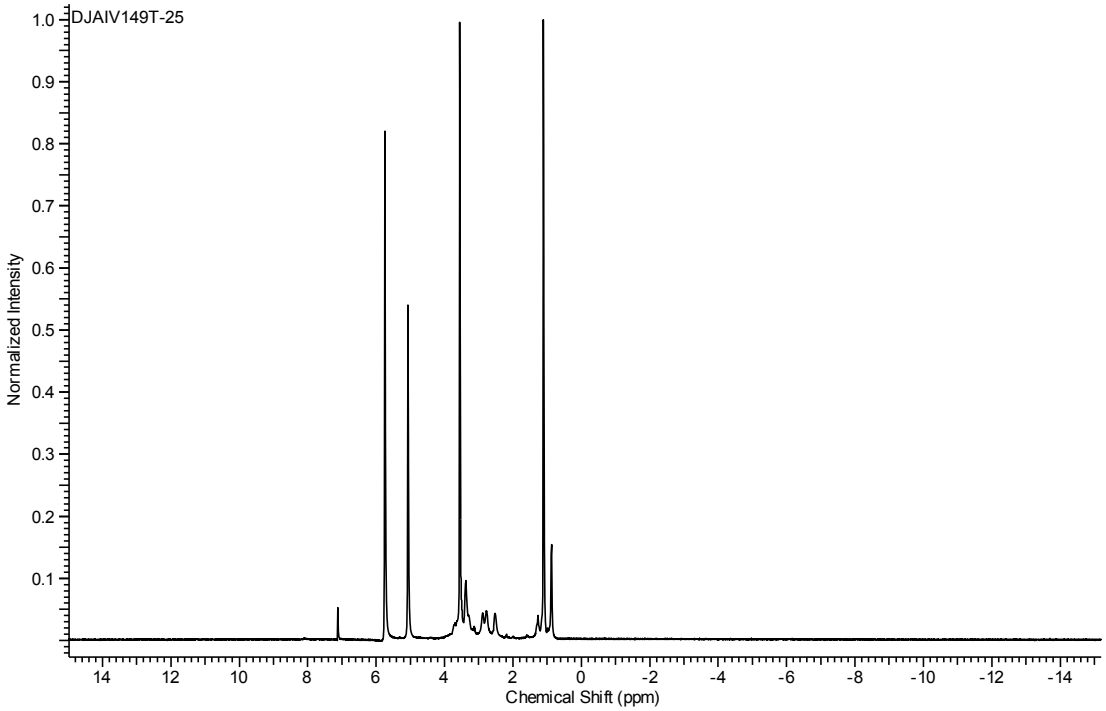

3-to-1 ligand 1.16 to $Eu(OTf)_3$, ^{1}H-NMR spectrum at –25 °C in 9:1 CD_3CD_2OD–D_2O with 1,1,1,2,2-pentachloroethane standard

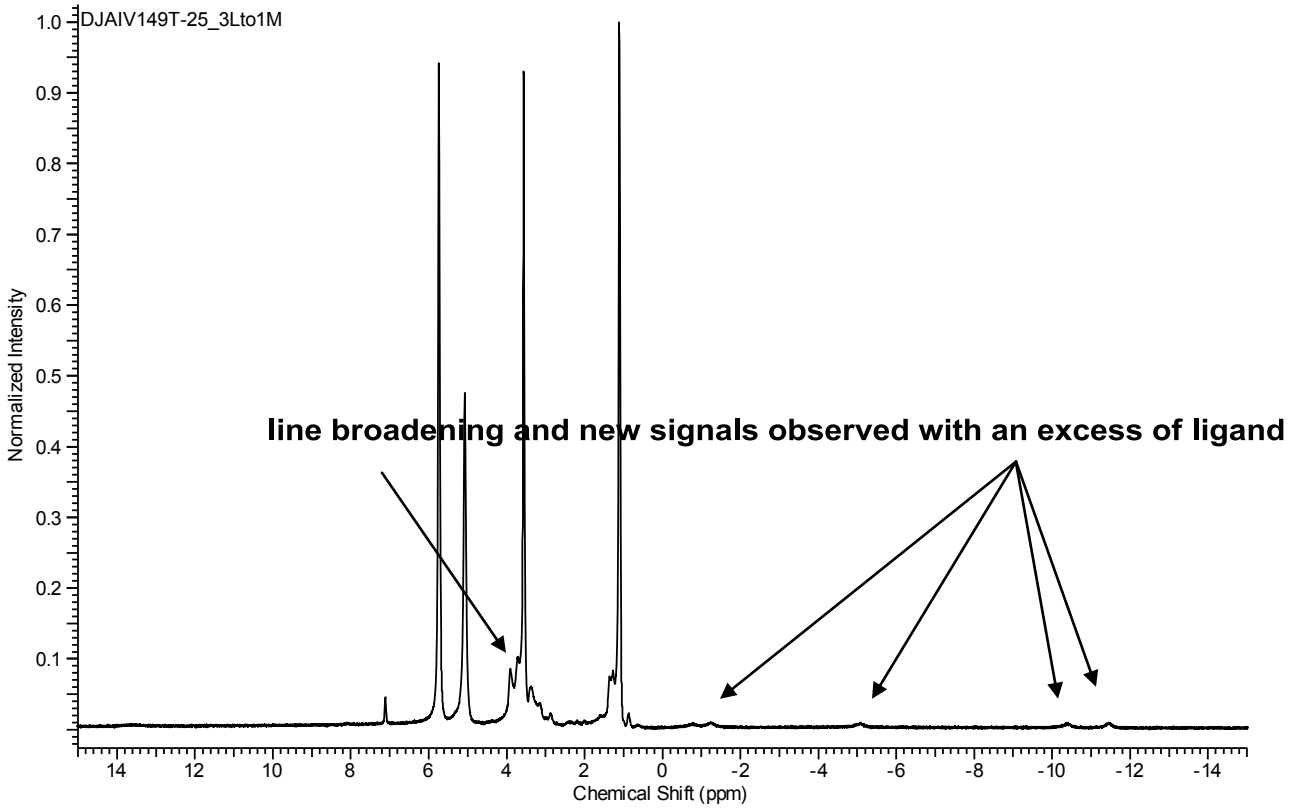

0.6-to-1 ligand 1.16 to $Eu(OTf)_3$, ^{1}H-NMR spectrum at –25 °C in 9:1 CD_3CD_2OD–D_2O with 1,1,1,2,2-pentachloroethane standard

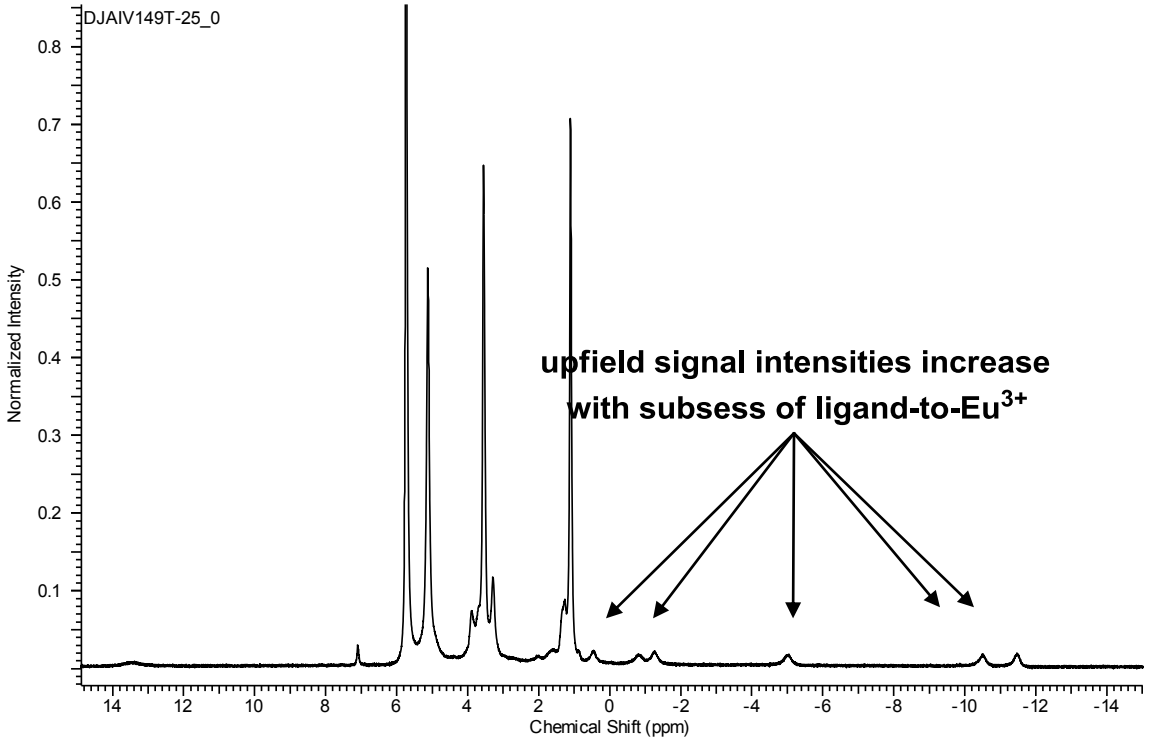

Ligand 1.17, ^{1}H-NMR spectrum at –25 °C in 9:1 CD_3CD_2OD–D_2O with 1,1,1,2,2-pentachloroethane standard

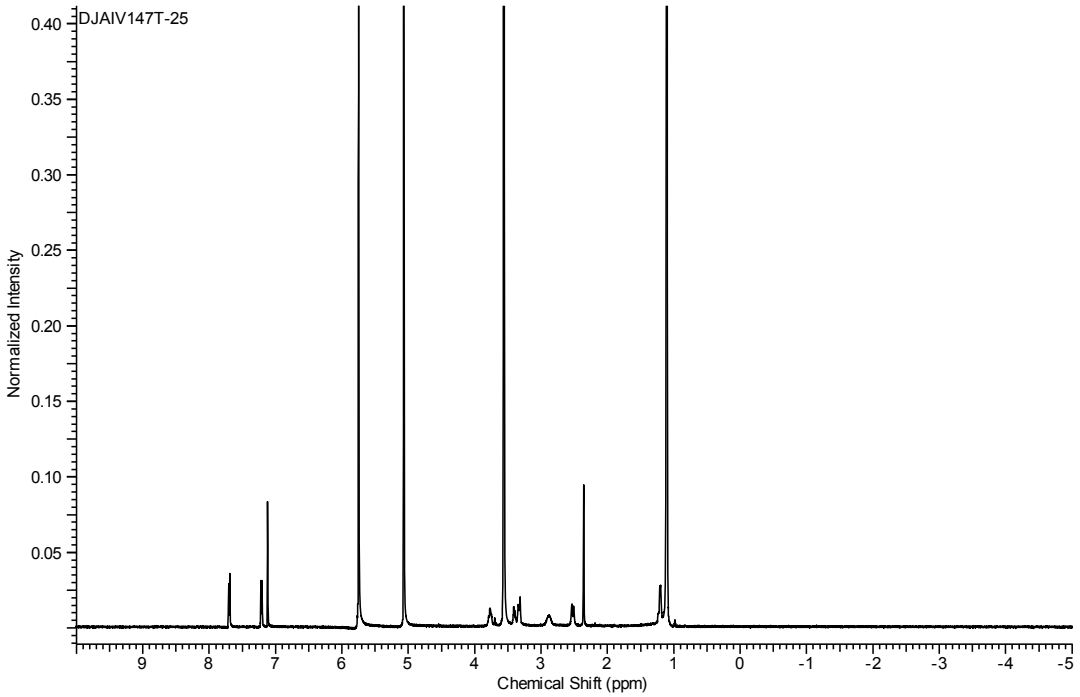

6-to-1 ligand 1.17 to $Eu(OTf)_3$, ^{1}H-NMR spectrum at –25 °C in 9:1 CD_3CD_2OD–D_2O with 1,1,1,2,2-pentachloroethane standard

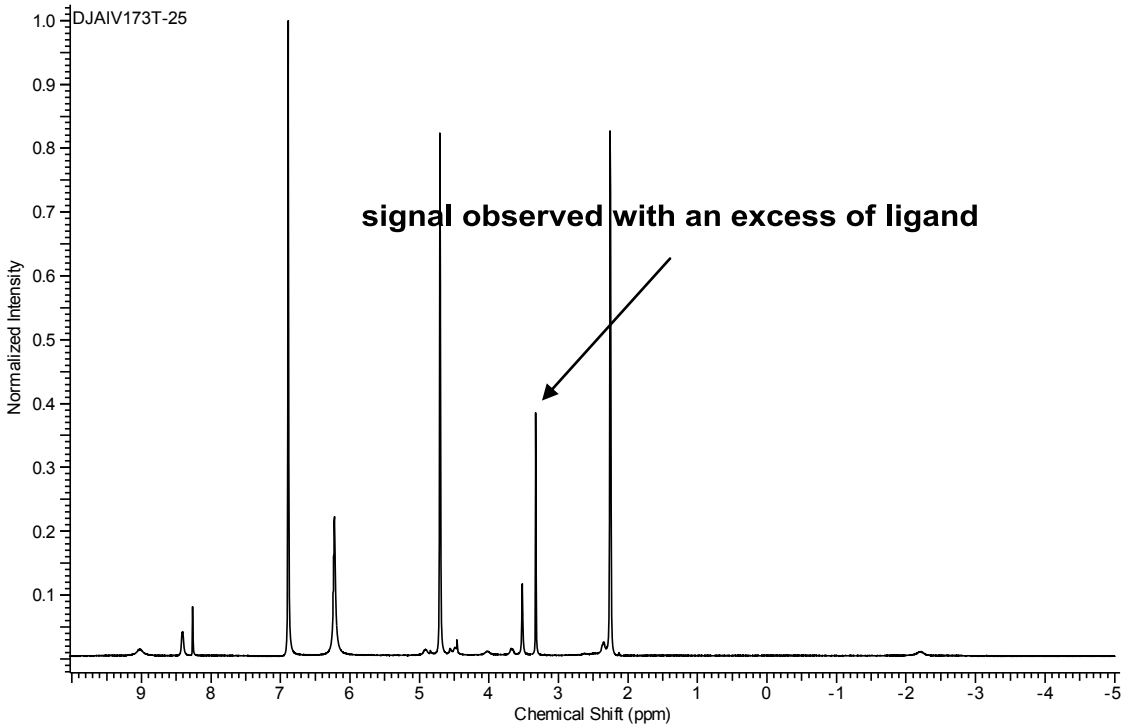

0.6-to-1 ligand 1.17 to $Eu(OTf)_3$, ^{1}H-NMR spectrum at –25 °C in 9:1 CD_3CD_2OD–D_2O with 1,1,1,2,2-pentachloroethane standard

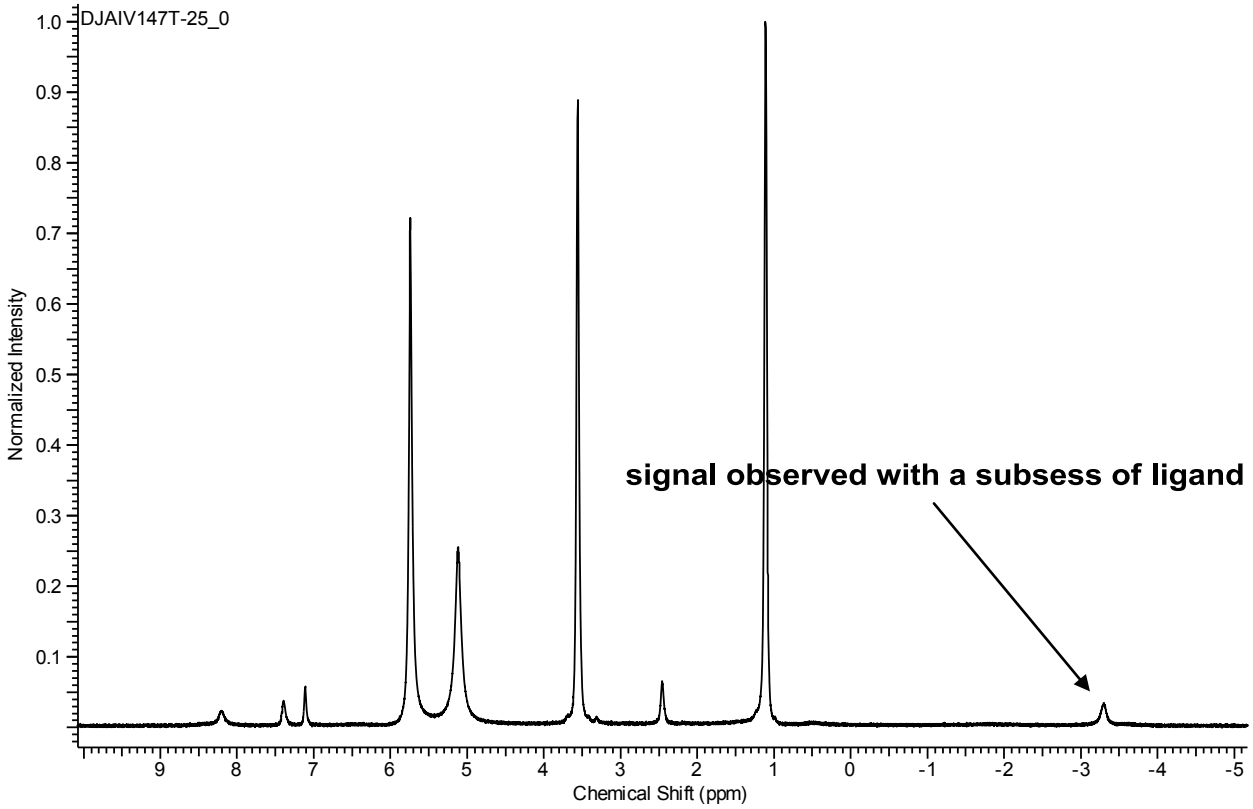

APPENDIX C

Page	Contents
85	Tetraaza crown ethers studied
86	Results and discussion
87	Experimental section
88	Conclusions

Introduction

In addition to exploring ligands **1.5** and **1.13**–**1.17**, tetraaza crown ether ligands **C1** and **C2** (Figure C1) were investigated. We hypothesized that ligands with the same chiral functional groups as **1.5** and either two alcohol donor arms or two methyl groups attached to the macrocyle would afford selective and stable metal complexes when mixed with Eu^{3+} in aqueous mixtures. Ligand **C1** was synthesized to test if alcohol sidearms increase Eu^{3+}-binding ability compared to **1.5**, and **C2** was synthesized with methyl substitutions to test if the substitutions could sterically hinder 2:1 ligand-to-metal interactions and, consequently, increase the reactivity of Eu^{3+}-based precatalysts compared to **1.5**. Briefly, ligand **C1** was synthesized by functionalizing two amines of 1,4,7,10-tetraazadodecane with alcohol sidearms and then adding chiral methyl ester sidearms to the remaining amines as shown in **Scheme C1**. Ligand **C2** was synthesized by functionalizing two amines of 1,4,7,10-tetraazadodecane with methyl groups followed by the subsequent addition of chiral methyl ester sidearms as shown in **Scheme C2**.

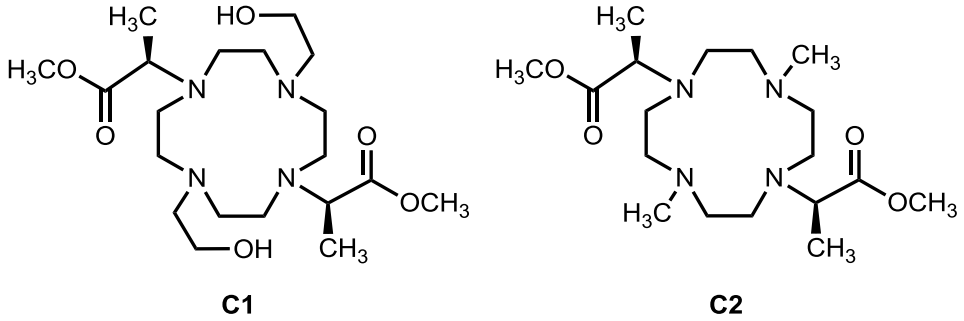

Figure C1. Tetraaza crown ether ligands synthesized for testing in Mukaiyama aldol reactions.

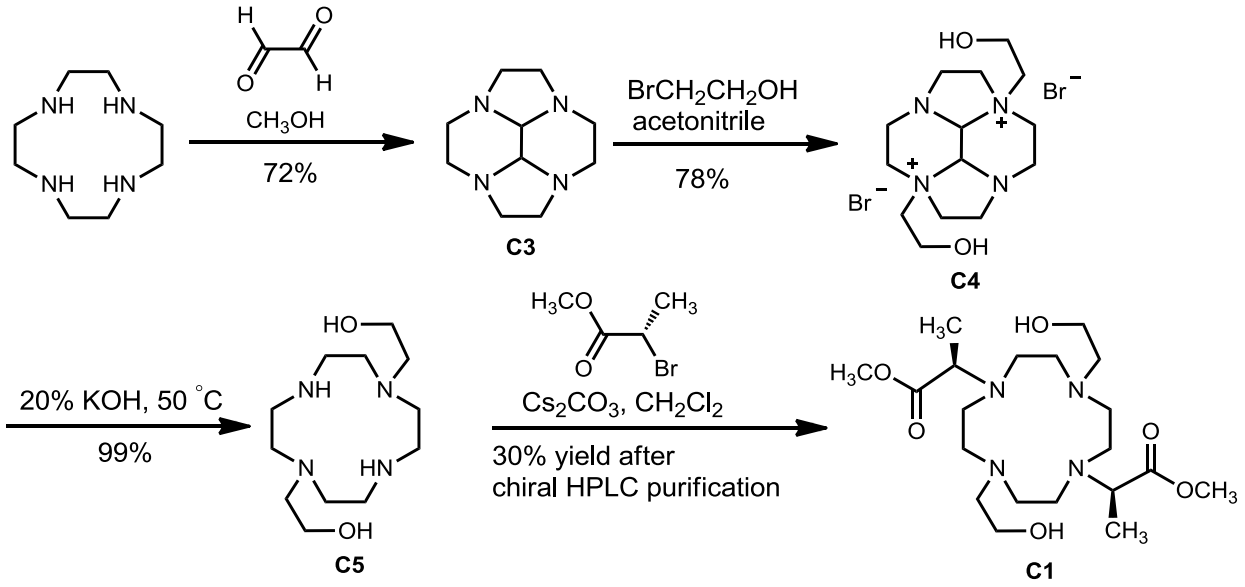

Scheme C1. Synthesis of octadentate ligand **C1**.

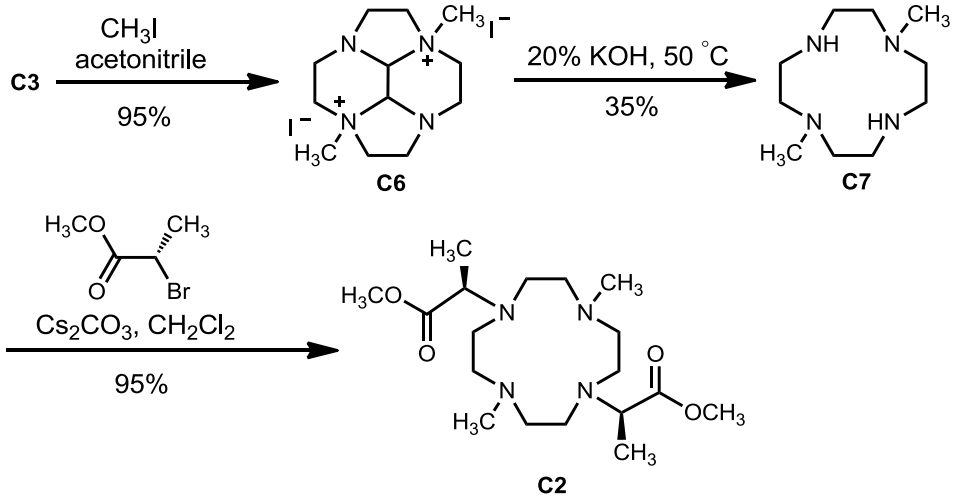

Scheme C2. Synthesis of hexadentate ligand **C2**.

Results and Discussion

Eu^{3+} combined with ligand **C1** in EtOH/H_2O (9:1) was unable to catalyze Mukaiyama aldol reactions. This lack of reactivity was attributed either to the possibility of the alcohol sidearms being deprotonated and causing a reduction in Lewis acidity at the metal center or to the lack of available coordination sites for the aldehyde to bind to Eu^{3+}. When Eu^{3+} was combined with ligand **C2** in EtOH/H_2O (9:1), products were observed but the reactions were not selective

(**Table C1**). These results are likely due to inefficient binding of Eu^{3+} by **C2** (unbound Eu^{3+} catalyzes racemic reactions).

Table C1. Mukaiyama aldol reaction results for Eu^{3+} combined with **C2** in EtOH/H_2O (9:1).

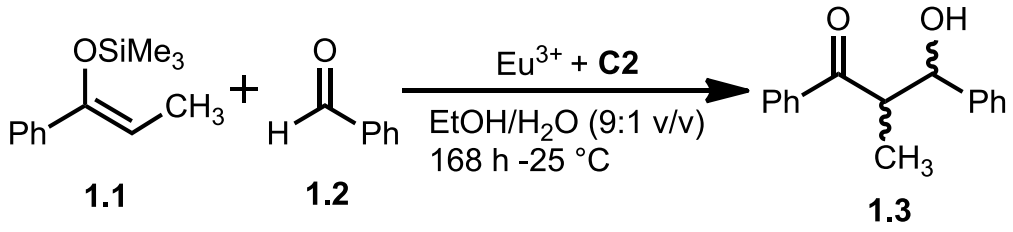

yield (%)	53[a]	34[b]
dr (*syn*:*anti*)	0.87:1[a]	0.81:1[b]
er (*syn*)	1:1[a]	1:1[b]

[a]ligand-to-Eu^{3+} ratio of 1.2:1 [b]ligand-to-Eu^{3+} ratio of 2.4:1

Experimental section

Materials. Commercially available chemicals were used without further purification. Water was purified using a PURELAB Ultra Mk2 (ELGA) water purification system. **1.1** (*Z*/*E* = 12:1) was synthesized according a previously published procedure.[17]

(2R,2'R)-dimethyl 2,2'-(4,10-bis(2-hydroxyethyl)-1,4,7,10-tetraazacyclododecane-1,7-diyl)dipropanoate (C1): Starting from **C5** the procedure from ref 3d was followed to add (*S*)-methyl 2-bromopropanoate to the two secondary amines to afford **C1** which was purified by chiral HPLC using a Chiracel OJ-H column using an isocratic method of hexanes/isopropanol (90:10) as the mobile phase. HRESIMS (*m*/*z*): $[M + H^+]^+$ calcd for $C_{20}H_{41}N_4O_6$, 433.3026; found 433.3012.

(2R,2'R)-dimethyl 2,2'-(4,10-dimethyl-1,4,7,10-tetraazacyclododecane-1,7-diyl)dipropanoate (C2): Starting from **C6** the procedure from ref 3d was followed to add (*S*)-methyl 2-bromopropanoate to the two secondary amines to afford **C2.** HRESIMS (*m*/*z*): $[M + H^+]^+$ calcd for $C_{18}H_{37}N_4O_4$, 373.2815; found 373.2813.

decahydro-2a,4a,6a,8a-tetraazacyclopenta[fg]acenaphthylene (C3): To a stirring mixture of 1,4,7,10-tetraazacyclododecane (5.00 g, 1.0 eq) in CH_3OH (350 mL) at 0 °C was added 3.5 mL of 40% w/w oxaldehyde in water (1.1 eq) over the course of 3 h. The mixture was allowed to come to room temperature and the solvents were removed under reduced pressure to afford a yellow oil. The oil was rinsed with ether and the rinsings were concentrated to yield 4.0 g of **C3**.

2a,6a-bis(2-hydroxyethyl)dodecahydro-2a,4a,6a,8a-tetraazacyclopenta[fg]acenaphthylene-2a,6a-diium bromide (C4): To a mixture of **C3** in acetonitrile was added bromoethanol (10 eq). The mixture was allowed to stir for 168 h and then concentrated under reduced pressure to give **C4**. HRESIMS (*m*/*z*): $[M - Br^-]^+$ calcd for $C_{14}H_{28}BrN_4O_2$, 363.1396; found 363.1404.

2,2'-(1,4,7,10-tetraazacyclododecane-1,7-diyl)diethanol (C5): **C4** was heated to 50 °C in 20 % KOH for 24 h and concentrated under reduced pressure to give a yellow oil containing **C5**. HRESIMS (*m*/*z*): $[M + H^+]^+$ calcd for $C_{12}H_{29}N_4O_2$, 261.2291; found 261.2282.

2a,6a-dimethyldodecahydro-2a,4a,6a,8a-tetraazacyclopenta[fg]acenaphthylene-2a,6a-diium iodide (C6): To a mixture of **C3** in acetonitrile was added iodomethane (10 eq). The mixture was allowed to stir for 24 h then concentrated under reduced pressure to give **C6**.

1,7-dimethyl-1,4,7,10-tetraazacyclododecane (C7): **C6** was heated to 50 °C in 20 % KOH for 24 h and concentrated under reduced pressure to give a yellow oil containing **C6**.

Conclusions

The two ligands described here were not published with the data reported in Chapter 3 of this dissertation because further characterization of these metal complexes is needed to have a thorough discussion.

APPENDIX D

Page	Contents
89	Table of contents
90	Copyright permission for Reference 3a
91	Copyright permission for Reference 3c
92	Copyright permission for Reference 8b
93	Copyright permission for Reference 9b
94	Copyright permission for Reference 10
95	Copyright permission for Reference 13
96	Copyright permission for Reference 15b

Copyright Clearance Center RightsLink®

Home | Account Info | Help

ACS Publications
MOST TRUSTED. MOST CITED. MOST READ.

Title: Lanthanide Trifluoromethanesulfonate-Catalyzed Asymmetric Aldol Reactions in Aqueous Media

Author: Shū Kobayashi,*, Tomoaki Hamada,Satoshi Nagayama, and, and Kei Manabe

Publication: Organic Letters

Publisher: American Chemical Society

Date: Jan 1, 2001

Copyright © 2001, American Chemical Society

Logged in as:
Derek Averill
LOGOUT

PERMISSION/LICENSE IS GRANTED FOR YOUR ORDER AT NO CHARGE

This type of permission/license, instead of the standard Terms & Conditions, is sent to you because no fee is being charged for your order. Please note the following:

- Permission is granted for your request in both print and electronic formats, and translations.
- If figures and/or tables were requested, they may be adapted or used in part.
- Please print this page for your records and send a copy of it to your publisher/graduate school.
- Appropriate credit for the requested material should be given as follows: "Reprinted (adapted) with permission from (COMPLETE REFERENCE CITATION). Copyright (YEAR) American Chemical Society." Insert appropriate information in place of the capitalized words.
- One-time permission is granted only for the use specified in your request. No additional uses are granted (such as derivative works or other editions). For any other uses, please submit a new request.

If credit is given to another source for the material you requested, permission must be obtained from that source.

Copyright Clearance Center RightsLink®

Home Account Info Help

ACS Publications
MOST TRUSTED. MOST CITED. MOST READ.

Title: A New Class of Ligands for Aqueous, Lanthanide-Catalyzed, Enantioselective Mukaiyama Aldol Reactions

Author: Yujiang Mei, Prabani Dissanayake, and Matthew J. Allen

Publication: Journal of the American Chemical Society

Publisher: American Chemical Society

Date: Sep 1, 2010

Copyright © 2010, American Chemical Society

Logged in as:
Derek Averill
LOGOUT

PERMISSION/LICENSE IS GRANTED FOR YOUR ORDER AT NO CHARGE

This type of permission/license, instead of the standard Terms & Conditions, is sent to you because no fee is being charged for your order. Please note the following:

- Permission is granted for your request in both print and electronic formats, and translations.
- If figures and/or tables were requested, they may be adapted or used in part.
- Please print this page for your records and send a copy of it to your publisher/graduate school.
- Appropriate credit for the requested material should be given as follows: "Reprinted (adapted) with permission from (COMPLETE REFERENCE CITATION). Copyright (YEAR) American Chemical Society." Insert appropriate information in place of the capitalized words.
- One-time permission is granted only for the use specified in your request. No additional uses are granted (such as derivative works or other editions). For any other uses, please submit a new request.

If credit is given to another source for the material you requested, permission must be obtained from that source.

Copyright Clearance Center RightsLink®

Home | Create Account | Help

ACS Publications
MOST TRUSTED. MOST CITED. MOST READ.

Title: Synthesis, Spectroscopic Characterization, and Reactivity of Water-Tolerant Eu3+-Based Precatalysts

Author: Derek J. Averill and Matthew J. Allen

Publication: Inorganic Chemistry

Publisher: American Chemical Society

Date: Jun 1, 2014

Copyright © 2014, American Chemical Society

User ID
Password
Enable Auto Login
LOGIN
Forgot Password/User ID?
If you're a copyright.com user, you can login to RightsLink using your copyright.com credentials. Already **a RightsLink user** or want to learn more?

PERMISSION/LICENSE IS GRANTED FOR YOUR ORDER AT NO CHARGE

This type of permission/license, instead of the standard Terms & Conditions, is sent to you because no fee is being charged for your order. Please note the following:

- Permission is granted for your request in both print and electronic formats, and translations.
- If figures and/or tables were requested, they may be adapted or used in part.
- Please print this page for your records and send a copy of it to your publisher/graduate school.
- Appropriate credit for the requested material should be given as follows: "Reprinted (adapted) with permission from (COMPLETE REFERENCE CITATION). Copyright (YEAR) American Chemical Society." Insert appropriate information in place of the capitalized words.
- One-time permission is granted only for the use specified in your request. No additional uses are granted (such as derivative works or other editions). For any other uses, please submit a new request.

BACK | CLOSE WINDOW

Copyright © 2014 Copyright Clearance Center, Inc. All Rights Reserved. Privacy statement.
Comments? We would like to hear from you. E-mail us at customercare@copyright.com

Copyright Clearance Center RightsLink®

Home | Account Info | Help

ACS Publications
Most Trusted. Most Cited. Most Read.

Title: Structural, Luminescence, and NMR Studies of the Reversible Binding of Acetate, Lactate, Citrate, and Selected Amino Acids to Chiral Diaqua Ytterbium, Gadolinium, and Europium Complexes

Author: Rachel S. Dickins et al.

Publication: Journal of the American Chemical Society

Publisher: American Chemical Society

Date: Oct 1, 2002

Copyright © 2002, American Chemical Society

Logged in as:
Derek Averill
Account #:
3000810832

LOGOUT

PERMISSION/LICENSE IS GRANTED FOR YOUR ORDER AT NO CHARGE

This type of permission/license, instead of the standard Terms & Conditions, is sent to you because no fee is being charged for your order. Please note the following:

- Permission is granted for your request in both print and electronic formats, and translations.
- If figures and/or tables were requested, they may be adapted or used in part.
- Please print this page for your records and send a copy of it to your publisher/graduate school.
- Appropriate credit for the requested material should be given as follows: "Reprinted (adapted) with permission from (COMPLETE REFERENCE CITATION). Copyright (YEAR) American Chemical Society." Insert appropriate information in place of the capitalized words.
- One-time permission is granted only for the use specified in your request. No additional uses are granted (such as derivative works or other editions). For any other uses, please submit a new request.

If credit is given to another source for the material you requested, permission must be obtained from that source.

Copyright Clearance Center RightsLink®

Home | Account Info | Help

ACS Publications
MOST TRUSTED. MOST CITED. MOST READ.

Title: Dynamic Measurements of Aqueous Lanthanide Triflate-Catalyzed Reactions Using Luminescence Decay

Author: Prabani Dissanayake and Matthew J. Allen

Publication: Journal of the American Chemical Society

Publisher: American Chemical Society

Date: May 1, 2009

Copyright © 2009, American Chemical Society

Logged in as:
Derek Averill
LOGOUT

PERMISSION/LICENSE IS GRANTED FOR YOUR ORDER AT NO CHARGE

This type of permission/license, instead of the standard Terms & Conditions, is sent to you because no fee is being charged for your order. Please note the following:

- Permission is granted for your request in both print and electronic formats, and translations.
- If figures and/or tables were requested, they may be adapted or used in part.
- Please print this page for your records and send a copy of it to your publisher/graduate school.
- Appropriate credit for the requested material should be given as follows: "Reprinted (adapted) with permission from (COMPLETE REFERENCE CITATION). Copyright (YEAR) American Chemical Society." Insert appropriate information in place of the capitalized words.
- One-time permission is granted only for the use specified in your request. No additional uses are granted (such as derivative works or other editions). For any other uses, please submit a new request.

If credit is given to another source for the material you requested, permission must be obtained from that source.

Inbox: Re: Fwd: permissions request (3 of 3182)

Mark as: Move Copy This message to

Delete Reply Forward Redirect View Thread Blacklist Whitelist Message Source Save

Date: Mon, 14 Jul 2014 14:31:54 +0800 [02:31:54 AM EDT]
From: Molecules Editorial Office / MDPI <molecules@mdpi.com>
To: djaveril@chem.wayne.edu
Reply-To: molecules@mdpi.com
Subject: Re: Fwd: permissions request

Dear Dr. Averill,

Thank you very much for your message and inquiry. It seems that all the figures in your following paper are prepared by the authors are therefore licensed under the CC-BY 3.0 license:

Averill, D.J.; Dissanayake, P.; Allen, M.J. The Role of Water in Lanthanide-Catalyzed Carbon-Carbon Bond Formation. Molecules 2012, 17, 2073-2081. http://www.mdpi.com/1420-3049/17/2/2073

Therefore, you can reuse all figures at your convenience under the sole condition of properly citing the paper (see above reference as an example of properly citing the paper).

Best regards,
Ms. Ran Dang
Assistant Editor
Molecules (http://www.mdpi.com/journal/molecules)

--
Ms. Ran Dang, M.Sc.
MDPI Branch Office, Beijing
Suite 2011, Ruidu International Center, No. 1 Cuijingbeili,
Tongzhou District, Beijing 101100, China
E-Mail: ran.dang@mdpi.com
Skype: adrian_sung
Tel./Fax: +86 10 8152 1170

MDPI AG
Molecules Editorial Office
Klybeckstrasse 64, 2nd Floor, Basel CH-4057, Switzerland
Tel. +41 61 683 77 34; Fax: +41 61 302 89 18
E-Mail: molecules@mdpi.com
http://www.mdpi.com/journal/molecules

Role of Water in Mukaiyar × Rightslink® by Copyright ×

https://s100.copyright.com/AppDispatchServlet

Copyright Clearance Center RightsLink®

Home Account Info Help Live Chat

ACS Publications
Most Trusted. Most Cited. Most Read.

Title: Role of Water in Mukaiyama–Aldol Reaction Catalyzed by Lanthanide Lewis Acid: A Computational Study

Author: Miho Hatanaka and Keiji Morokuma

Publication: Journal of the American Chemical Society

Publisher: American Chemical Society

Date: Sep 1, 2013

Copyright © 2013, American Chemical Society

Logged in as:
Derek Averill
Account #:
3000810832

LOGOUT

PERMISSION/LICENSE IS GRANTED FOR YOUR ORDER AT NO CHARGE

This type of permission/license, instead of the standard Terms & Conditions, is sent to you because no fee is being charged for your order. Please note the following:

- Permission is granted for your request in both print and electronic formats, and translations.
- If figures and/or tables were requested, they may be adapted or used in part.
- Please print this page for your records and send a copy of it to your publisher/graduate school.
- Appropriate credit for the requested material should be given as follows: "Reprinted (adapted) with permission from (COMPLETE REFERENCE CITATION). Copyright (YEAR) American Chemical Society." Insert appropriate information in place of the capitalized words.
- One-time permission is granted only for the use specified in your request. No additional uses are granted (such as derivative works or other editions). For any other uses, please submit a new request.

BACK CLOSE WINDOW

Copyright © 2014 Copyright Clearance Center, Inc. All Rights Reserved. Privacy statement.
Comments? We would like to hear from you. E-mail us at customercare@copyright.com

REFERENCES

(1) (a) Ouchi, K.; Saito, S.; Shibukawa, M. *Inorg. Chem.* **2013**, *52*, 6239–6241. (b) Caillé, F.; Bonnet, C. S.; Buron, F.; Villette, S.; Helm, L.; Petoud, S.; Sezenet, F.; Tóth, É. *Inorg. Chem.* **2012**, *51*, 2522–2532. (c) Andolina, C. M.; Mathews, R. A.; Morrow, J. R. Helv. Chim. Acta **2009**, 92, 2330–2347. (d) Choppin, G. R.; Wang, Z. M. *Inorg. Chem.* **1997**, *36*, 249–252. (e) Lochhead, M. J.; Wamsley, P. R.; Bray, K. L. *Inorg. Chem.* **1994**, *33*, 2000–2003. (f) Horrocks, W. D., Jr.; Sudnick, D. R. *J. Am. Chem. Soc.* **1979**, *101*, 334–340. (g) Wu, S. L,; Horrocks, W. D., Jr. *Inorg. Chem.* 1995, 34, 3724–3732. (h) Sánchez-Lombardo, I.; Andolina, C. M.; Morrow, J. R.; Yatismirsky, A. K. *Dalton Trans*. **2010**, ***39***, 864–873. (i) Kobayashi, S.; Hachiya, I. *Tetrahedron Lett.* **1992**, *33*, 1625–1628. (j) Kobayashi, S.; Hachiya, I. *J. Org. Chem.* **1994**, *59*, 3590−3596. (k) Kobayashi, S.; Nagayama, S.; Busujima, T. *J. Am. Chem. Soc.* **1998**, *120*, 8287–8288. (l) Kitanosono, T.; Kobayashi, S. *Adv. Synth. Catal.* **2013**, *355*, 3095–3118.

(2) (a) Miyahara, Y.; Ito, Y. N. *J. Org. Chem.* **2014**, *79*, 6801–6807. (b) Rigo, M.; Canu, P.; Angelin, L.; Valle, G. D. *Ind. Eng. Chem. Res.* **1998**, *37*, 1189–1195. (c) Kulszewicz-Bajer, I.; Proń, A.; Abramowicz, J.; Jeandey, C.; Oddou, J.-L.; Sobczak, J. W. *Chem. Mater*. **1999**, *11*, 552–556. (d) Denmark, S. E.; Heemstra, J. R., Jr. *Org. Lett.* **2003**, *5*, 2303−2306.

(3) (a) Kobayashi, S.; Hamada, T.; Nagayama, S.; Manabe, K. *Org. Lett.* **2001**, *3*, 165−167. (b) Hamada, T.; Manabe, K.; Ishikawa, S.; Nagayama, S.; Shiro, M.; Kobayashi, S. *J. Am. Chem. Soc.* **2003**, *125*, 2989−2996. (c) Mei, Y.; Dissanayake, P.; Allen, M. J. *J. Am. Chem. Soc.* **2010**, *132*, 12871−12873. (d) Mei, Y.; Averill, D. J.; Allen, M. J. *J. Org. Chem.* **2012**, *77*, 5624–5632. (e) Pandya, S. U.; Dickens, R. S.; Parker, D. *Org. Biomol. Chem.* **2007**, *5*, 3842–3846. (f) Robinson, J. R.; Fan, X.; Yadav, J.; Carroll, P.J.; Wooten, A.J.; Pericàs, M.A.; Schelter, E.J.; Walsh, P.J. *J. Am. Chem. Soc*. **2014**, *136*, 8034–8041.

(4) (a) Richardson, F. S. *Chem. Rev.* **1982**, *82*, 541–552. (b) Bünzli, J.-C. G.; Piguet, C. *Chem. Soc. Rev.*, **2005**, *34*, 1048–1077. (c) Kan, S. B. J.; Ng, K. K. –H.; Paterson, I. *Angew. Chem. Int. Ed.* 2013, 52, 9097–9108. (d) Mlynarski, J.; Paradowska, J.; *Chem. Soc. Rev.* **2008**, *37,* 1502–1511. (e) Kobayashi, S.; Sugiura, M.; Kitagawa, H.; Lam, W. W. *Chem. Rev.* **2002**, *102*, 2227–2302. (f) Kobayashi, S.; Manabe, K. *Acc. Chem. Res.* **2002**, *35*, 209–217.

(5) (a) Lee, Y.; Choi, J. Y.; Fu, H.; Harvey, C.; Ravindran, S.; Roush, W. R.; Boothroyd, J. C.; Khosla, C. *J. Med. Chem.* **2011**, *54*, 2792−2804. (b) Tosin, M.; Smith, L.; Leadlay, P. F. *Angew. Chem., Int. Ed.* **2011**, *50*, 11930−11933. (c) Morar, M.; Pengelly, K.; Koteva, K.; Wright, G. D. *Biochemistry* **2012**, *51*, 1740−1751. (d) Park, J. W.; Oh, H.-S.; Jung, W. S.; Park, S. R.; Han, A. R.; Ban, Y.-H.; Kim, E. J.; Kang, H.-Y.; Yoon, Y. *J. Chem. Commun*. **2008**, 5782−5784. (e) Green, A. P.; Lee, A. T. L.; Thomas, E. J. *Chem. Commun.* **2011**, *47*, 7200–7202. (f) Oh, H.-S.; Kang, H.-Y. *J. Org. Chem.* **2012**, *77*, 1125−1130.

(6) (a) Kobayashi, S.; Nagayama, S.; Busujima, T. *Chem. Lett.* **1999**, 71−72. (b) Kobayashi, S.; Nagayama, S.; Busujima, T. *Tetrahedron* **1999**, *55*, 8739−8746. (c) Nagayama, S.; Kobayashi, S. *J. Am. Chem. Soc.* **2000**, *122*, 11531−11532. (d) Ollevier, T.; Plancq, B. *Chem. Commun.* **2012**, *48*, 2289−2291.

(7) (a) Kim, Y. S.; Matsunaga, S.; Das, J.; Sekine, A.; Ohshima, T.; Shibasaki, M. *J. Am. Chem. Soc.* **2000**, *122*, 6506–6507. (b) Mikami, K.; Mikami, H.; Matsuzawa, H.; Matsumoto, Y.; Nishikido, J.; Yamamoto, F.; Nakajima, H. *Tetrahedron* **2002**, *58,* 4015–4021.

(8) (a) Bradshaw, J. S.; Huszthy, P.; McDaniel, C. W.; Zhu, C. Y.; Dalley, N. K.; Izatt, R. M. *J. Org. Chem.* **1990**, *55*, 3129–3137. (b) Averill, D. J.; Allen, M. J. *Inorg. Chem.* **2014**, *53*, 6257–6263.

(9) (a) Harada, T.; Tsumatori, H.; Nishiyama, K.; Yuasa, J.; Hasegawa, Y.; Kawai, T., *Inorg. Chem.* **2012**, *51*, 6476–6485. (b) Dickins, R. S.; Aime, S.; Batsanov, A. S.; Beeby, A.; Botta, M.; Bruce, J. I.; Howard, J. A. K.; Love, C. S.; Parker, D.; Peacock, R. D.; Puschmann, H. *J. Am. Chem. Soc.* **2002**, *124*, 12697–12705.

(10) Dissanayake, P.; Allen, M. J. *J. Am. Chem. Soc.* **2009**, *131*, 6342−6343.

(11) (a) Supkowski, R. M.; Horrocks, W. D., Jr. *Inorg. Chim. Acta* **2002**, *340*, 44–48. (b) Beeby, A.; Clarkson, I. M.; Dickens, R. S.; Faulkner, S.; Parker, D.; Royle, L.; de Sousa, A. S.; Williams, J. A. G.; Woods, M. *J. Chem. Soc.*, *Perkin Trans. 2* **1999**, 493–504. (c) Dissanayake, P.; Mei, Y.; Allen, M. J. *ACS Catal*. **2011**, *1*, 1203–1212.

(12) Lin, Z.; Allen, M. J. *Dyes Pigments* **2014**, *110*, 261–269.

(13) Averill, D. J.; Dissanayake, P.; Allen, M. J. *Molecules* **2012**, *17*, 2073−2081.

(14) (a) Dehaen, G.; Absillis, G.; Driesen, K.; Binnemans, K.; Parac-Vogt, T. N. *Helv. Chim. Acta* **2009**, *92*, 2387–2397. (b) Bemquerer, M. P.; Bloch, C. Jr.; Brito, H. F.; Teotnio, E. E.S.; Miranda, M. T. M. *J. Inorg. Biochem.* **2002**, *91*, 363–370.

(15) (a) Hatanaka, M.; Maeda, S.; Morokuma, K. *J. Chem Theory Comput.* **2013**, *9*, 2882–2886. (b) Hatanaka, M.; Morokuma, K. *J. Am. Chem. Soc.* **2013**, *135*, 13972–13979.

(16) (a) Kobayashi, S.; Manabe, K. *Pure. Appl. Chem.* **2000**, *72*, 1373–1380. (b) Mikami, K.; Kotera, O.; Motoyama, Y.; Sakaguchi, H. *Synlett* **1995**, 975–977. (c) Bernardelli, P.; Moradei, O. M.; Friedrich, D.; Yang, J.; Gallou, F.; Dyck, B. P.; Doskotch, R. W. *J. Am. Chem. Soc.* **2001**, *123*, 9021–9032. (d) Qian, C.; Huang, T. *Tetrahedron Lett.* **1997**, *38*, 6721–6724. (e) Aspinall, H. C.; Greeves, N.; McIver, E. G. *Tetrahedron Lett.* **1998**, *39*, 9283–9286. (f) Kinsman, A. C.; Kerr, M. A.; *Org. Lett.* **2000**, *2*, 3517–3520. (g) Crousse, B.; Bégué, J.-P.; Bonnet-Delpon, D. *J. Org. Chem.* **2000**, *65*, 5009–5013. (h) Sanchez-Blanco, A. I.; Gothelf, K. V.; Jørgensen, K. A.

Tetrahedron Lett. **1997**, *38*, 7923–7926. (i) Kawada, A.; Mitamura, S.; Kobayashi, S. *Chem. Commun.* **1993**, 1157–1158. (j) Kobayashi, S.; Ishitani, H.; Komiyama, S.; Oniciu, D. C.; Katritzky, A. R. *Tetrahedron Lett.* **1996**, *37*, 3731–3734.

(17) Li, H. -J.; Tian, H. –Y.; Wu, Y. –C.; Chen, Y. –J.; Liu, L.; Wang, D.; Li, C. –J. *Adv. Synth. Catal.* **2005**, *347*, 1247–1256.

(18) Cossy, C.; Helm, L.; Merbach, A. E. *Inorg. Chem.* **1988**, *27*, 1973–1979.

(19) Hwang, B. J.; *Ind. Eng. Chem. Res.* **1994**, *33*, 1897–1900.

(20) Bünzli, J. –C. G.; Merbach, A. E.; Nielson, R. M. *Inorg. Chim. Acta.* **1987**, *139*, 151–152.

(21) Barge, A.; Cravotto, G.; Gianolio, E.; Fedeli, F. *Contrast Med. Mol. Imaging* **2006**, *1*, 184–188.

(22) (a) Xuan, R.; Oh, H. –S.; Lee, Y.; Kang, H.-Y. *J. Org. Chem.* **2008**, *73*, 1456–1461. (b) Pearson, A. J.; Panda, S. *Org. Lett.* **2011**, *13*, 5548–5551.

(23) (a) Denmark, S. E.; Wong, K.-T.; Tavenger, R. A. *J. Am. Chem. Soc.* **1997**, *119*, 2333–2334. (b) Desimoni, G.; Faita, G.; Piccinini, F.; Toscanini, M. *Eur. J. Org. Chem.* **2006**, 5228–5230.

(24) Li, H.-J.; Tian, H.-Y.; Chen, Y.-J.; Wang, D.; Li, C.-J. *Chem. Commun.* **2002**, 2994–2995.

(25) (a) Mlynarski, J.; Jankowska, J. *Adv. Synth. Catal.* **2005**, *347*, 521–525. (b) Jankowska, J.; Mlynarski, J. *J. Org. Chem.* **2006**, *71*, 1317–1321. (c) Jankowska, J.; Paradowska, J.; Rakiel, B.; Mlynarski, J. *J. Org. Chem.* **2007**, *72*, 2228–2231.

(26) Still, W. C.; Kahn, M.; Mitra, A. *J. Org. Chem.* **1978**, *43*, 2923–2925.

(27) (a) Brittain, H. G. *Inorg. Chem.* **1980**, *19*, 640–643. (b) George, M. R.; Golden, C. A.; Grossel, M. C.; Curry, R. J. *Inorg. Chem.* **2006**, *45*,1739–1744.

(28) Binnemans, K.; Herck, K. V.; Gorller-Warland, C. *Chem. Phys. Lett.* **1997**, *266*, 297–302.

(29) Billard, I.; Georg, S. *Helv. Chim. Acta* **2009**, *92*, 2227–2237.

(30) (a) Baranyai, Z.; Bányai, I.; Brücher, E.; Király, R.; Terreno, E. *Eur. J. Inorg. Chem.* **2007**, 3639–3645. (b) Tóth, É.; Brücher, E.; Lázár, I.; Tóth, I. *Inorg. Chem.* **1994**, *33*, 4070–4076. (c) Chin, A. K. O.; Morrow, J. R.; Lake, C. H.; Churchill, M. R. *Inorg. Chem.* **1994**, *33*, 656–664.

(31) (a) Kobayashi, S.; Wakabayashi, T.; Nagayama, S.; Oyamada, H. *Tetrahedron Lett.* **1997**, *38*, 4559–4562. (b) Nomiya, K.; Ohta, K.; Sakai, Y.; Hosoya, T.-A; Ohtake, A.; Takakura, A.; Matsunaga, S. *Bull. Chem. Soc. Jpn.* **2013**, *86*, 800–812.

ABSTRACT

LANTHANIDE-BASED PRECATALYSTS FOR CARBON–CARBON BOND FORMING REACTIONS IN AQUEOUS MEDIA.

by

DEREK JAMES AVERILL

December 2014

Advisor: Dr. Matthew J. Allen

Major: Chemistry

Degree: Doctor of Philosophy

The formation of carbon–carbon bonds is of great interest to synthetic chemists because these bonds make up the majority of biologically active compounds. The Mukaiyama aldol reaction is a Lewis-acid-catalyzed carbon–carbon bond-forming reaction that has the ability to produce optically active β-hydroxy carbonyls which can be found in many pharmaceuticals and natural products. Because of precatalyst instability towards hydrolysis, anhydrous solvents are commonly used. Recent efforts have focused on water-tolerant versions of enantioselective Mukaiyama aldol reactions because of the financial and environmental benefits of using aqueous media. Consequently, the Lewis-acidic and water-tolerant features of Ln^{3+} ions have aroused great interest in lanthanide-catalyzed bond-forming reactions in aqueous media.

Several Ln^{3+}-based Lewis acid precatalysts that were designed for Mukaiyama aldol reactions have been shown to be enantioselective, water-tolerant, and recoverable. Limiting the usefulness of these precatalysts are high ligand loadings and long reaction times that are necessary for high enantiomeric ratios. An understanding of water-coordination number, counter anion identitiy, solvent system, and ligand type effect(s) are necessary to improve upon existing Ln^{3+}-based precatalysts.

We used luminescence-decay measurements and high performance liquid chromatography analyses to study the effects of water-coordination number, counter anion identitiy, and solvent system on reaction rates of Mukaiyama aldol reactions. We found that higher water-coordination numbers and higher water compositions gave rise to more reactive precatalysts for Mukaiyama aldol reactions that were catalyzed by Eu^{3+}. The effects of ligand type on reactivity and selectivity of Eu^{3+}-based precatalysts for Mukaiyama aldol reactions were studied by synthesizing and characterizing four new hexadentate ligands in the presence of Eu^{3+}. Eu^{3+} emission spectra and ^{1}H-NMR experiments were used to study changes in Eu^{3+} coordination while titrating hexadentate ligands into solutions of Eu^{3+} and it was found that Eu^{3+} is able to be coordinatively saturated in the presence of excess hexadentate ligands.

Trends in reactivity and selectivity were found by studying Eu^{3+} in the presence of different anions and several chiral hexadentate ligands that contain ester, carboxylic acid, alcohol and amide donating groups. The results described in this thesis are likely to contribute to the development of highly reactive and selective Ln^{3+}-based precatalysts.

AUTOBIOGRAPHICAL STATEMENT

College Education
Oakland Community College, Auburn Hills, Michigan: A.A. 2003–2006
Oakland University, Rochester Hills, Michigan: B.S. 2006–2009
Wayne State University, Detroit, Michigan: Ph.D. 2009–2014

Honors and Awards
Thompson Undergraduate Chemistry Award: 2008 and 2009
Wayne State University Chemistry Excellence in Teaching Award: 2011
Wayne State Graduate Student Travel Award: 2012
Schaap Graduate Student Fellowship: 2012–2013
Heller Fellowship: 2013–2014
Esther and Stanley Kirschner Graduate Award in Inorganic Chemistry: 2014

Professional Affiliations
American Chemical Society, 2009 and 2012

Research Experience
Oakland University 2007–2009, Advisor: Dr. Ferman Chavez
Wayne State University 2009–2014, Advisor: Dr. Matthew J. Allen

Teaching Experience
Undergraduate Teaching Assistant, Oakland University, 2008–2009
Graduate Teaching Assistant, Wayne State University, 2009–2011

Publications

"Oxalate Oxidase Model Studies: Substrate Reactivity" Pawlak, P. L.; Panda, M.; Li, J.; **Averill, D. J.**; Nikolovoski, B,; Brennessel, W. W.; Chavez, F. A. Submitted

Averill, D. J.; Allen, M. J. **2014**, in press, *Catal. Sci. Technol.* DOI: 10.1039/C4CY01117A

Averill, D. J.; Allen, M. J. *Inorg. Chem.* **2014**, *53*, 6257–6263.

Banerjee, A.; Li, J.; Fugitt, J. B.; **Averill, D. J.**; Rumshlag, A. T.; Tyminska, N.; Brennessel, W. W.; Sevilla, M. D.; Chavez, F.A. *Inorg. Chim. Acta.* **2013,** *405*, 295–301.

Mei, Y.; **Averill, D. J.**; Allen, M. J. *J. Org. Chem*. **2012,** *77*, 5624–5632.

Averill, D. J.; Dissanayake, P.; Allen, M. J. *Molecules* **2012,** *17*, 2073–2081.

Averill, D. J.; Garcia, J.; Siriwardena-Mahanama, B. N.; Vithanarachchi, S. M.; Allen, M. J. *J. Vis. Exp.* **2011,** *53,* e2844.

Dissanayake, P.; **Averill, D. J.**; Allen, M. J. Lanthanide-Catalyzed Mukaiyama Aldol Reactions. In Science of Synthesis, Knowledge Updates 2011/4; Marek, I., Ed.; Georg Thieme Verlag KG: Stuttgart, Germany, 2012; pp 1–9. (review article)